WORKSHOP REPORT

NEUTRON MACROMOLECULAR CRYSTALLOGRAPHY AT THE SPALLATION NEUTRON SOURCE

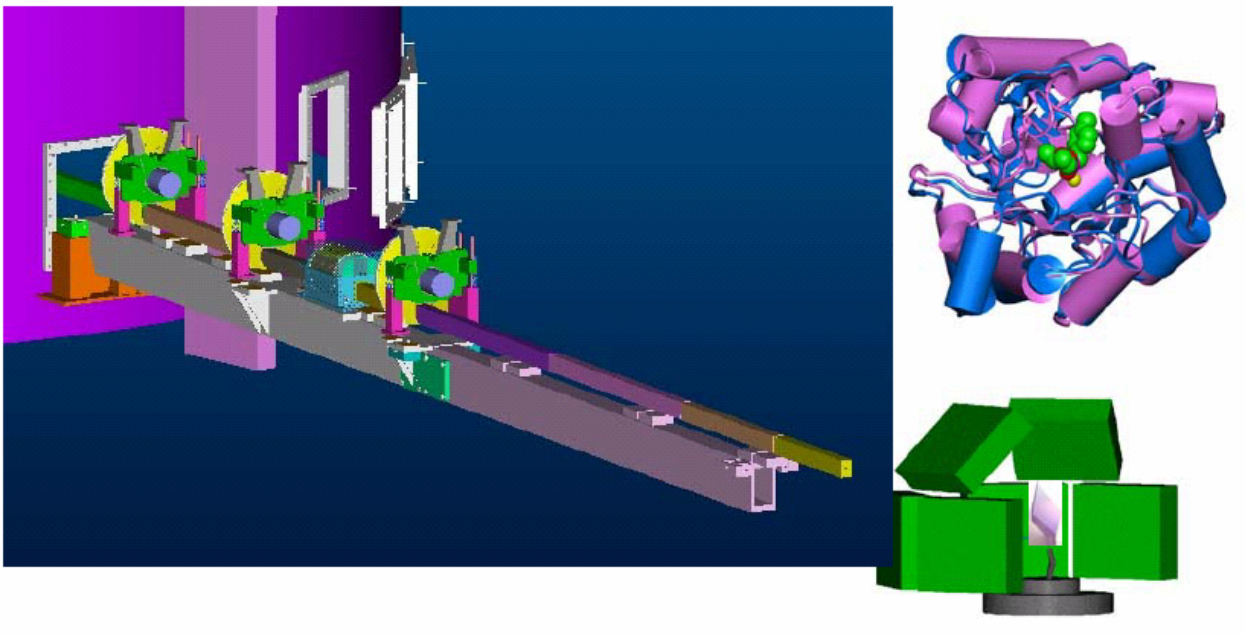

OCTOBER 2 - 3, 2003

AT THE INTENSE PULSED NEUTRON SOURCE (IPNS)

ARGONNE NATIONAL LABORATORY
ARGONNE, IL, USA

IPNS

UIC University of Illinois at Chicago

Office of Basic Energy Sciences · Serving the Present, Shaping the Future ·

ORAU
OAK RIDGE ASSOCIATED UNIVERSITIES

SNS
SPALLATION NEUTRON SOURCE

TABLE OF CONTENTS

EXECUTIVE SUMMARY AND RECOMMENDATIONS

Neutron Macromolecular Crystallography (NMC) is able to accurately determine proton locations, protonation states and hydration, and hydrogen/deuterium exchange in macromolecular crystals even at a moderate resolution (2 Å to 2.5 Å). Characterization of the protonation states of amino acid residues in the active sites of enzymes is crucial for an understanding of reaction mechanisms. The large difference in the neutron scattering cross-sections of hydrogen and deuterium nuclei has been exploited to extract important structural information on exchangeable protons and bound water in macromolecules. Such information is difficult to obtain from other techniques, and NMC accordingly offers a number of unique capabilities to address important problems in enzymology, bioenergetics, and structural biology.

In order to exploit the high neutron flux that will become available by 2006 at the Spallation Neutron Source (SNS), and to leverage the strong support and interest of the macromolecular crystallography community, a workshop on "Neutron Macromolecular Crystallography at the Spallation Neutron Source" was organized at the Intense Pulsed Neutron Source (IPNS), Argonne National Laboratory, on October 2-3, 2003. The workshop was co-sponsored by the SNS, IPNS, and Oak Ridge Associated Universities (ORAU). The objectives of the workshop were to assemble a broad spectrum of researchers, in order to determine the current and future scientific needs for macromolecular neutron crystallography and to seek input on design criteria for a next generation, best-in-class, Macromolecular Neutron Diffractometer (*MaNDi*) at the SNS. The workshop brought together a diverse group of over fifty participants. Attendees included biologists, enzymologists, biochemists, molecular biologists, computational chemists, physicists, NMR spectroscopists, and x-ray and neutron protein crystallographers who require accurate structural information on the positions of hydrogen atoms and water molecules in the active sites of enzymes and receptors, in order to elucidate the mechanistic details involved in their function, as well as information on hydration in nucleic acid systems. Leading scientists from the United States and abroad, representing both academia and industry, gave presentations and participated in organized discussions that enabled them to present their scientific cases and to define the needs for macromolecular neutron diffraction in their research.

The participants unanimously agreed that there is a strong and continuing need within the scientific community for macromolecular neutron crystallography but noted that work to date has been limited by the small number of available instruments, especially in the United States, and by the low, effective neutron flux of the available neutron beams, which leads to a requirement for large crystals (>1 mm^3) and limits the size of the unit cells (<100 Å) that can be studied. The group enthusiastically welcomed factors of 10 to 50-fold gains in performance promised by the proposed *MaNDi* beamline and agreed that this advance would help revolutionize the field of macromolecular neutron diffraction. The group unanimously favored the formation of an Instrument Development Team (IDT) and strongly recommended that high priority be given to building *MaNDi* at the SNS as soon as possible. The ability to work with much smaller crystals, approaching the size that are now commonly used for laboratory single-crystal x-ray studies, and the greatly increased throughput, will open up new fields of research and is expected to stimulate rapid growth in the user community.

The design concepts for *MaNDi* were well received by the community. The participants mandated the IDT to further develop and evaluate the instrument design, with recommendations that *MaNDi* be optimized for the rapid measurement of Bragg intensities to resolutions of 1.5 Å to 2.0 Å, on macromolecular crystals with volumes of less than 1 mm^3, and with unit cell dimensions between 50 Å and 150 Å. It was anticipated that these design specifications would fulfill the data collection requirements for more than 80% of the samples being studied by the

user community. Moreover, to maximize the potential scientific impact of *MaNDi*, it was recommended that the instrument design should be flexible enough to collect data to resolutions higher than 1.5 Å from crystals with smaller unit cell dimensions, and to collect data from crystals with unit cell sizes larger than 150 Å at the expense of the higher resolution data. The latter specifications are for contrast variation studies of large and complex systems. To achieve these objectives, and to collect both high-resolution and low-angle reflections, it was recommended that the instrument design incorporate an adjustable detector or detector-array for data collection over a wide area, and have the capability to select different wavelength ranges as needed.

The workshop participants also strongly recommended that a number of additional and supporting scientific areas be co-developed and implemented at *MaNDi* and at the recently commissioned Protein Crystallography Station (PCS) at Los Alamos National laboratory in order to support and strengthen the macromolecular neutron community. First, protein perdeuteration capabilities were deemed to be essential because deuterated proteins would deliver increases in coherent scattering, and large reductions in incoherent scattering background, which would result in a reduction in the crystal size requirements by as much as order of magnitude. It was recommended that deuteration capabilities and facilities be established to support the neutron community at *MaNDi* and at the PCS. Second, development and refinement of methods and apparatus for growing larger crystals of macromolecules and for performing hydrogen/deuterium exchange were recommended. Finally, it was recommended that user-friendly software for neutron data collection, processing, and refinement should be co-developed with the PCS.

In the final round-table discussion, the scientific community as represented through the workshop participants, from the USA and abroad, expressed strong endorsement and support for construction of a next generation macromolecular neutron diffractometer at the SNS, and strongly recommended the co-development and implementation of a number of biological neutron science support areas and facilities. It is anticipated that *MaNDi* will have a major impact on macromolecular neutron crystallography and consequent biological structure studies worldwide.

INTRODUCTION

Neutron Macromolecular Crystallography (NMC) can fill an important niche in structural biology [1-23], enzymology, and functional genomics due to its versatility in the accurate determination of protons, protonation states, and hydration in macromolecular crystals even at a moderate 2 to 2.5 Å resolution [18, 24, 25]. Although ultra-high resolution macromolecular x-ray crystallography (UHRMXC) at third generation synchrotron sources on cryo-protected highly ordered protein crystals can locate the ordered hydrogen atoms [26-28] and protonation states of amino acid side chains [29], there are many instances where the information obtained is inadequate. For instance, in myoglobin, even at resolutions better than 1.15 Å, UHRMXC did not give hydrogen positions [30-32], whilst NMC enabled the same hydrogen atom positions to be visualized in a perdeuterated structure determined to 2.0 Å resolution [33].

The knowledge about protonation states of amino acid residues in the active sites of enzymes is crucial for an understanding of reaction mechanisms. Identification of protonated amino acids in the catalytic center would allow discrimination between two or more competing reaction models [34]. Such critical information from NMC help to solve the question about which of the two amino acids, Asp-102 or His-57, in trypsin is the origin of the catalytic proton [35].

The large difference in the neutron scattering cross-sections of hydrogen and deuterium nuclei has been exploited to extract important structural information on exchangeable protons and bound water in macromolecules. At a higher resolution (1.5 Å) neutron diffraction shows the degree of order of different water molecules in the crystals [36]. Such information is difficult to obtain from other techniques.

Crystals of perdeuterated proteins provide enhanced visibility of deuterons in the neutron crystallographic data [33] due to the combined effects of large coherent and small incoherent scattering cross-sections of deuterium that increases the signal-to-noise ratio by a factor of 8 when compared to normal proteins. Perdeuterated crystals offer unique advantages in determining the exchangeable protons and provide access to information on the charge density distribution from x-ray and neutron difference maps. Thus, NMC offers a number of unique advantages with respect to addressing important problems in enzymology and structural biology.

Another area where NMC has a great potential to make a strong impact is the structural biology of the membrane proteins. Although XMC has enormous success in solving the crystal structures of aqueous proteins [over 25,000 total entries in the Protein Data Bank (PDB)], only a handful of membrane proteins (36 entries in the PDB) have been solved to date despite the fact that about 40% of the genome consists of membrane bound proteins. One obvious reason for this limited success is the difficulty in growing high quality crystals of membrane proteins. Another advantage with NMC is its ability to reveal detergent envelopes around the membrane proteins at much lower resolution [37, 38] when measurements are done at different contrasts. Thus, NMC can readily serve as an indispensable complementary tool to XMC in advancing the important field of structural biology.

Even though NMC is a powerful technique, its productivity has been severely constrained by the lack of facilities and intrinsic low brightness of available neutron sources. Currently there are only limited instruments that are recognized to be useful for high resolution single crystal macromolecular neutron crystallography: LADI at the Institut Laue-Langevin (ILL), Grenoble, France; BIX3/BIX4 at the Japan Atomic Energy Research Institute (JAERI); and PCS

at Los Alamos National Laboratory (LANL). While the reactor based LADI and BIX3 instruments were operational during the past 5-7 years, the time-of-flight diffractometer PCS at the spallation source at Los Alamos National Laboratory has become available during early 2003.

Since its inception in 1995, LADI has raised the molecular weight ceiling above 30 kDa for NMC studies of proteins such as aspartic proteinase at 2 Å resolution [39]. Gilboa et al [40] took this to new limits with the 50 kDa case of glucose bound concanavalin A with a cubic unit cell size of 167 Å . The large incoherent background inherent to Laue diffraction is greatly ameliorated by predeuteration and recent work has shown that it is possible to collect high resolution data (~2.4 Å) from small (0.15mm^3) crystals, though spatial overlap of reflections at the detector limits application with unit cells > 80 Å. The time-of-flight Laue diffraction technique at the PCS instrument [41] offers indisputable advantage over the conventional Laue method at LADI in using a large wavelength band (0.7 - 7 Å) and spreading the diffraction peaks as well as the background into a large number of wavelength channels. in This has enabled diffraction data to be collected for D-Xylose isomerase [42], which, with a molecular unit cell of (94 x 99 x 103 Å^3.), is one of the largest systems addressed date by NMC at high resolution (~2.0 Å) . Recognition in the scientific community of the unique information obtainable with NMC has already resulted in an oversubscription factor > 2 on neutron instruments worldwide and by a factor > 3 for the PCS instrument at LANL. Higher flux is needed for studies on crystals of smaller volumes and larger unit cells (>100 Å) at resolution in the range of 1.5 Å. Thus, there is a dire need for powerful high resolution diffractometers for NMC.

With the advent of the Spallation Neutron Source (SNS) at Oak Ridge National Laboratory, an excellent opportunity exists for the development of a powerful high resolution neutron diffractometer for structural biology. Since SNS is currently under construction and will have more than an order of magnitude higher intensity than the Los Alamos facility, a great deal of flexibility currently exists for designing a fully optimized diffractometer for NMC. Furthermore, state-of-the art neutron guides, cryogenic moderators, and high sensitivity and high resolution detectors would allow additional factors of increases in data rates and resolution. Hence it is proposed to develop a dedicated, best-in-class and high resolution time-of-flight single crystal macromolecular neutron diffractometer (*MaNDi*) at the SNS high power target station (HPTS) that operates at 60 Hz.

Design calculations using analytical equations and Monte Carlo simulations show that the data rates at the *MaNDi* instrument will be over 50 times greater than at PCS. Thus, it will become possible to investigate larger unit cell systems at high resolution with smaller crystals. It is expected that the unprecedented high data rates and resolution with **MaNDi** for the high resolution NMC will revolutionize and greatly advance the fields of structural biology and enzymology.

To provide impetus to the development of *MaNDi* at the SNS, a workshop entitled "Neutron Macromolecular Crystallography at the Spallation Neutron Source" was organized at the Intense Pulsed Neutron Source Division, Argonne National Laboratory, during October 2-3, 2003. The objectives of the workshop were:

1) Inform the scientific community about the exciting opportunity available at the SNS for the development of a versatile diffractometer for high resolution NMC.
2) Obtain input from the scientific community on the leading edge scientific problems that will require NMC.
3) Obtain input on the design parameters for *MaNDi* with regard to the range of size of the unit cell, resolution, sample environment, deuteration facilities, and other related facilities for structural biology at the SNS site.

4) Officially form an instrument development team (IDT) and document a strong scientific case to obtain funding for the construction of the *MaNDi* instrument.

Over 50 scientists including many pioneers and experts, as well as younger scientists, attended this workshop where a number of talks emphasizing the need for facilities for NMC were presented. Summaries of the talks, list of attendees, the instrument development team (IDT), and IDT executive committee are given below.

References

1. Tsyba, I. and R. Bau, *Chemtracts-Inorganic Chemistry*, 2002. **15**: p. 233-257.
2. Schoenborn, B.P., in *Nature in Biology, Basic Life Sciences*, B.P. Schoenborn, Editor. 1984, Plenum Press: New York. p. 261-281.
3. Schoenborn, B.P., *Methods Enzymol.*, 1985. **114**: p. 510.
4. Schoenborn, B.P., in *Neutrons in Biology, Basic Life Sciences*, R.B. Knott, Editor. 1996, Plenum Press: New York. p. 1-16.
5. Kossiakoff, A.A., *Annu. Rev. Biophys. Bioeng.*, 1983. **12**: p. 159.
6. Kossiakoff, A.A., *Basic Life Sci.*, 1984. **27**: p. 281.
7. Kossiakoff, A.A., *Annu. Rev. Biochem.*, 1985. **54**: p. 1195.
8. Wlodawer, A., *Prog. Biophys. Mol. Biol.*, 1982. **40**: p. 115.
9. Raghavan, N.V. and A. Wlodawer, *Methods Exp. Phys. Part C*, 1987. **23**: p. 335.
10. Timmins, P.A., *Physica B*, 1995. **213-214**: p. 26.
11. Helliwell, J.R., *Nature Struct. Biol.*, 1997. **11**: p. 874.
12. Niimura, N., *Curr. Op. Struct. Biol.*, 1999. **9**: p. 602.
13. Gutberlet, T., U. Heinemann, and M. Steiner, *Acta Cryst. D*, 2001. **D57**: p. 349.
14. Shu, F., V. Ramakrishnan, and B.P. Schoenborn, *Proc. Natl. Acad. Sci. USA*, 2000. **97**: p. 3872.
15. Coates, L., et al., *Biochemistry*, 2001. **40**: p. 13149.
16. Niimura, N., et al., *Nat.Struct.Biol.*, 1997. **4**: p. 909.
17. Ostermann, A., et al., *Biophys.Chem*, 2002. **95**: p. 183.
18. Bon, C., M.S. Lehmann, and C. Wilkinson, *Acta Cryst. D*, 1999. **55**: p. 978-987.
19. Wlodawer, A. and W.A. Hendrickson, *Acta Crystallogr.*, 1982. **A38**: p. 239-247.
20. Wlodawer, A., et al., *J. Mol. Biol.*, 1984. **180**: p. 301-329.
21. Borah, B., et al., *Biochemistry*, 1985. **24**: p. 2058.
22. Wlodawer, A., H. Savage, and G. Dodson, *Acta Crystallogr.*, 1989. **B45**: p. 99.
23. Habash, J., et al., *Acta Cryst. D*, 2000. **56**: p. 541-550.
24. Kurihara, K., et al., *J. Phys. Soc. Jpn. Suppl.*, 2001. **A 70**: p. 400-402.
25. Ostermann, A., et al., *Biophys Chem*, 2002. **95**(3): p. 183-93.
26. Longhi, S., et al., *J. Mol. Biol.*, 1997. **268**: p. 779-799.
27. Kuhn, P., et al., *Biochemistry*, 1998. **37**: p. 13446-13452.
28. Jelsch, C., et al., *Proc. Natl. Acad. Sci. USA*, 2000. **97**: p. 3171-3176.
29. Berisio, R., et al., *J. Mol. Biol.*, 1999(292): p. 845-854.
30. Miele, A.E., et al., *Acta Crystallogr D Biol Crystallogr*, 2003. **59**: p. 982.
31. Kachalova, G.S., A.N. Popov, and H.D. Bartunik, *Science*, 1999. **284**: p. 473.
32. Vojtechovsky, J., et al., *Biophys. J.*, 1999. **77**: p. 2153-2174.
33. Shu, F., V. Ramakrishnan, and B.P. Schoenborn, *PNAS*, 2000. **97**: p. 3872-3877.
34. Schmidt, M., B. Meier, and F. Parak, *J. Biol. Inorg. Chem.*, 1996. **1**: p. 532-541.
35. Kossiakoff, A.A. and S.A. Spencer, *Biochemistry*, 1981. **20**: p. 6462-6474.
36. Engler, N., et al., *PNAS*, 2003. **100**(18): p. 10243-10248.
37. Pebay-Peyroula, E., et al., *Structure*, 1995. **3**: p. 1051 - 1059.
38. Penel, S., et al., *Biochimie*, 1998. **80**: p. 543 - 551.
39. Coates, L., et al., *Biochemistry*, 2001. **40**(44): p. 13149-57.
40. Kalb (Gilboa), A.J., et al., *J. Appl. Cryst.*, 2001. **34**: p. 454-457.
41. Langan, P., G. Greene, and B.P. Schoenborn, *J. Appl. Cryst.*, 2004. **37**: p. 24-31.
42. Hanson, B.L., et al., *Acta Cryst. D*, 2004. **60**: p. 241-249.

Neutron Macromolecular Crystallography at the Spallation Neutron Source

AGENDA

Thursday, October 2, 2003

8:15 AM Continental Breakfast

General Introduction

8:45 AM Ray Teller: Welcome

8:50 AM Andy Mesecar: Introduction and Objective

Morning Session Chair, Andy Mesecar

Challenges in Structural Biology

9:00 AM Anthony Kossiakoff: Picking the Right Systems for the Right Problems

9:40 AM Alex Wlodawer: What Can We Learn From Neutron Crystallographic Studies of Enzymes and Other Proteins?

10:20 AM Coffee

Neutron Diffraction in Biology

10:45 AM Dean Myles: Recent Trends and Advances in Neutron Macromolecular Crystallography

11:15 AM Ian Anderson: The Spallation Neutron Source: Project Update

11:45 AM P. Thiyagarajan: *MaNDi* - Design of the Proposed Instrument at SNS

12:15 PM Lunch

Afternoon Session Chair, Anthony Kossiakoff

Hydrogens and Water in Macromolecular Systems

1:30 PM Alberto Podjarny: The Aldose Reductase Case: Ultra High Resolution X-Ray Structure and Preliminary Neutron Diffraction Results

2:10 PM John Helliwell: Getting the Complete Protein (Crystal) Structure; Concanavalin A and beta-crustacyanin Case Studies at Current Capabilities and Beyond

2:40 PM Martin Egli: Limits of XMC: DNA-Cation Interactions and Water-Nucleobase 'Stacking'

3:15 PM Coffee

3:45 PM Patrick Loria: Enzyme Dynamics, Catalysis, and Water

4:15 PM Michael Johnson: NMR, X-ray and Computational Analysis of Sickle Hemoglobin Aggregation Inhibitors -- Importance of Protonation States

4:45 PM Hong Guo: Quantum Mechanical/Molecular Mechanical MD Simulations of Cytidine and Adenosine Deaminase: Importance of Proton Positions

Drug Development

5:15 PM Chris Dealwis: Towards Elucidating Catalytic Mechanism of Dihydrofolate Reductase Using Neutron and Ultra High Resolution X-ray Crystallography

5:45 PM Geoffrey Stamper: Structure-Based Drug Design in the Pharmaceutical Industry: Is There a Role for NMC?

6:15 PM End of Session

7:00 PM Workshop Banquet (Argonne Guest House), Cash Bar Opens at 6:30 pm

MaNDi Workshop Schedule - continued

Friday, October 3, 2003

8:00 AM Continental Breakfast

Morning Session Chair, John Helliwell

Current Neutron Macromolecular Crystallography Research

8:30 AM Martha Teeter: Modeling Protein Dynamics with Neutron Crystallography at 1 Å Resolution

9:00 AM Peter Timmins: Detergent Structures in Membrane Protein Crystals

9:30 AM Petra Fromme: Neutron Diffraction on Membrane Protein Crystals

10:00 AM Coffee

10:30 PM Dan Carter: Counter-diffusion Methods in the Growth of Macrocrystals for Neutron Diffraction
11:00 AM Nobuo Niimura: Hydrogen and Hydration in Proteins and DNA Obtained by BIX-3 and BIX-4
11:30 AM Paul Langan: Protein Crystallography with Spallation Neutrons: Results from the PCS at Los Alamos
12:15 PM Lunch
1:30 PM **Discussion of the Scientific Case and Formation of an Instrumentation Development Team**
Discussion Chairs: Andy Mesecar, Alex Wlodawer, Art Schultz and Bernard Santarsiero
Discussion Topics:

- *MaNDi* Capabilities
- Scientific Case
- IDT Formation
- Strategy for Securing Funding
- Development of Proposals

3:30 PM Close of Workshop

WORKSHOP PRESENTATION SUMMARIES

Introduction and Objectives

Andrew Mesecar

The University of Illinois at Chicago, Center for Pharmaceutical Biotechnology

A brief history of Neutron Macromolecular Crystallography at the SNS was presented and outlined to explain the formation of the workshop and why the participants were there.

- 2000: Bunick proposed an instrument for NMC
- Dec 2000: workshop at Knoxville – Bunick
- March 2001: Scientific case to EFAC - Dealwis
- EFAC recommendation: NMC can be done on the single crystal instrument for chemical crystallography
- 2002 ACA meeting: Steering committee formed to push this effort
- Oct 2002: Mesecar presented scientific case to the EFAC
- EFAC: Positive response - requested a LOI by the community
- March 2003: Design of MaNDi presented by Schultz and Thiyaga at the EFAC
- EFAC was enthusiastic about the expected performance of MaNDi (Mar 03)
- Workshop at Argonne to build a science case (Oct 2003)

General workshop objectives were then outlined:

- Develop a plan to extend, broaden, and strengthen the neutron diffraction community
- Identify the experimental capabilities of MaNDi that the neutron diffraction user community requires or desires
- Develop a Scientific Case for MaNDi
- Form the Instrument Development Team (IDT)
- Develop Proposals for the SNS and Funding Agencies
- Develop a Strategy to Secure Funding

Picking the Right Systems for the Right Problems

Anthony Kossiakoff
The University of Chicago, Department of Biochemistry and Molecular Biology

Several examples of NMC were presented in the area of enzymology and neutron protein crystallography. The wealth of information that can be obtained from neutron density maps including the location of protons, exchangeable hydrogens, charge distributions, and protein dynamics was illustrated. Neutron macromolecular crystallography (NMC) was the key to solving the question about which of the two amino acids, Asp-102 or His-57 in trypsin, was the origin of the catalytic proton (Figure 1). A perspective on the current challenges for NMC is:

- Lack of neutron facilities for NMC in US as well as the world.
- Even with its advantages, NMC will be very challenging, especially in comparison to synchrotrons where one can collect data very fast.
- Emphasized quality over quantity - 1.5 Å resolution structure will be needed to address questions on protein function.
- For NMC to succeed and make a strong impact, systems have to be perdeuterated.

Structural opportunities at SNS:

- Systems where H atoms perform function, but structural details are lacking.
- H/D exchange: Powerful and unbiased method to locate exchangeable H's using the D_2O minus H_2O solvent difference maps (Kossiakoff, A. A., et al., Proteins (1992) 12, 223-236). High resolution data unequivocally determines which sites exchange and which do not. This provides information about protein dynamics, structural strength, and changes in time-averaged structure, which tells you where weak points in secondary structure are located and which are sites of local unfolding. Perdeuteration of proteins will take this technique to a new level.
- Hydroxyl orientations are the most valuable probe to assess electrostatic/van der Waals forces in protein packing (J. Mol. Biol. (1995) 250, 553-570.)
- Assignment of charge distributions using X-N difference maps, especially using perdeuterated crystals in D_2O and H_2O.

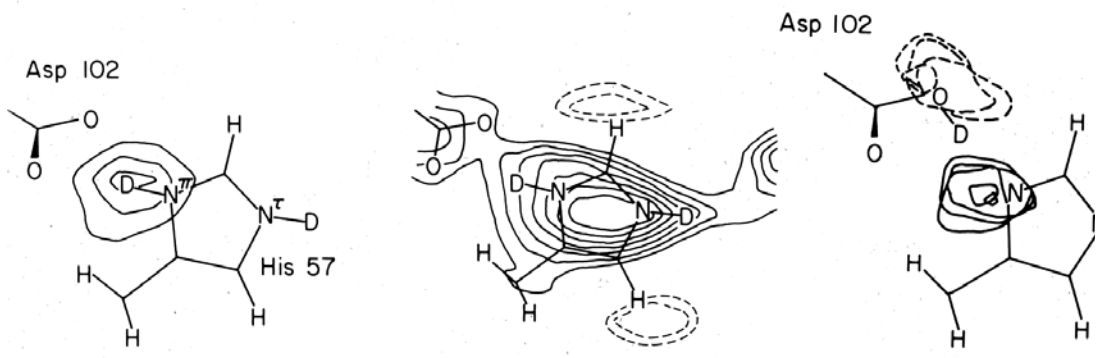

Figure 1. The serine protease charge-relay system.

What Can We Learn from Neutron Crystallographic Studies of Enzymes and Other Proteins?

Alex Wlodawer
National Cancer Institute, National Institutes of Health

Examples from his neutron macromolecular crystallography studies of BPTI, insulin, and RNase A at NIST were presented. BPTI, ribonuclease A, and insulin crystals soaked in D_2O provided information on the exchangeable H atoms. Most protective amide H atoms were found to be involved in H-bonds in beta sheets and some in helices.

Structural Opportunities at the SNS:

- HIV protease (PR) Apoenzyme. Within the active site of aspartic proteases, the catalytic residue is presumable a water molecule that is bonded between two aspartic acids. Knowledge of the exact hydrogen positions is crucial for fully understanding the mechanism of this important enzyme. The enzyme is symmetric at the active site yet it works on an asymmetric substrate. The enzyme has to become asymmetric when active.

- Protonation of residues was seen in neutron density maps of endothiapepsin at 2 Å resolution. Ultra-high resolution x-ray structures to 0.93 Å reveal the protonation of the inhibitor statine but not the two Asp residues (Cooper). There is a strong need for high-resolution neutron data for learning about the function of this enzyme.

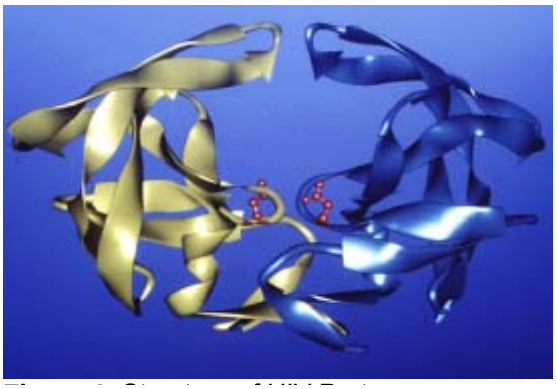

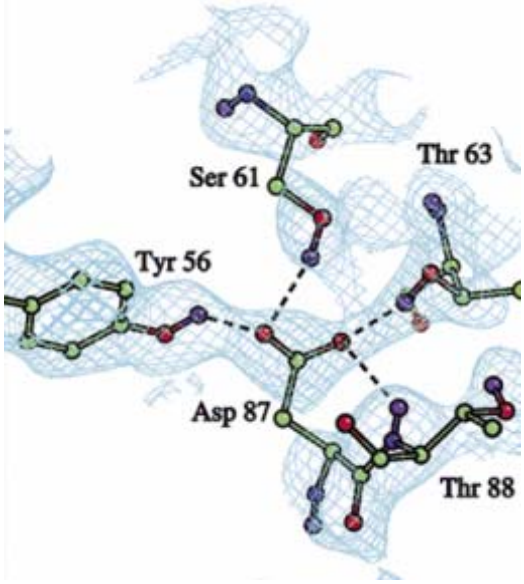

Figure 2. Neutron density map of endothiapepsin.

Recent Trends and Advances in Neutron Macromolecular Crystallography

Dean Myles
Director, Center for Structural Molecular Biology, Oak Ridge National Laboratory

Hydrogen bonding interactions mediate much of biological structure and function and the determination of the hydrogen atom and water substructure in biological molecules can provide fundamental insights into the key processes of life. Whilst much of our knowledge of the 3-dimensional structure of proteins has been provided by x-ray crystallography, hydrogen atoms can only be seen (if at all) by x-rays if they are well-ordered and if data are available at atomic resolutions (<1.2Å). The positions of more mobile and more labile hydrogen atoms can therefore be exceedingly difficult to locate and must usually be determined by other techniques. High-resolution neutron crystallography can complement x-ray structure determination by enabling hydrogen atoms and water positions to be located that cannot be seen by x-ray analysis alone, thus allowing a more complete description of the structure (and dynamics) to be developed.

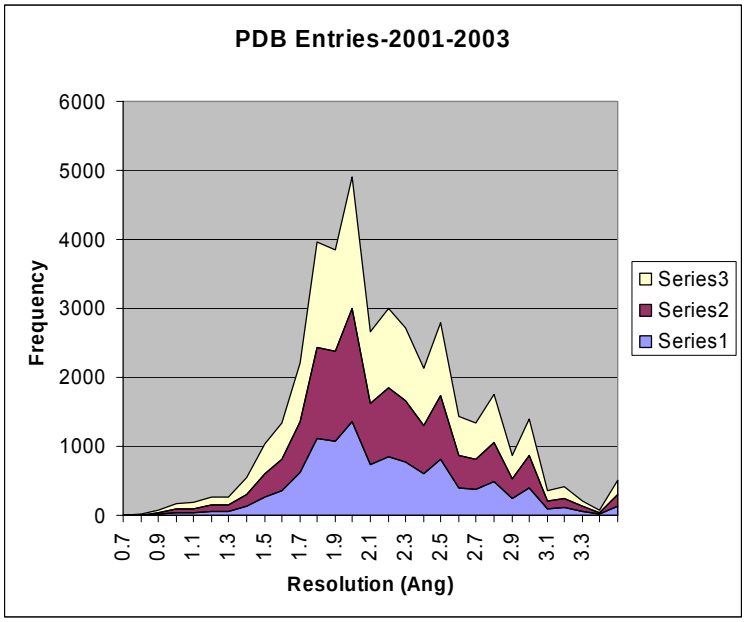

Figure 1. Graph showing cumulative frequency of x-ray protein structures deposited in the PDB as a function of resolution. Hydrogen atoms can only be located in x-ray structures if data extend below 1.2Ang resolution (marked in Blue) – neutrons show information on H/D positions at below 2.5Ang resolution (marked in Red).

Although neutron protein crystallography has provided key and fundamental insights into enzyme mechanism, hydrogen bonding interactions and the water structure in a number of small protein systems, wider application has been seriously hampered by the relatively low neutron flux available at most neutron facilities and by the limited capacity of the instrumentation to exploit it. For example, the available neutron fluxes are many orders of magnitude lower than x-ray fluxes at third generation synchrotrons, *c.f.* neutron 10^{15} s^{-1} m^{-2} $ster^{-1}$ versus x-ray 10^{33} at the APS. The introduction of more efficient neutron diffractometers that use large 2-dimensional image plate detector systems at reactor neutron sources and the recent commissioning of a spallation neutron source protein crystallography station (PCS) at LANL have provided step function improvements in performance that promise to open up the field to more demanding problems in biology.

The LADI instrument at the Institute Laue Langevin (ILL) was designed to speed up data collection for protein crystallography. LADI uses Laue geometry to provide a more rapid and efficient survey of reciprocal space, maximizing the flux on the sample by using all available neutrons within a broad spectral range ($\delta\lambda/\lambda$ > 20%) and stimulating very large numbers of reflections ($\propto \delta\lambda/\lambda$) at all possible wavelengths ($\lambda_{min} > \lambda > \lambda_{max}$) over many different angles. The layout of the detector is shown in Figure 2.

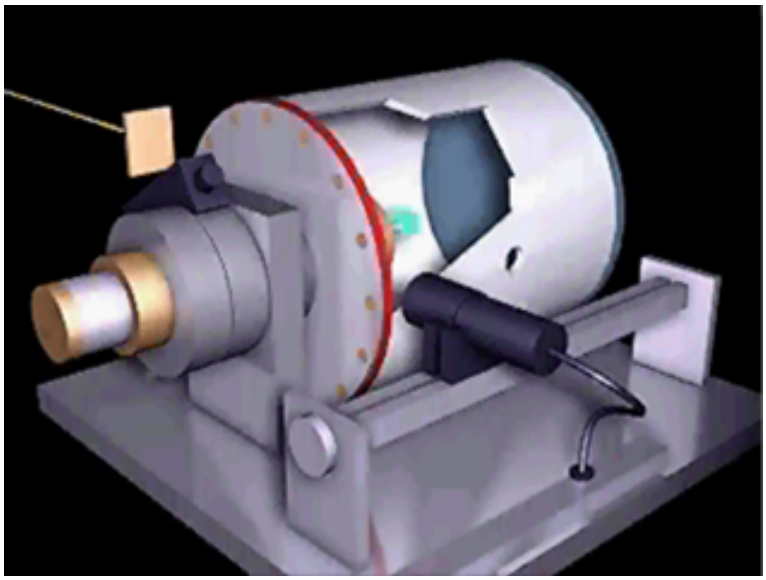

Figure 2. Detector Geometry

The sample is centered on the rotation axis of a cylindrical camera. Four Gd_2O_3 doped BaF(Br.I):Eu^{2+} Fuji image plate screens (400x200mm) are bonded onto the outer surface of the drum (318 mm diameter and 400 mm in length), subtending a very large solid angle of detection of 288° around and 103° across the drum. Reciprocal space is surveyed by rotating the sample about the cylinder axis in steps. Each setting covers a large and continuous volume of reciprocal space and the number of steps required is dependent upon the wavelength (λ) and bandpass ($d\lambda/\lambda$) of the incident neutron beam, the symmetry and unit cell volume of the crystal and upon the required resolution of the data. The combination of broad bandpass quasi-Laue geometry with a large cylindrical area detector provides 10-100 fold gains in efficiency compared with conventional neutron diffractometers. A typical quasi-Laue diffraction image is shown in Figure 3.

This has made feasible studies of larger biological complexes and smaller crystals than previously possible and has re-defined the role and expectations of neutron protein crystallography. Current studies are addressing questions of important biological significance concerning enzymatic mechanism, ligand-binding interactions, solvent effects, structure dynamics and their implications. The ability to determine the position *and* orientation of complete D_2O water molecules in protein crystals at physiological meaningful temperatures has led to a picture of water molecules forming an extended constantly fluctuating network covering the protein surface. Many biological processes involve the transfer of hydrogen, and neutron

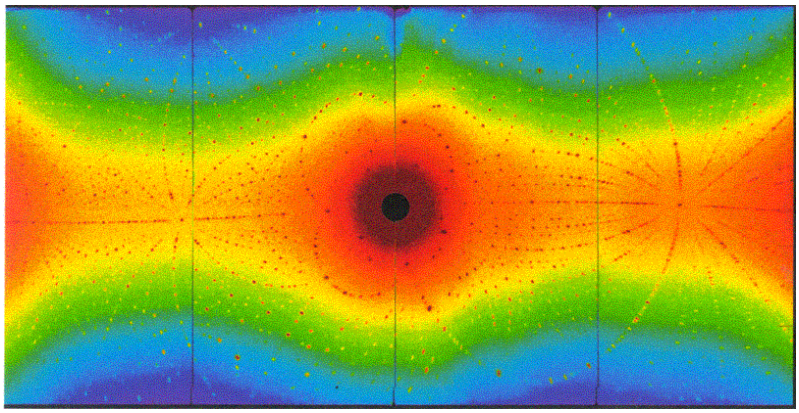

Figure 3. Quasi-Laue diffraction image

diffraction can allow the position of important hydrogen atoms to be determined. Results from a number of LADI studies concerned with enzymatic mechanisms have shown that H/D locations determined at medium resolution (~2 Å) on LADI have been shown to provide additional information that could not be determined from atomic resolution (<1.2 Å) synchrotron x-ray data alone. For example, the 2.0 Å neutron structure of an aspartic protease, Endothiapepsin, in a transition state analogue complex, directly revealed the key hydrogen positions at the catalytic site of the protein, helping resolve the long-standing controversy over the catalytic mechanism in this important family of enzymes (Figure 4) (Coates et al, 2001).

The potential of the instrument for more demanding applications is being assessed and explored, notably in analysis of large unit cell systems and in cryo-crystallography. Diffraction data measured from extremely large unit cell systems, such as the cubic crystal form of concanavalin A/methyl alpha-D-glucoside complex ($I2_13$, a = 167 Å) (ref) and from the large iron storage protein complex ferritin ($F432$, a = 183 Å), have demonstrated the potential to collect useful data to medium resolutions (3.5 Å) but highlight the problems of resolving densely packed reflections on the present (fixed radius) detector. The ferritin complex contains 24 protein subunits that assemble to form a capsid with a combined molecular weight of 450,000 Dalton - an order of magnitude bigger than anything envisaged in the design stage of LADI.

A number of low temperature studies (12 K) have been completed and the results are being critically compared with cryogenic x-ray (typically 100 K) and room temperature x-ray and neutron structures. Preliminary results suggest that the neutron diffraction at cryogenic temperatures yields fuller information on the water structure at the protein surface (see Helliwell et al.)

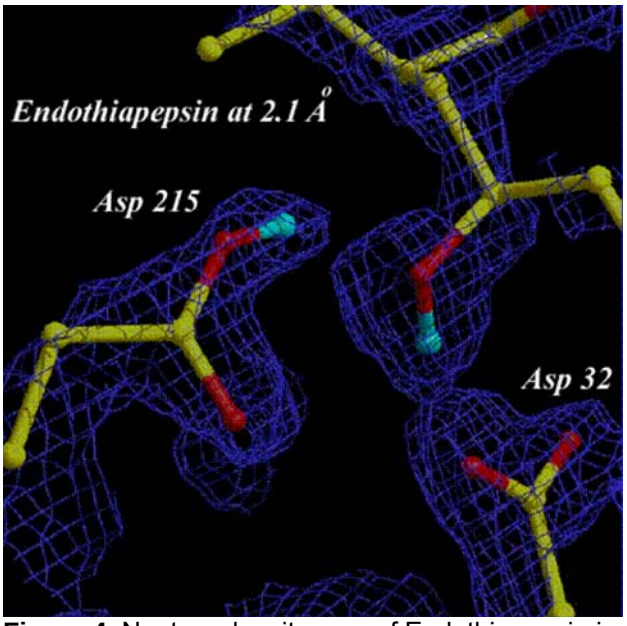

Figure 4. Neutron density map of Endothiapepsin in a transition state analogue. (Coates et al, 2001).

These technical advances have delivered 10-100 fold improvements in efficiency for small protein systems, but even at the most powerful facilities the relatively large crystal volumes of 1 – 2 mm^3 that are required still remains a major hurdle. One way to help address this is by manipulating and "improving" the scattering behavior of the sample. Hydrogen has a large incoherent scattering cross section (80.27 barns) that dominates the background in neutron scattering experiments from biological material, and thus hides weak reflections. The signal to noise in experiments can be significantly improved by replacing hydrogen with deuterium (2.05 barns).

Fully D-labeled protein can be produced most readily by over-expression of the target protein in a microbial system that has been adapted to growth in a fully deuterated environment (100% D_2O and deuterated carbon sources). For a typical protein crystal, the gain approaches a factor of 10 on full (per)deuteration. The ILL and EMBL Outstation in Grenoble have recognized this huge benefit to neutron diffraction and have established a Deuteration Laboratory that allows users to produce fully D-labeled protein within a few weeks. The first successful external user of this facility was the group of Alberto Podjarny (Strasbourg), who has produced fully

perdeuterated aldose reductase. Diffraction experiments performed on LADI have produced data of good quality that extend beyond 2.5 Å resolution from a crystal of 0.14 mm^3 size.

Life scientists are now presenting state of the art problems in biology that challenge the current capabilities of these instruments and further order of magnitude gains in performance would now be decisive in opening new fields of research. The further developments planned at existing facilities will bring significant advance in capabilities, whilst the new instruments planned at the next generation spallation neutron sources will provide unprecedented capability for neutron analysis of biological macromolecules such as proteins and DNA/RNA and their complexes.

The Spallation Neutron Source: Project Update

Ian Anderson
Director, Experimental Facilities Division, Spallation Neutron Source

At SNS neutrons will be produced by the short pulsed 1-GeV proton beam bombarding on a liquid mercury target. For every proton striking the nucleus, 20 to 30 neutrons are expelled. SNS will produce pulses that each contain neutron intensity 50 to 100 times higher than that obtainable from the best continuous source. Intense, short-pulse neutron beams from accelerator-based sources make it possible to perform time-of-flight analysis of the scattered neutrons and to study a wide range of scientific problems and perform real-time analysis. Four types of moderators will be available for delivering neutrons with slightly different spectra. Most appropriate moderators for NMC would be coupled liquid hydrogen and decoupled liquid hydrogen moderators that produce cold neutrons with a peak around 3 Å. Flux at the coupled hydrogen moderator will be about 8 times that at the decoupled moderator. This is due to the long tail in the emission time of neutrons of a given wavelength. The target is designed for 2 MW and will be upgraded at a later stage.

The current layout of the experimental facility is shown in Fig. 1. It can be seen that most of the beam lines have been assigned to different scientific groups and only a few are available for which several scientific groups are competing. Given the unique information that the NMC can provide to structural biology and the advancements made during the past decades in the areas of neutron production, instrumentation, molecular biology techniques, deuteration and crystallization, it is crucial that the US macromolecular crystallography community take advantage of the highest neutron flux that will be available at SNS. The instrument design team should evaluate the performance of a diffractometer at different moderators so that the best diffractometer for NMC can be built at SNS to address the scientific challenges for the community. It is important that the instrument design simulate data for real crystals so that the performance of the instrument at various configurations can be meaningfully compared.

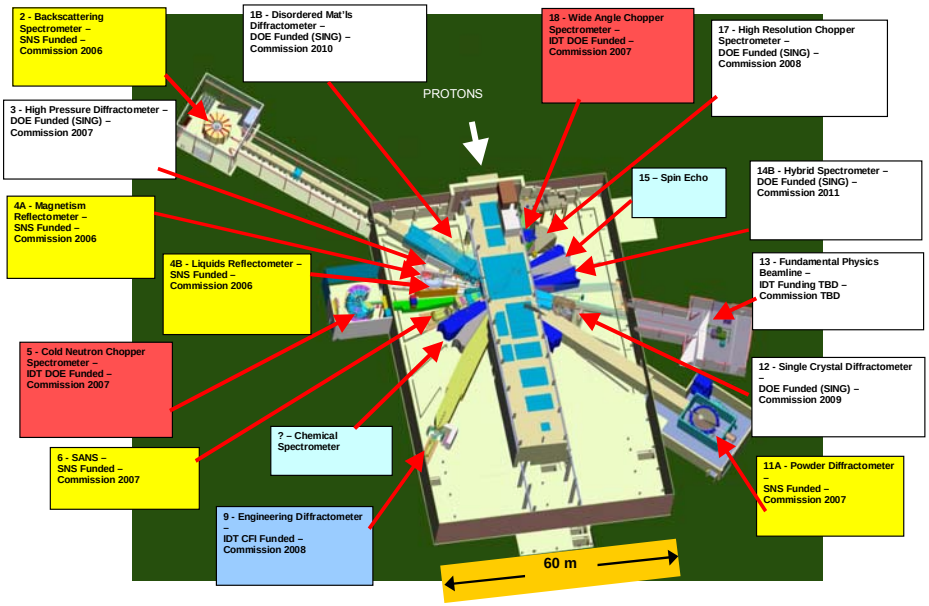

Figure 1. Instrument Layout at the Experimental facility at the SNS

MaNDi – Design of the Proposed Instrument at SNS

P. Thiyagarajan
Intense Pulsed Neutron Source (IPNS), Argonne National Laboratory

Neutron macromolecular crystallography (NMC) can provide accurate information on the positions of the protons and water molecules at active sites of enzymes even at a moderate 2.0 Å resolution. In order to exploit the high neutron flux (8 times ISIS and 14 times LANSCE peak thermal neutron flux and 50 times ILL) that will become available by 2006 at the Spallation Neutron Source (SNS), and to leverage the enormous interest shown by the macromolecular crystallography community, it is proposed to develop a dedicated best-in-class high throughput and high resolution time-of-flight single crystal macromolecular neutron diffractometer (*MaNDi*) at the SNS high power target station. *MaNDi* has been designed to be able to collect a full hemisphere of Bragg data with a resolution of 1.5 to 2 Å, on a macromolecular crystal with a lattice constant up to 150 Å, in a few days to a week. A thorough evaluation of the instrument performance at different moderators using analytical equations and Mote Carlo simulations shows that the decoupled hydrogen moderator at SNS would be the best choice for *MaNDi*. State-of-the-art neutron guides and optics will be used for efficient beam transport and optimization of collimation at the sample. A curved guide section in the middle will steer the beam gently so that the crystal will not view the moderator that emits a large amount of fast neutrons and γ-rays that can cause damage to the crystal. The high throughput is accomplished by the use of a wide band width of cold neutrons (1.8 Å < λ < 4.5 Å) sorted by time-of-flight and an array of high resolution position-sensitive area detectors covering a large solid angle. The performance of *MaNDi* has been calculated (Figure 1) based on counting times necessary to obtain a complete data set for protein crystals with different unit cell sizes, by taking into consideration the data precision, Debye-Waller factor, flux, and incoherent background.

For crystals of deuterated proteins, with a 150 Å unit cell and a volume of 0.125 mm^3, a complete data set for a d_{min} = 2 Å can be obtained from *MaNDi* in a few days (Fig. 1). Our calculations indicate that a similar amount of beam time will be required to obtain data of similar precision for 1 mm^3 normal protein crystals.

The counting times for a d_{min} = 1.5 Å for the above systems will be an order of magnitude higher than that for d_{min} = 2.0 Å. For instance, counting times for crystals with a 60 Å unit cell axis will require about 7 days, while those with a 100 Å unit cell axis will require about 30 days to obtain data of similar precision. Current instruments for NMC require counting times that are 10 to 50 times longer than the above times. Furthermore, *MaNDi* will enable studies of crystals with larger lattice constants than is possible at the current facilities for NMC. It is expected that the unprecedented high data rates and resolution obtainable with *MaNDi* for the high resolution NMC will open up new avenues thus far not available and will greatly advance the fields of structural biology and enzymology.

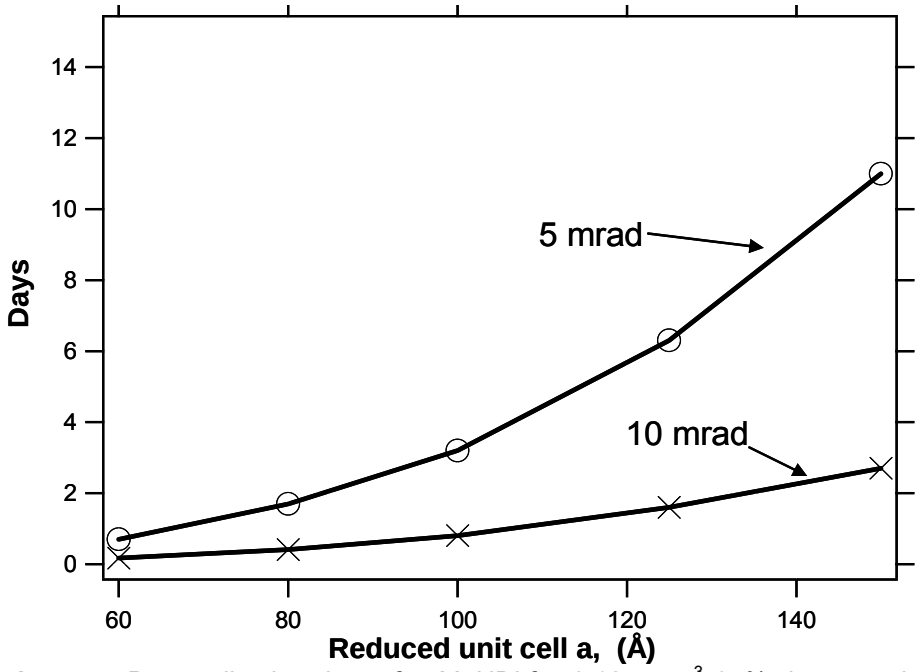

Figure 1. Data collection times for *MaNDi* for 0.125 mm^3 95% deuterated protein crystals for a d_{min} = 2 Å with different unit cell dimensions. The flux on the sample can be increased at the expense of higher beam divergence (10 mrad vs. 5 mrad). However, for crystals that can tolerated the higher divergence, the data collection time is significantly reduced.

The Aldose Reductase Case: Ultra High Resolution X-ray Structure and Preliminary Neutron Diffraction Results

Alberto Podjarny
IGBMC, Department of Structural Biology

Aldose reductase (AR; EC 1.1.1.21) is a 316-amino acid enzyme that reduces a wide range of substrates, such as aldehydes, aldoses, and corticosteroids. As it reduces D-glucose into D-sorbitol, it is believed to be involved in degenerative complications of diabetes, since the accumulation of excess sorbitol resulting from diabetic hyperglycemia has been shown to play a role in the development of diabetic complications such as retinopathy, neuropathy and nephropathy (Yabe-Nishimura 1998; Oates and Mylari 1999).

Several x-ray (Rondeau et al. 1992; Wilson et al. 1992; Wilson et al. 1993; Tete-Favier et al. 1995; Urzhumtsev et al. 1997), site-directed mutagenesis (Tarle et al. 1993; Bohren et al. 1994; Schlegel et al. 1998; Schlegel et al. 1998) and modeling studies (Lee, Chen et al. 1998) of AR, its enzymatic mechanism (Cachau et al. 2000) and its inhibitor binding (Singh et al. 2000) have been carried out. AR folds as a $(\beta/\alpha)_8$ barrel with the $NADP^+$ nicotinamide ring buried at the bottom of the active site cleft of approximate dimensions 9 Å (diameter) and 11 Å (depth). Our previous crystallographic studies, done at 2 Å resolution (Urzhumtsev et al. 1997), showed that AR inhibitors of the carboxylic acid (e.g., tolrestat) and of the spirohydantoin (e.g., sorbinil) families bind at the catalytic site, making hydrogen bonds with Tyr 48, His 110, and Trp 111.

In the presented work, we were able to push the limits of the resolution of x-ray diffraction (to 0.62 Å) for the structure of the ternary complex of human aldose reductase, its cofactor $NADP^+$ and the inhibitor IDD 594 refined at 0.66 Å resolution, the highest resolution ever reported so far for a monomeric enzyme with a molecular weight of 36 kDa and no S-S bonds (Howard et al., in press).

As shown in Figure 1, the electron density maps give a very clear image of the inhibitor and of its interactions with the enzyme.

The high resolution structure is important for drug design, as it explains

1) The specificity ratio (1100) of Aldose vs. Aldehyde reductase: Aldehyde has a Tyr in the 113 position
2) The need for bromine in the aromatic ring in the specificity pocket. For example, chlorine (which

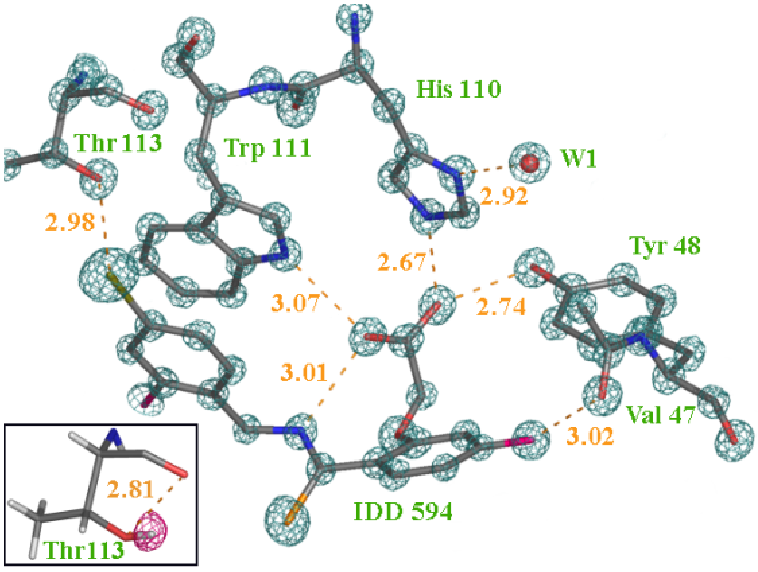

Figure 1: σA weighted 2Fo-Fc maps, contoured blue at 4.15 e/Å^3 (4σ) together with color-coded atoms (same code as Figure 2b). The respective peak volumes correlate well with the atomic number. Insert: Close view of Thr 113, superimposed with the Fo-Fc (Omit-H, σA-weighted, magenta contours at 0.25 e/Å^3 (2.5σ.showing the position of the hydrogen atom which makes an internal H-bond.

does not have an electropositive character on the nodal plane) does not bind as well.

3) The non competitive character of inhibitors; substrates bind to NADPH complex, negatively charged inhibitors bind to the anionic site defined by His 110, Tyr 48 and NADP+ coenzyme.

The ultra-high resolution structure shows 54% of the total number of hydrogen atoms. As shown in Figure 2, the possibility of seeing a hydrogen atom is linearly dependent of the B-factor of the bound atom.

In particular, the ultra high resolution maps have shown the protonation states of His 110 (Figure 3) and the position of the H-atom of Thr 113 (Insert, Figure 1).

The determination of protonation states and H-atom positions is essential for understanding the critical contacts of the inhibitor, in particular:

1) The H of OG-Thr 113 is making an internal H-bond, and therefore the interaction with the Bromine is purely electrostatic with a very short distance (2.98 Å).
2) His 110 is singly protonated at the position Ne2, and thus the charged inhibitor makes H-bonds with His 110 and Tyr 48 and electrostatic interaction with NADP+.

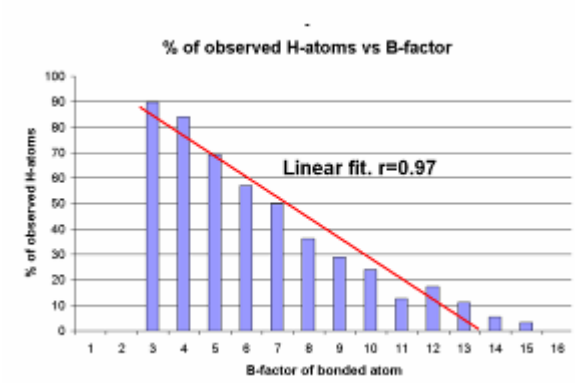

Figure 2. Histogram of percentage of observed hydrogen atoms as a function of the B factor of the bonded heavy atom.

To see more hydrogen atoms, and in particular to determine protonation states of critical residues for catalysis and inhibitor binding, neutron studies have been started. Fully perdeuterated protein (verified by mass spectrometry) has been produced through collaboration with the ILL (Grenoble), crystallized at the IGBMC and measured at the LADI instrument. The resolution limit of the neutron diffraction was 2.6 Å for a 0.14 mm^3 crystal, a clear improvement from the resolution of 4.5 A observed with hydrogenated protein exchanged in heavy water.

The table shows the preliminary results of a partial treatment of the neutron data (12 frames out of 33). A clear but weak signal can be observed up to 2.6 Å.

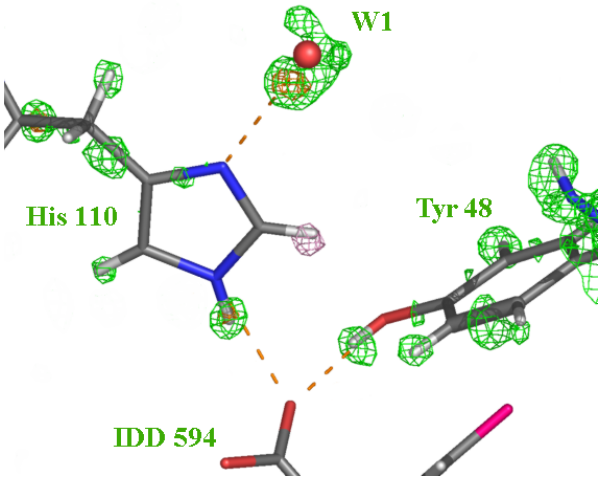

Figure 3: σA-weighted Fo-Fc map of the active site region with omitted hydrogen atoms, contoured gold at 0.44 e/Å^3 (4.0σ), green at 0.31 e/Å^3 (2.8 σ), and pink at 0.11 e/Å^3 (1.0σ). The single protonation of His 110 at NE2 is clearly visible, while the strong peak near the W1 water molecule indicates that W1 is the proton donor in the W1-His110 ND1 hydrogen bond. The hydrogen atoms (white) are observed in the maps, as interpreted by SHELXL. The 1.0σ contour is restricted to the neighborhood of the H atom.

Dmin		Rmerge		I / Sig		
6,97		**0,076**		8,4		
5,66		**0,107**		6,4		
4,89		**0,1**		6,8		
4,37		**0,096**		6,6		
3,98		**0,112**		6,2		
3,68		**0,118**		6,1		
3,44		**0,133**		5,5		
3,25		**0,123**		6		
3,08		**0,15**		5		
2,93		**0,154**		2,2		
2,81		**0,13**		5,5		
2,7		**0,159**		4,7		
2,6		**0,201**		2,3		
overall		**0,12**		**3,8**		

Conclusions and Perspectives

Ultra high resolution crystallography has identified critical protonation states and solvation, but not all H-atoms are visible.

Neutron structure determination is currently under way, as well as efforts to produce larger crystals, to obtain neutron diffraction at atomic resolution.

References.

Bohren, K. M., C. E. Grimshaw, et al. (1994). "Tyrosine-48 is the proton donor and histidine-110 directs substrate stereochemical selectivity in the reduction reaction of human aldose reductase: enzyme kinetics and crystal structure of the Y48H mutant enzyme." Biochemistry **33**(8): 2021-32.

Cachau, R., E. Howard, et al. (2000). "The subatomic resolution structure of human aldose reductase shows the catalytic mechanism." Journal de Physique IV France, 10, 3-13, (2000).

Howard, E., R. Sanishvili, R.E. Cachau, A. Mitschler, B. Chevrier, P. Barth, V. Lamour, M. Van Zandt, E. Sibley, C. Bon, D. Moras, T. R. Schneider, A. Joachimiak & A. Podjarny. "Ultra-high resolution drug design I: Human aldose reductase – inhibitor complex at 0.66 Å shows experimentally protonation states and atomic interactions which have implications for the inhibition mechanism" Proteins: Struct. Funct. Genet. in press

Lee, Y. S., Z. Chen, et al. (1998). "Molecular modeling studies of the binding modes of aldose reductase inhibitors at the active site of human aldose reductase." Bioorg. Med. Chem. **6**: 1811-1819.

Oates, P. J. and B. L. Mylari (1999). "Aldose reductase inhibitors: therapeutic implications for diabetic complications." Expert Opin Investig Drugs **8**: 2095-2119.

Rondeau, J. M., F. Tete-Favier, et al. (1992). "Novel NADPH-binding domain revealed by the crystal structure of aldose reductase." Nature **355**: 469-472.

Schlegel, B. P., J. M. Jez, et al. (1998). “Mutagenesis of 3 alpha-hydroxysteroid dehydrogenase reveals a "push-pull" mechanism for proton transfer in aldo-keto reductases.” Biochemistry **37**: 3538-3548.

Schlegel, B. P., K. Ratnam, et al. (1998). “Retention of NADPH-linked quinone reductase activity in an aldo-keto reductase following mutation of the catalytic tyrosine.” Biochemistry **37**: 11003-11011.

Singh, S. B., M. S. Malamas, et al. (2000). “Molecular Modeling of the Aldose Reductase-Inhibitor Complex Based on the X-ray Crystal Structure and Studies with Single-Site-Directed Mutants.” J. Med. Chem. **43**: 1062-1070.

Tarle, I., D. W. Borhani, et al. (1993). “Probing the active site of human aldose reductase. Site-directed mutagenesis of Asp-43, Tyr-48, Lys-77, and His-110.” J. Biol. Chem. **268**: 25687-25693.

Tete-Favier, F., P. Barth, et al. (1995). “Aldose Reductase from Pig Lens.” Eur. J. Med. Chem. **30S**(30): 589s-603s.

Urzhumtsev, A., F. Tete-Favier, et al. (1997). “A 'specificity' pocket inferred from the crystal structures of the complexes of aldose reductase with the pharmaceutically important inhibitors tolrestat and sorbinil.” Structure **5**: 601-612.

Wilson, D. K., K. M. Bohren, et al. (1992). “An unlikely sugar substrate site in the 1.65 A structure of the human aldose reductase holoenzyme implicated in diabetic complications.” Science **257**(5066): 81-4.

Wilson, D. K., I. Tarle, et al. (1993). “Refined 1.8 A structure of human aldose reductase complexed with the potent inhibitor zopolrestat.” Proc. Natl. Acad. Sci. U S A **90**(21): 9847-51.

Yabe-Nishimura, C. (1998). “Aldose reductase in glucose toxicity: a potential target for the prevention of diabetic complications.” Pharmacological Review **50**: 21-33.

Getting the Complete Protein Crystal Structure: Concanavalin A and Crustacyanin: Case Studies at Current Capabilities and Beyond

John Helliwell
University of Manchester

Whilst the determination of many of the hydrogens in proteins is now feasible with ultra-high, atomic resolution x-ray macromolecular crystallography (XMC), the mobility of particular hydrogens can still kill their diffraction signal. But, since neutron protein crystallography determination of deuteriums at around 2 Å or better resolution matches that at 1.0 Å by XMC, then more mobile hydrogens are still determinable by neutron macromolecular crystallography (NMC) [1]. Indeed the bound solvent is a whole category of deuterium atoms that are more efficiently sought by neutron techniques [1].

One of the largest proteins that has been studied by both UHRXMC (0.94 Å) [2] NMC (2.4 Å) [1] is the protein concanavalin A (Figure 1). As an illustration of the need for further neutron facilities development, two further case studies were given. The first case was that of concanavalin A with bound glucoside. This system offers very large crystals (up to 100 mm^3 in volume), but the unit cell (space group $I2_13$, a = 168 Å) means that the LADI neutron data can be measured to only ~4 Å resolution, insufficient for detailed structural analysis [3].

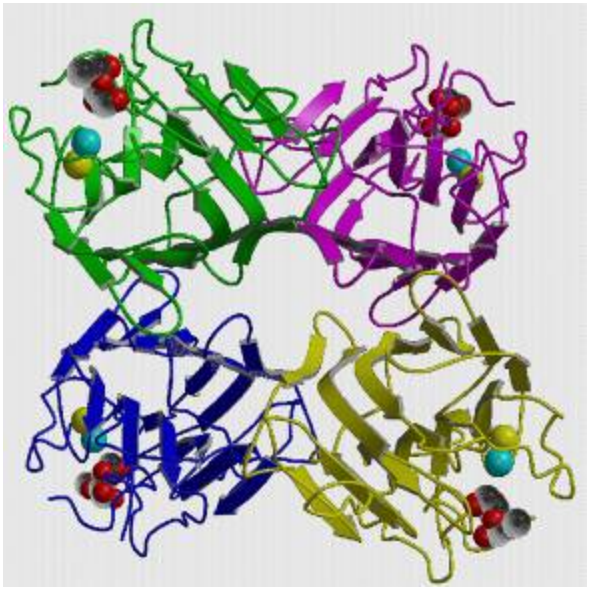

Figure 1. Structure of concanavalin A tetramer (100 kDa).

In a final case study, well beyond current neutron facility capability, was the case described of the structure of the lobster shell coloration protein crustacyanin, which binds astaxanthin. This structure was determined using XMC to 3.2 Å resolution [4] (Figure 2), and involves a bound water molecule at one end of each of the two carotenoids (Figure 3). The very short H-bond distances of the bound water oxygens to the keto oxygens of the astaxanthin end rings (2.65 Å and 2.7 Å) arouses an interest in further defining the state of these bound waters especially with respect to a biophysical understanding of the molecular basis of the bathochromic shift effect. The crustacyanin crystal sample size and the unit cell size put it completely outside the capabilities of the current diffractometers for NMC. However, enhancements of LADI at ILL are planned and the proposed MaNDi on SNS offers important further gains to global NMC users (as well as a vital USA NMC capability).

One hopes and dreams then of new protein crystal sample cases being brought within the range of application of NMC capabilities. A very recent breakthrough on the sample treatment is that of successful freezing of large neutron-sized protein crystals of concanavalin A as an example from which high resolution x-ray and neutron diffraction data were collected [5].

This has allowed improved nuclear density definition and opens up freeze trapping time-resolved neutron protein crystal structure studies to be envisaged.

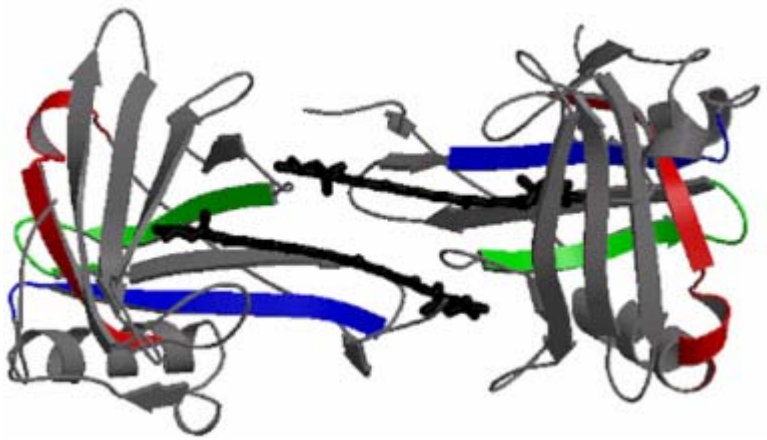

Figure 2. Structure of crustacyanin.

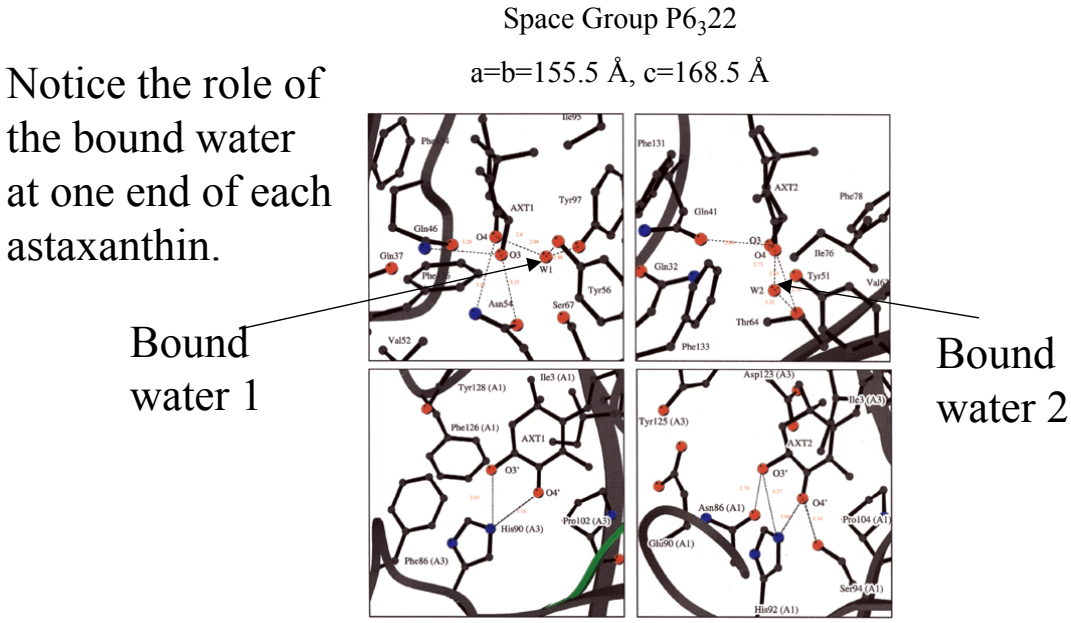

Figure 3. Bound water molecules in the active site of crustacyanin.

References.

1. Habash, J., Raftery, J., Nuttall, R., Price, H. J., Wilkinson, C., Kalb (Gilboa), A. J. & Helliwell, J. R. (2000) Acta Cryst. D56, 541-550.
2. A.Deacon, T.Gleichmann, A.J. Kalb (Gilboa), H.J.Price, J.Raftery, G.Bradbrook, J.Yariv and J.R.Helliwell (1997) J. Chem. Soc. Faraday Trans.
24, 4305 4312.
3. Kalb (Gilboa), A. J., Myles, D. A. A., Habash, J., Raftery, J. & Helliwell, J. R. (2001).J. Appl. Cryst. 34, 454-457.
4. Cianci, M., Rizkallah, P J, Olczak, A., Raftery, J., Chayen, N E and Helliwell, J. R. (2002) PNAS. USA 99, 9795-9800.
5. M Blakeley, A J K Gilboa, J R Helliwell and D A A Myles (2003) submitted to J Appl Cryst.

Limits of X-ray Macromolecular Crystallography: DNA-Cation Interactions and Water Nucleobase "Stacking"

Martin Egli
Department of Biochemistry, Vanderbilt University

Two current topics in the area of nucleic acid structure and function were presented. The first concerns the reliable detection of ordered alkali metal ions (i.e. Na^+ and K^+) coordinated to DNA and RNA molecules in crystals. The other is the precise mode of interaction between water molecules and hetero- (the base moieties of nucleic acids and certain amino acid side chains, i.e. His and Trp) and homo-nuclear (Phe or benzene as the simplest model) aromatic systems. Although both topics have been studied extensively with x-ray macromolecular crystallography (XMC) this technique cannot provide a complete understanding of either.

Due to the poly-anionic nature of DNA and RNA, metal ions play a crucial role in the thermodynamic stability and conformation of nucleic acids. It is clear that more complicated folding motifs such as those encountered in G-rich DNA quadruplexes (**Figure 1**) or in the tertiary structure of large RNA molecules are often associated with metal ion coordination and Mg^{2+} is of particular importance in this regard. By comparison, metal ions probably play a less important role in shaping the overall structure of simple nucleic acid duplexes. X-ray crystallography can shed light on the whereabouts of so-called site-bound or ordered metal ions. However, it does not give any clues about the localizations of diffuse cations although these can be of significance for the thermodynamic stability of nucleic acids.

With ever more high-resolution crystal structures of DNA and RNA becoming available our understanding of the preferred coordination modes of metal ions and the potential effects on nucleic acid structure has greatly improved. In addition, solution NMR and computational simulations (molecular dynamics, MD) have also shed light on localizations of metal ions surrounding nucleic acid molecules. However, in spite of the fact that ions are often visible in structures of nucleic acids it is not straightforward to determine how they affect the structure. Thus, many metal ions visible in crystal structures may simply stabilize the crystal lattice by bridging phosphate groups from neighboring molecules.

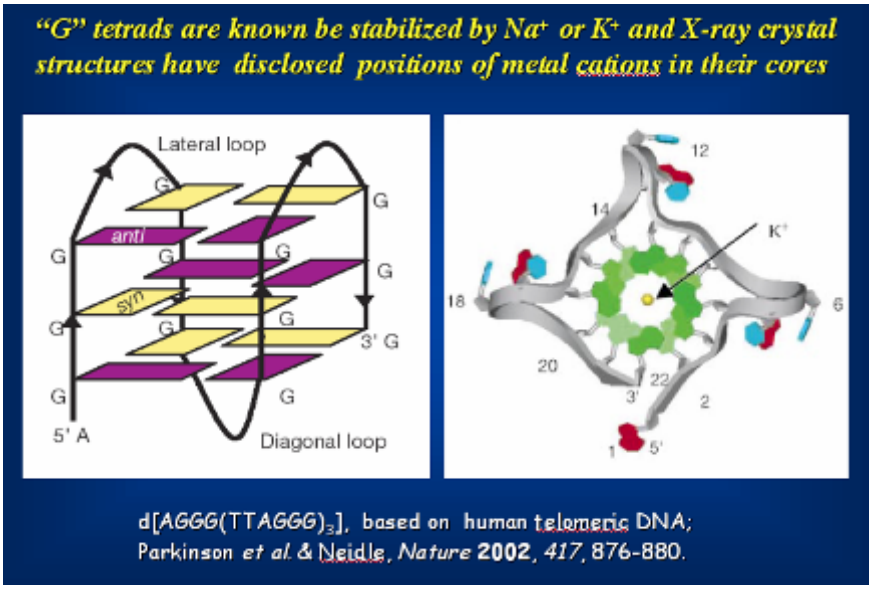

Figure 1

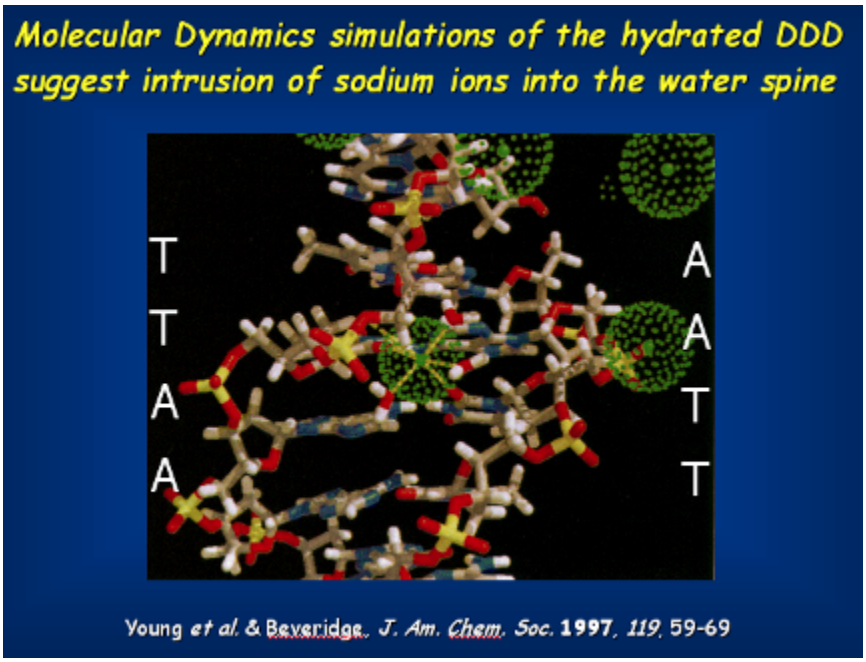

Figure 2

Recently, MD simulations indicated that Na^+ ions invade the so-called spine of hydration in the minor groove of the DNA dodecamer with sequence CGCGAATTCGCG (the Dickerson-Drew Dodecamer or DDD) (**Figure 2**). The presence of a single metal ion at the central ApT was subsequently confirmed by the structure of a DDD based on crystals soaked in Rb^+, a heavier alkali metal ion that is easier to detect in electron density maps than Na^+ (**Figure 3**). Subsequently, it was demonstrated that high-resolution structures of DNA crystals soaked in a variety of alkali metal ion solutions of different concentration in combination with single wavelength anomalous dispersion experiments provided more reliable information on metal ion binding sites than high-resolution structures alone (**Figure 4**). Nevertheless, Na^+ ions remain

difficult to locate as the scattering contributions of Na^+ and water are similar and the geometries of tetrahedrally coordinated water molecules and Na^+ ions vary only slightly.

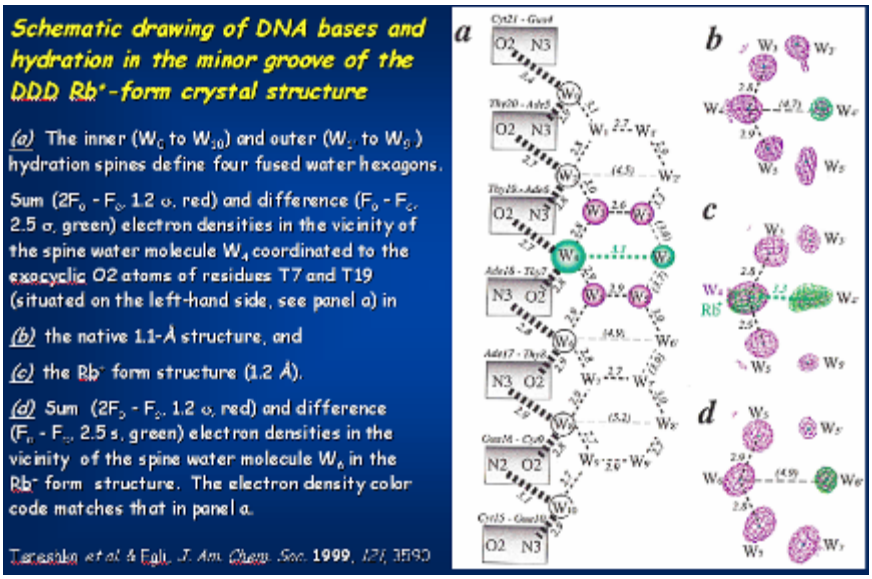

Figure 3

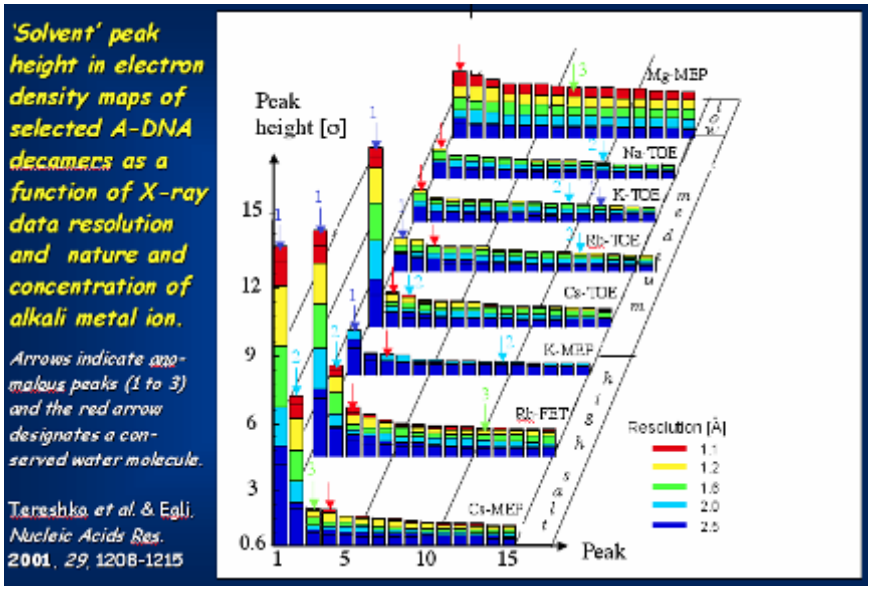

Figure 4

Not only may certain ions be invisible in electron density maps based on XMC experiments, an additional problem concerns the determination of the precise effects of metal ion coordination on duplex structure. Thus, the question whether metal ions can assume specific roles in the control of DNA duplex conformation has stirred up controversy in recent years. Some in the field believe that cation localization within the grooves of DNA represents a significant factor in sequence-specific helical structure. Others are of the opinion that sequence dictates local DNA conformation and thus binding of metal ions. According to this second group, metal ions can bind to DNA in a sequence-specific manner and in turn modulate the local structure, but ions should not be considered the single most significant driving force of a number of DNA conformational phenomena.

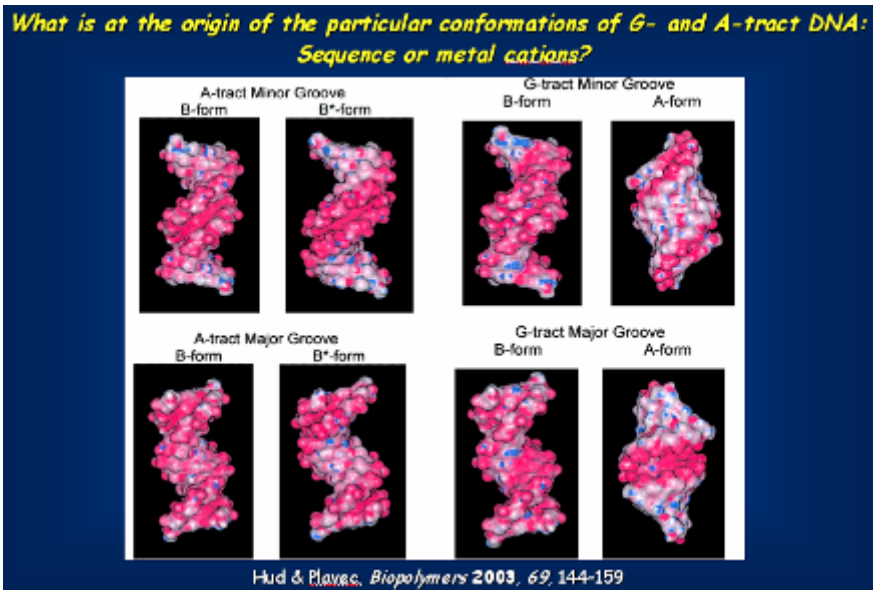

Figure 5

To study the possible effects of metal ions on DNA conformation, all sequences can be divided into three principal groups: A-tracts, G-tracts and generic DNA, the latter representing the vast majority of DNA sequences. A-tracts have an unusually narrow minor groove, are straight and have high base-pair propeller twist (**Figure 5**). G-tracts have a propensity to undergo the B-form → A-form transition at increased ionic strengths. The proponents of the 'ions are dominant' model believe that the DNA grooves are flexible ionophores and that DNA duplex structure is modulated by a tug of war between the two grooves for cation localization. They argue that the duplex geometry adopted by A-tracts (referred to as B*-DNA, **Figure 5**) is due to ion localization in the minor groove as a result of the highly negative electrostatic potentials there. Conversely, G-tract DNA exhibits a highly negative electrostatic potential in the major groove (**Figure 5**), leading to preferred localization of cations there and consequently a collapse of the DNA around the ions. Generic DNA on the other hand would have a more balanced occupation of its major and minor grooves by cations, consistent with a more or less canonical B-form geometry. By contrast, those emphasizing the dominating role of sequence in the control of DNA conformation will argue that it is sequence that shapes the DNA in the first place and that the narrow minor groove of A-tract or B*-DNA is narrow even before ions settle in the groove.

Neutron macromolecular crystallography (NMC) experiments can potentially provide important new insights into the two above issues, namely reliable determination of alkali metal ion binding sites and, subsequent to the retrieval of ions, the structural consequences of ion binding for duplex geometry. NMC is also expected to be of great help in the analysis of the precise modes of interaction between water molecules and the aromatic moieties of nucleic acids and proteins. Hydrogen bonds between water molecules and π acceptors are a common element of macromolecular crystal structures. The donor group is N-H, O-H, S-H or C-H and a comprehensive analysis of the relative donor and acceptor efficiencies in X-H$\cdots\pi$ interactions has recently been published (**Figure 6**).

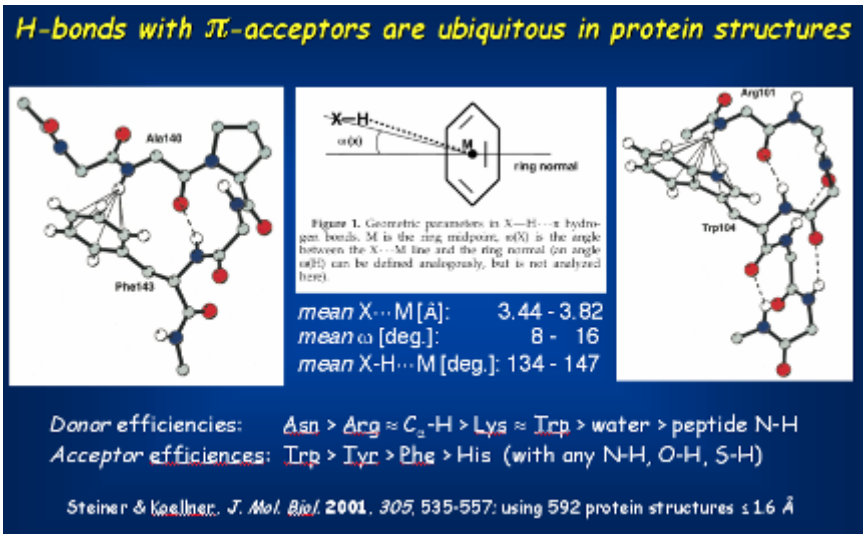

Figure 6

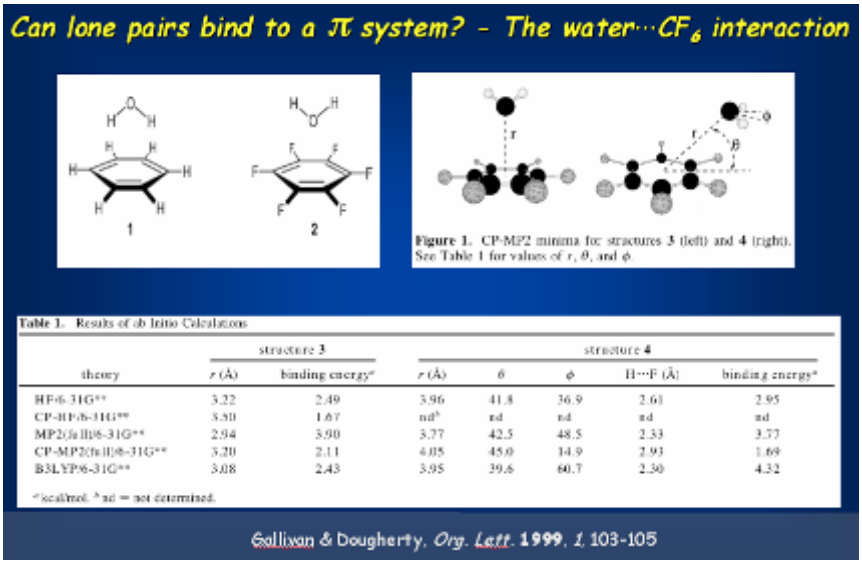

Figure 7

Benzene, the basic model system for studying the interactions between water and aromatics, forms hydrogen bonds with water (**Figure 6**). Consistent with the negative electric quadrupole moment of benzene the hydrogen atoms of water are directed into the six-membered ring and two different relative orientations between an isolated water and benzene molecules have been established spectroscopically. Conversely, the hydrogen atoms are directed away from the ring plane in the case of hexafluorobenzene which exhibits a positive electric quadrupole moment (**Figure 7**). Similarly, high-resolution crystal structures of DNA and RNA have established that lone pairs of oxygen atoms can be directed into the π electron systems of nucleobases (**Figures 8, 9**). Although this finding is initially somewhat counterintuitive, such lone-pair$\cdots\pi$ (l.p.$\cdots\pi$) interactions can be explained by a partially positive polarization of nucleobases due to coordination of metal ions or the particular environment.

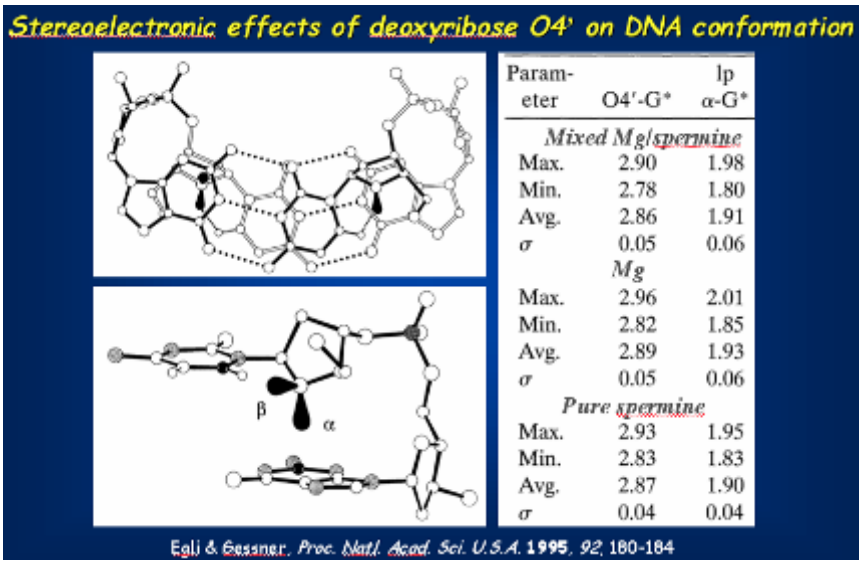

Param-eter	O4'-G*	lp α-G*
Mixed Mg/spermine		
Max.	2.90	1.98
Min.	2.78	1.80
Avg.	2.86	1.91
σ	0.05	0.06
Mg		
Max.	2.96	2.01
Min.	2.82	1.85
Avg.	2.89	1.93
σ	0.05	0.06
Pure spermine		
Max.	2.93	1.95
Min.	2.83	1.83
Avg.	2.87	1.90
σ	0.04	0.04

Figure 8

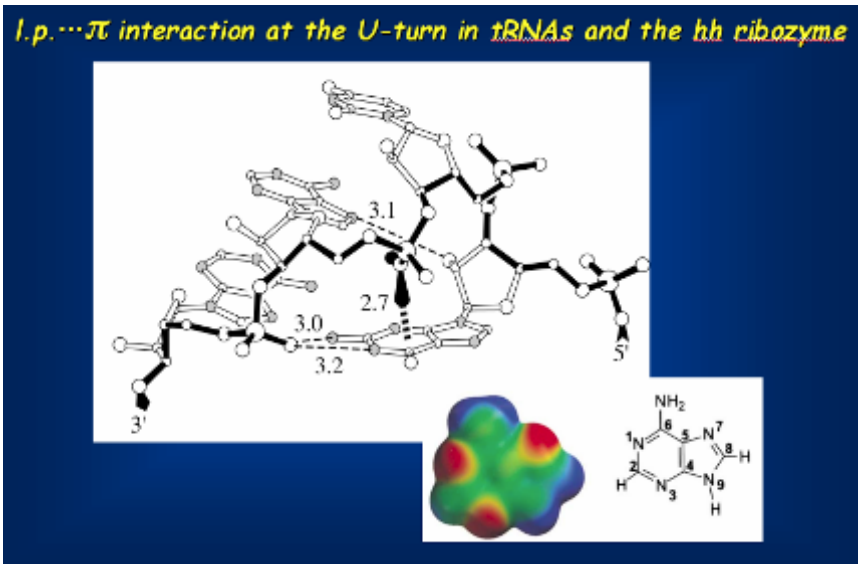

Figure 9

Such l.p.···π interactions can become energetically relevant and their stabilities can surpass those of O-H···π interactions. This was recently established for imidazole and protonated imidazole on the basis of semi empirical calculations (**Figure 10**).

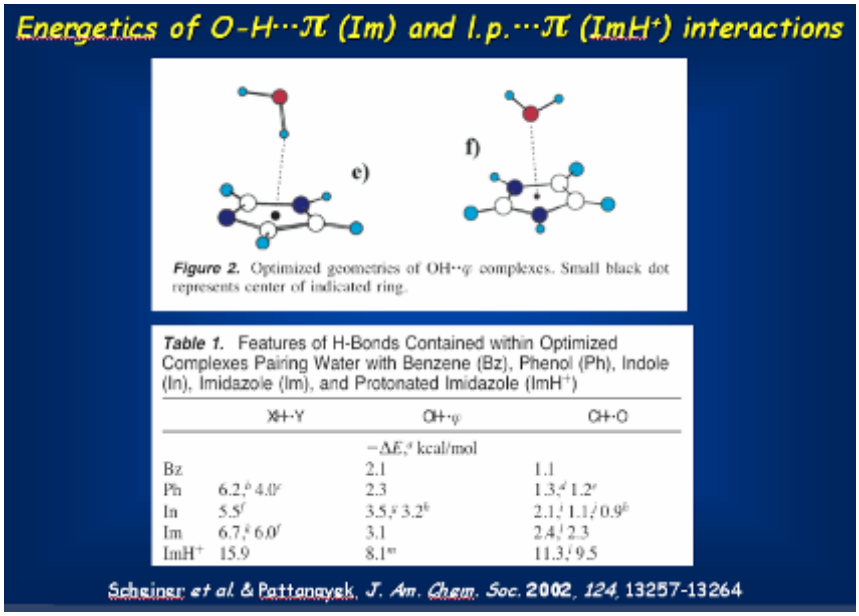

Figure 10

We have observed l.p.···π interactions as well as O-H···π interactions between water and nucleobases in a high-resolution crystal structure of an RNA frameshifting pseudoknot (**Figure 11**). In this structure, water mimics stacking of one base on another. In one case water is located directly above the protonated cytosine ring that is engaged in a quadruple base interaction that is absolutely required for efficient frameshifting.

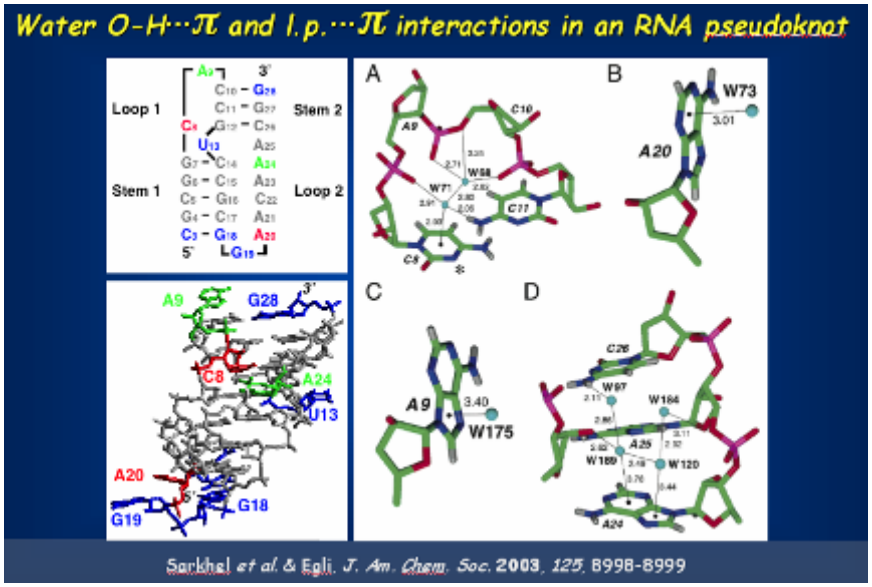

Figure 11

Although counterintuitive l.p.···π interactions may not be uncommon. A recent survey of water molecules located within hydrogen bonding distance from aromatic side chains in 75 protein crystal structures refined to atomic resolution identified 18 cases (**Figure 12**). However, despite the excellent quality of these structures, it appears difficult to determine whether the interaction between water and the aromatic system is of the l.p.···π or the O-H···π type. NMC

experiments would undoubtedly help to resolve this ambiguity as neutron scattering is ideally suited to differentiate between hydrogen atoms and lone pairs.

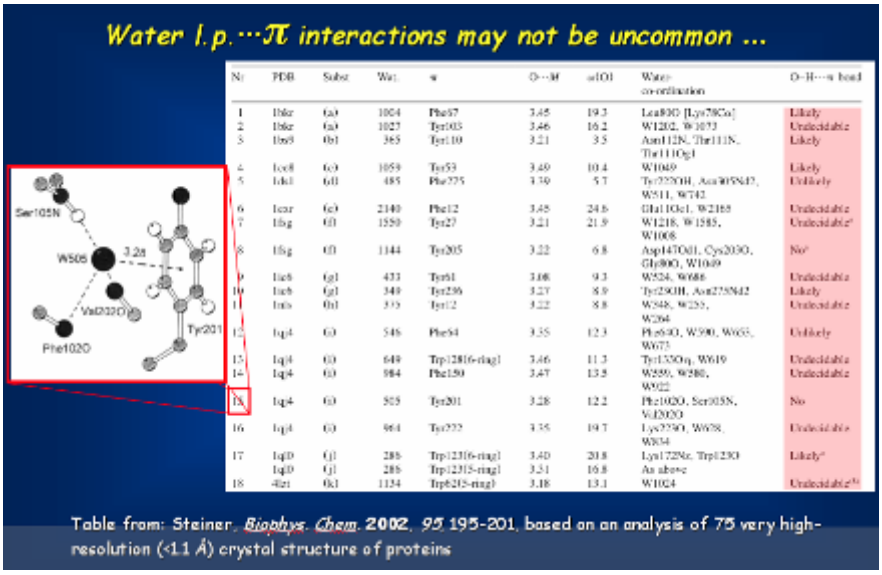

Figure 12

NMR Dynamic Studies of Ribonuclease A and the Role of Protons and Water in the Catalytic Mechanism

Patrick Loria
Department of Chemistry, Yale University

The intramolecular dynamics of Ribonuclease A (RNase A) were characterized by solution NMR in the absence and presence of a nanomolar inhibitor (pTppAp) to address the role of protein flexibility in enzyme function. NMR spin-relaxation rate measurements provide evidence for protein motion occurring at a rate of ~1500 s^{-1}. A subset of the amino acid residues displays conformational flexibility and these residues are located at the enzyme active site and substrate-binding site. The timescale and activation energies for this motional process are similar to the overall catalytic rate and activation barrier, implicating the motion in the rate-determining step. A conserved water molecule was identified by both x-ray crystallography and NMR and located in position to provide the only connection between two flexible regions of RNase A. To address the role of this water in mediating protein mobility, one of its hydrogen bonding partners, D121 was mutated to alanine. In the D121A mutant enzyme, both previously flexible regions show a loss of motion on the millisecond timescale implicating an important role for this specific water molecule (Figure 1).

Additionally, the dynamics in RNase A exhibit a pH dependence. Motion in a loop located at the base of the enzyme active site is dampened as the solution pH is lowered. Histidine 48 is located in the vicinity of this active site loop and shows titration behavior, by NMR, similar to that of loop motion. We suggest that deprotonation of H48 is correlated with an increase active-site flexibility.

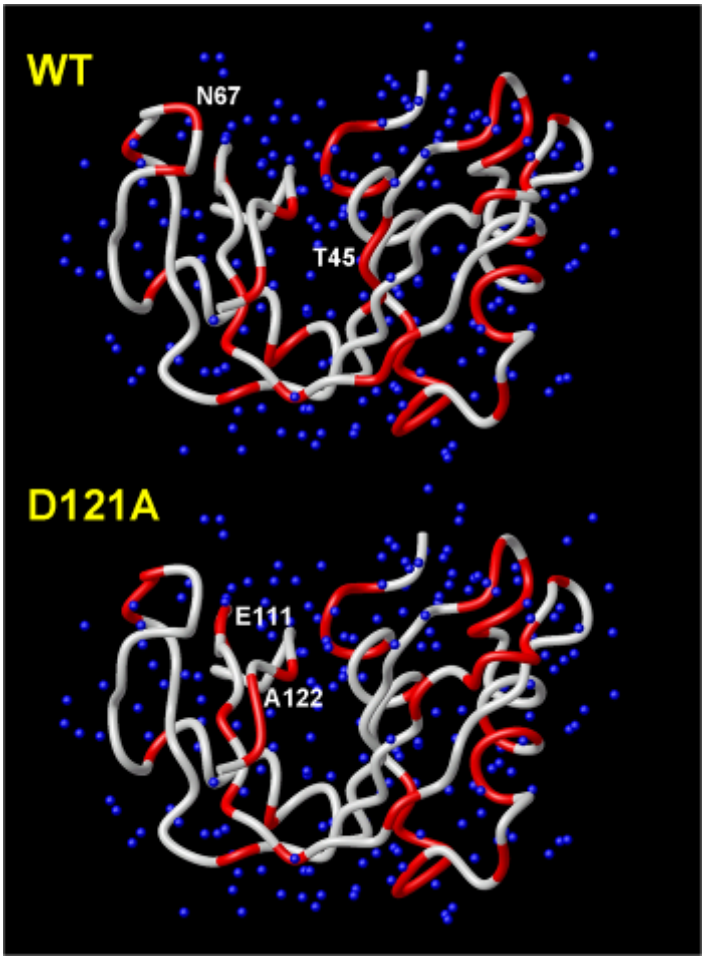

Figure 1. Water structure in wild-type and mutant (D121A) RNase A. Water positions determined by NMR in our lab are indicated by red ribbons. The crystallographic waters are shown as blue balls and were determined by; Wlodawer, Svensson, Sjolin, Gilliland (1988) Biochemistry 27, 2705-17. Schultz, Quirk, Raines (1998) Biochemistry 37, 8886-98.

NMR, X-ray and Computational Analysis of HbS Aggregation Inhibitors – Importance of Protonation States

Michael E. Johnson
Center for Pharmaceutical Biotechnology, University of Illinois at Chicago

Although the molecular defect in sickle hemoglobin that produces sickle cell disease has been known for decades, there is still no effective drug treatment that acts on hemoglobin itself. It has been known for some time that a variety of hydrophobic compounds inhibit the polymerization of sickle hemoglobin (HbS). Early NMR studies showed binding of such compounds in a region proximate to the binding site for biphosphoglycerate, the native allosteric effector, provided only an approximate binding location. More recently, a series of diversely substituted isothiocyanates were examined for their regio-selective covalent reaction with hemoglobin in an attempt to more selectively alter the solubility properties of sickle hemoglobin. Electrospray mass spectrometry, molecular modeling, x-ray crystallography and conventional protein chemistry were used to study this regio-selectivity and the resulting increase in solubility of the modified hemoglobin. The x-ray crystal structure of Hb shows that one of the most effective compounds in the series, 2-(N,N-dimethylamino)ethyl isothiocyanate, selectively reacts with the thiol of Cysβ93 (Figure 1), which in conjunction with the cationic group was seen to perturb the local hemoglobin structure. This modified HbS shows an approximately 30% increase in solubility for the fully deoxygenated state, along with a significant increase in oxygen affinity. A close inspection of the modified Hb shows that insertion of a cationic group at Cysβ93 occurs in a "gap" region where the overall electrostatic potential would be dominated by four Lys residues on neighboring molecules (Lysβ8, Lysβ120, and two Lysβ17's), as well as two other Lys residues slightly further away from the Cysβ93 modification (Lysβ65 and Lysβ66). Besides these Lys residues on the neighboring molecules of the adjacent strand(s), there are three Lys residues near the covalently modified Cysβ93 (Lysα40, Lysβ95, and Lysβ144) for the native HbS polymer fiber. Some of these Lys residues are neutralized locally by nearby Glu or Asp residues. This is the case for the Gluβ121 next to Lysβ120, as well as the Gluβ90 near Lysβ144, and Lysβ95 on the other side of Aspβ94.

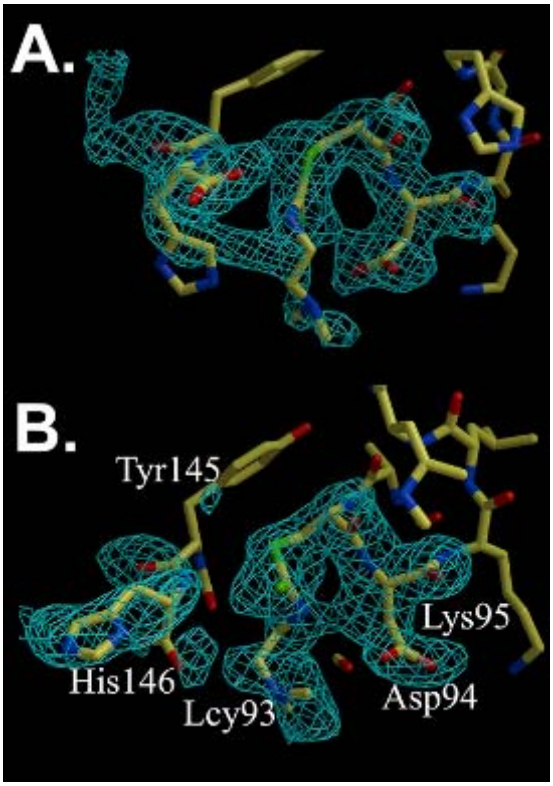

Figure 1. Electron Density surrounding Cysβ93 in covalently modified human hemoglobin. Cysβ93 was modified by 2-(N,N-dimethylamino)ethyl isothiocyanate which has anti-sickling properties. (A) and (B) are the different subunits in the asymmetric unit. Structure determined by the A. Mesecar lab.

In the native structure Aspβ94 forms a salt bridge with Hisβ146, effectively neutralizing the charge for both residues. Upon adduct formation at Cysβ93, the imidazole ring of Hisβ146 is displaced, inserting a weakly basic (cationic) group approximately into the center of the positive electrostatic potential generated by these Lys residues. Local charge neutralization of Aspβ94 appears to be maintained by the cationic group, as well

as a likely hydrogen bond formation between the protonated amine of the adduct and the carboxylate group of Aspβ94. Calculations suggest a change in the electric field surrounding Hisβ146 that is more likely due to the movement of the imidazole ring being pushed down from the Aspβ94 and minimally due to the nearby positively charged ligand (Figure 2). The change of the field surrounding the Aspβ94, however, from one which is pointed away from the Asp's COO^- group in the unbound Hb to one where a portion of the field has been eliminated in the liganded Hb, is likely due to the additional positive charge of the ligand influencing the electric field vectors in and around this COO^-.

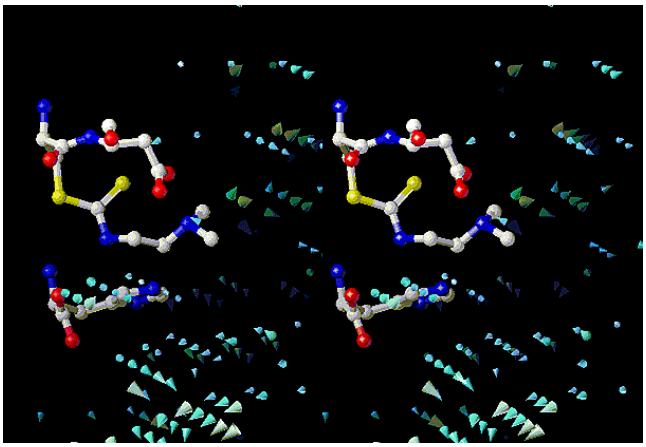

Figure 2. Stereo diagram of calculated electric field vectors surrounding Cysβ93.

Detailed interpretation of the various electrostatic effects consequent to the introduction of a cationic group at Cysβ93 would substantially benefit from methods such as neutron diffraction that can unequivocally determine the protonation states of the various ionic groups in the intermolecular region. Detailed analysis of the electrostatic influence on polymerization remains to be fully elucidated, and is highly dependent on ionization states of the various residues described above.

Quantum Mechanical/Molecular Mechanical Molecular Dynamics Simulations of Cytidine and Adenosine Deaminases

Hong Guo
University of Tennessee, Biochemistry & Molecular Biology

Molecular dynamics (MD) simulations can provide detailed information about the motions of proteins in which the Newtonian equations of motion for the atoms in proteins are solved numerically. The initial coordinates of the atoms used in molecular dynamics simulations are normally obtained from the x-ray structures, and the accuracy of these initial structures is crucial for the correctness of the simulations results (Figure 1). The lack of hydrogen and proton positions in many of x-ray structures of proteins and inaccuracy of the widely used procedures in determining their locations pose a serious problem for molecular dynamics simulations, as the incorrect positions would lead to both wrong initial conditions for the motions as well as artificial interactions (potential energy functions).

Here we use quantum mechanical/molecular mechanical (QM/MM) MD simulations to study the motions and interactions of transition state analogs in the active sites of cytidine deaminase (CDA) and adenosine deaminase (ADA) and to elucidate the mechanism of the CDA and ADA-catalyzed reactions. In the case of CDA, the simulations reveal that the covalent bond between C_4 and the 4-OH group in zebularine 3,4 hydrate (TSA) undergoes transient bond breaking and making on a picoseconds scale in the active site, resembling the process of the nucleophilic attack by the zinc hydroxide group on C_4 during the catalysis. The role of the active-site interactions in stabilizing zebularine 3,4-hydrate as well as the transition state during the enzyme-catalyzed reaction is also discussed. In the case of ADA, unless the proton is located at a different position as people thought, we found that the transition state analog is unstable in the wild-type enzyme.,

The results from the MD simulations indicate that the availability of neutron structures with correct hydrogen and proton positions will not only provide an important testing ground for theoretical predictions, but also help theoreticians to identify the deficiencies in theoretical approaches (e.g., force fields) for biological systems and make better predictions in the future.

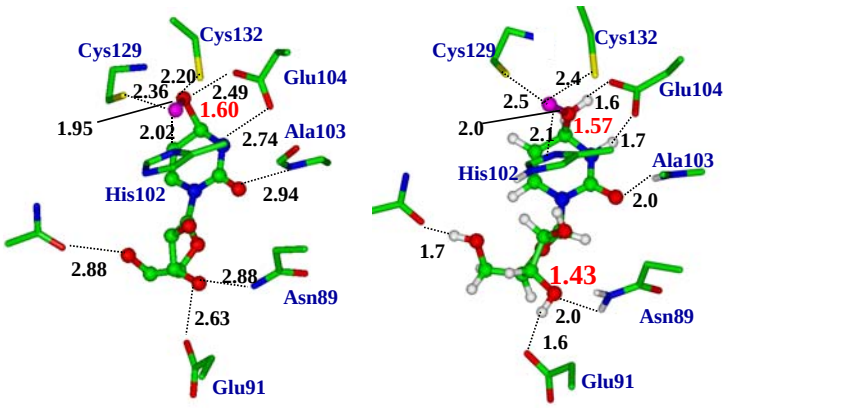

X-ray structure **Average structure from simulations**

Figure 1. Comparison of the active site structures from x-ray and the simulations.

Towards Elucidating Catalytic Mechanism of Dihydrofolate Reductase Using Neutron and Ultra High Resolution X-ray Crystallography

Chris Dealwis
University of Tennessee

Dihydrofolate reductases (DHFR) are ubiquitous housekeeping enzymes critical in the regeneration of tetrahydrofolate (THF). Although there are several medium to high-resolution (2-1.6 Å) *E. coli* DHFR crystallographic structures, a controversial question relating to the protonation state of the active site residue, aspartic acid 27, still remains unanswered. Resonance Raman data suggest Asp27 becomes protonated during the catalytic cycle while NMR data on the homologous *L. casei* DHFR indicate this Asp remains ionized. Using a combination of ultra-high resolution x-ray diffraction and neutron diffraction studies of DHFR ternary complexes we intend to independently determine the protonation state of Asp27 and determine proton positions of catalytically relevant water molecules. Currently the DHFR-MTX complex is being refined to 0.9 Å resolution. The two DHFR molecules in the asymmetric unit are found in the closed and occluded conformations, respectively (Figure 1). In order to conduct neutron diffraction experiments, we have produced perdeuterated E. coli DHFR and crystallized the DHFR-MTX complex. At present the crystal dimensions are 0.7x0.4x0.3 mm^3.

Future work will involve determining the neutron diffraction structure of DHFR-MTX and the DHFR-NADP+-Folate complexes.

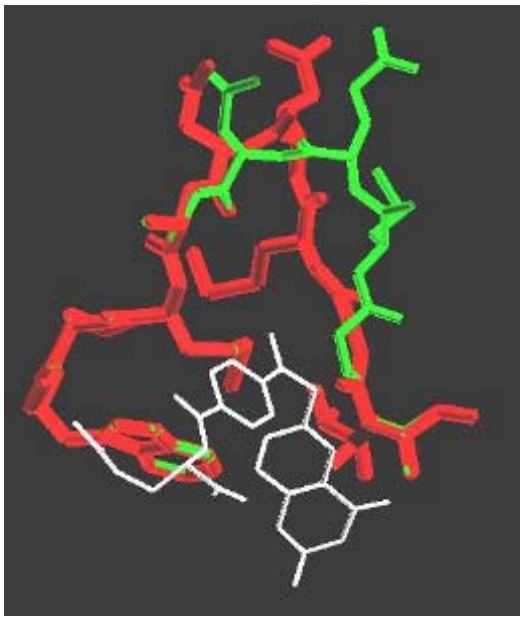

Figure 1. Conformational differences at the MET20 loop between the occluded and closed conformations.

Structure-Based Drug Design in the Pharmaceutical Industry: Is There a Role for NMC?

Geoffrey Stamper
Abbott Laboratory, Department of Structural Biology

The need to lower the costs associated with the drug discovery process has in part driven the development of technologies allowing for high-throughput protein x-ray crystallography.

High-throughput protein x-ray crystallography allows for the:

- Rapid identification of binding mode of the small molecule ligand.
- Provide insight into the flexibility of the target molecule.
- Provides a template for directed medicinal chemistry efforts to improve binding.
- Validate/interpret SAR.

Areas where HTP x-ray crystallography could improve:

- Prospective predictability of potency gains by improved understanding of SAR.

What does neutron macromolecular crystallography provide? Could it impact the improvement of HTP x-ray crystallography?

- Improve understanding of target-compound interactions.
- Map H-bond network at the active site.
- Monitor modulations of H-bonds in presence of ligand.
- Resulting affinity changes.
- Identify active tautomers.
- A database of structures with experimentally derived hydrogen positions.
- Allows for data collection of cryo-sensitive crystals.

Practical issues to overcome for viability of technique to Industrial Crystallographers:

- Time is short in high-throughput mode - collection times HAVE to be comparable.
- Software - easy to use, resulting intensities need to move seamlessly into refinement packages, etc.
- Ultra-high resolution x-ray diffraction data provide the same information on a shorter time scale.
- Sample issues:
- Currently no effort to optimize crystal size.
- Deuterium requirement.
- Not clear how this addition informational, namely hydrogen positions, would immediately impact current VLS/modeling efforts.

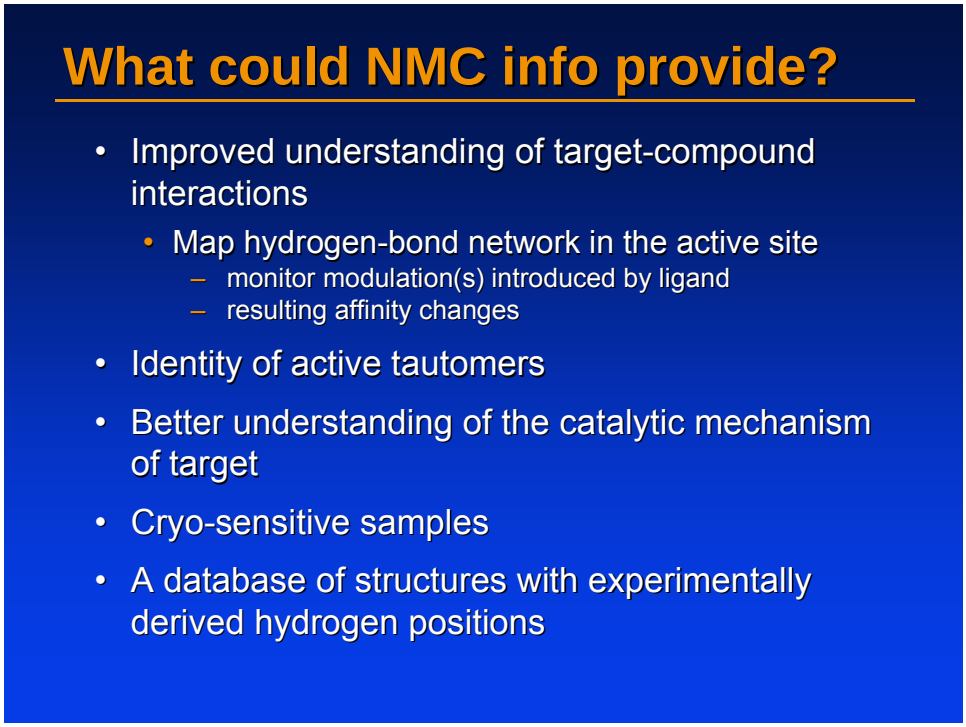

Summary: There is some general interest in this technique among some industrial crystallography labs. Serious consideration to implement the technique would first require addressing the issues outlined above.

Modeling Protein Dynamics with Neutron Crystallography at 1 Å.

Martha Teeter
Department of Chemistry, Boston College and the University of California, Davis

NMC at high resolution is critical to understanding protein structure and function for two key reasons. First, at high resolution (higher than ~1.2 Å), protein and water discrete disorder can be modeled accurately and this disorder is key to protein function. Second, hydrogens on the protein and on water can be uniquely visualized by neutron diffraction. These hydrogens, best modeled following discrete disorder, can provide clear enzyme mechanisms.

How do we know discrete disorder is important? The energy surface of proteins appears to be rough and their dynamics principally anharmonic.[1] Kinetic studies of myoglobin and bacteriorhodpsin suggest proteins exist in multiple stable states of almost equal energy.[2] Protein and water discrete disorder can define these states. High-resolution crystal structures are needed to model discrete disorder. These multiple states contribute to protein function (Figure 1).

At 200 K protein function appears to cease.[3] Analysis of 1 Å x-ray models of crambin, a 4.7 kDa, hydrophobic protein, from 300 K to 100 K.[4] reveals a break in slope for vibrational factor (*B)* vs. *T* at around 180 K. Further, for water vibrational factors the sign of the slope changes to negative below 180 K due to glassy nature of water. The same negative slope is seen for discretely disordered but not for ordered atoms. Thus dynamics for water and discretely disorder protein atoms are uniquely coupled. This coupling is linked to the function temperature.

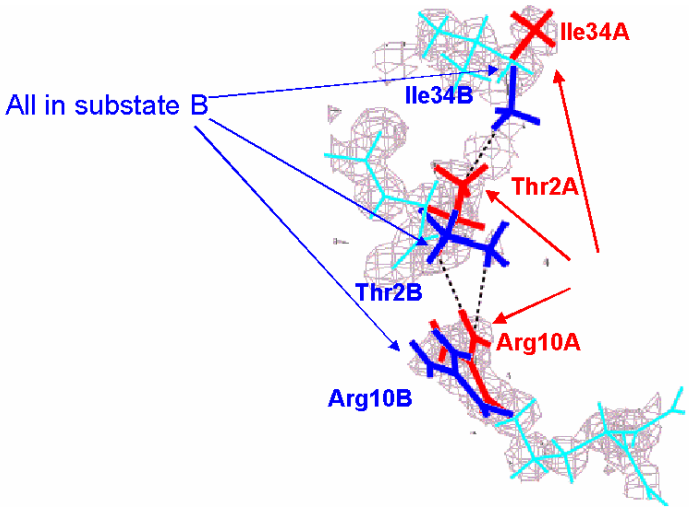

Figure 1. Conformational substates in Crambin.

Crambin structures at 0.54 Å by x-ray diffraction and 1.1 Å neutron data reveal residues with correlated multiple discretely-disordered states (substates) both along the surface of the protein and buried within the protein. On the surface, discretely disordered water connects substates of the protein. Interestingly, this water connection can extend over tens of Ångstroms, suggesting water stabilizes each global substate.

Myoglobin has three spectroscopically observed ground states to which photolyzed CO returns. Such multiple ground states are quantitatively correlated with discrete disorder in the distal His to three positions (Figure 2). I have rationalized correlated discrete disorder over the entire myoglobin protein for two of the three states and examined cavity formation for both states. This analysis shows that with a low energy cost correlated conformations of four residues can produce cavities to move the ligand from the distal to the proximal side of the heme, as was experimentally observed. For the one of these spectroscopic states adopted for L29F myoglobin, a movie of Mb-CO* picosecond dynamics from x-ray Laue diffraction data shows exactly these residues move near the heme Fe when cavities form and disappear.[5]

Myoglobin can use these cavities to bind and oxidize NO to higher oxides, like its homolog neuroglobin may do.

The key role of discrete disorder of protein and water to protein function is also clear for cholesterol oxidase at 1 Å.[6] Here correlated substates at the active site explain the mechanism.

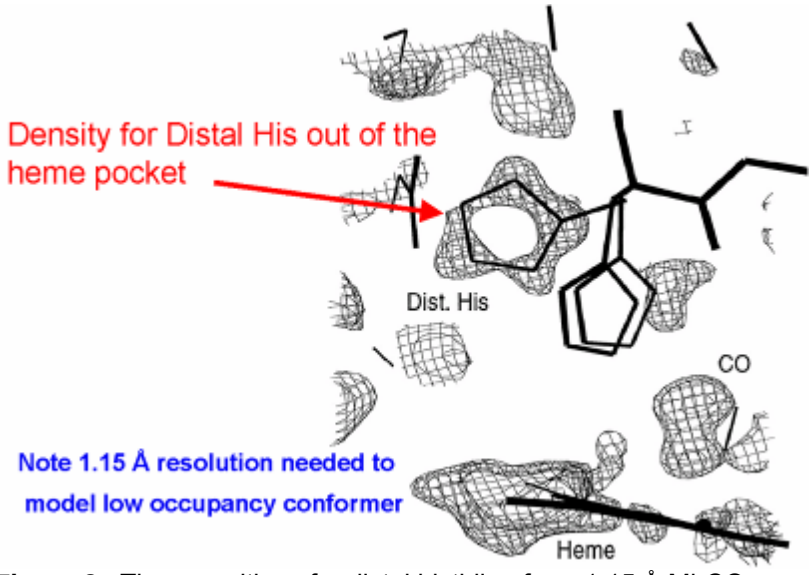

Figure 2. Three positions for distal histidine from 1.15 Å MbCO x-ray structure.

References

1. Doster, W., S. Cusack, and W. Petry, *Dynamic instability of liquid-like motions in globular proteins observed by inelastic neutron scattering.* Phys. Rev. Lett., 1990. **65**: p. 1080-1083.
2. Austin, R.H., et al., *Dynamics of ligand binding to myoglobin.* Biochem., 1975. **14**: p. 5355-5373.
3. Rasmussen, B.F., et al., *Crystalline ribonuclease A loses function below the dynamic transition at 220 K.* Nature, 1992. **357**: p. 423-424.
4. Teeter, M.M., et al., *On the nature of the glassy state of matter in hydrated protein: Relation to protein function.* Proc. Natl. Acad. Sci. USA, 2001. **98**: p. 11242-11247.
5. Schotte, F., et al., *Watching a protein as it functions with 150-ps time-resolved X-ray crystallography.* Science, 2003. **300**: p. 1944-1947.
6. Lario, P.I., N. Sampson, and A. Vrielink, *Sub-atomic resolution crystal structure of cholesterol oxidase: what atomic resolution crystallography reveals about enzyme mechanism and the role of the FAD cofactor in redox activity.* J. Mol. Biol., 2003. **326**: p. 1635-1650.

Small Angle Neutron Crystallography – Detergent Binding to Membrane Proteins.

Peter Timmins
Institut Laue Langevin, DS Divison

The use of contrast variation in protein crystallography is very old. It was used by Bragg & Perutz to determine the molecular envelope of hemoglobin before MIR was available for high-resolution crystallography. With x-rays, contrast variation is carried out by soaking crystals in sucrose or salt solutions which may have deleterious effects on the crystal. With neutrons, exchanging the water for H_2O/D_2O mixtures is all that is required.

Contrast

The scattering density of all components of biological macromolecules (sugar, protein, nucleic acids, lipids) can be matched by that of a particular H_2O/D_2O mixture. (e.g. 40% D_2O for proteins, 65 – 70 % D_2O for nucleic acids). The only exception is when these molecules are perdeuterated when they have a scattering density even higher than pure D_2O. (A laboratory specialized in *in vivo* deuteration exists at ILL - http://www.ill.fr/deuteration)

Instrumentation

Dedicated instrument for low-resolution crystallography, DB21, exists at ILL. Operates at wavelength = 7.5 Å, unit cells of 100-300 Å. Gives data to 10 – 15 Å resolution. Requires MUCH SMALLER crystals than for high resolution studies - <0.1 mm^3.

Systems studied

- protein-nucleic acid complexes, e.g. viruses
- lipoproteins
- membrane protein/detergent complexes - Detergent structures mimics lipid binding giving information about real membranes.
- hetero oligomeric proteins (use of specific deuteration)
- Protein envelopes for *ab initio* phasing – as yet not exploited

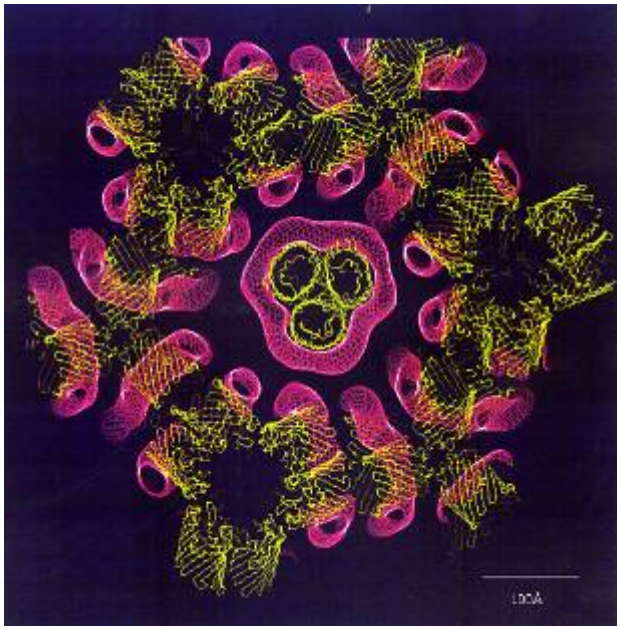

Figure 1. Packing of OmpF trimers in the tetragonal crystal form.

Data analysis

Phasing of crystal data is analogous to SIR. It is necessary to know the structure of one part of the complex, e.g. the protein in a membrane protein/detergent complex detergent. The phases are then known at the contrast where the detergent is invisible, e.g. ~10% D_2O and the contrast variation relationships allow phases to be calculated at any other contrast but with an ambiguity of sign. As with SIR this ambiguity can be resolved using *a priori* knowledge such as the known location of one component, non-crystallographic symmetry, solvent flattening etc.

Examples

- OmpF porin from E. coli Tetragonal form Pebay-Peyroula, E., Garavito, R.M., Rosenbusch, J.P., Zulauf, M. and Timmins, P.A. (1995). Detergent structure in tetragonal crystals of Ompf porin. Structure **3**, 1051 – 1059. Belt of detergent with not only protein-protein contacts being important but also detergent-detergent contacts (Figure 1).

- OmpF porin from E. Coli in trigonal form. Detergent belts coalesce in the crystal and induce hydrophobic protein-protein interactions which cannot be present in solution. Penel, S. Pebay-Peyroula, E., Rosenbusch, J., Rummel, G., Schirmer, T. and Timmins, P.A. (1998. Detergent binding in trigonal crystals of OmpF porin from *Escherichia coli*. Biochimie **80**, 543 – 551.

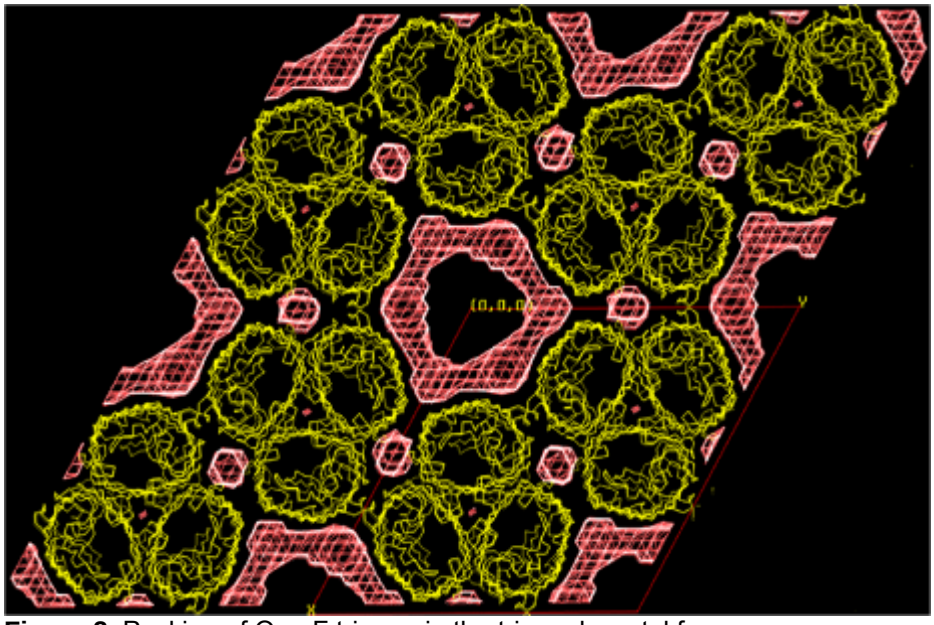

Figure 2. Packing of OmpF trimers in the trigonal crystal form.

Neutron Diffraction on Membrane Proteins

Petra Fromme
Department of Chemistry and Biochemistry, Arizona State University

Results were presented on ongoing neutron diffraction experiments on Photosystem I crystals which show how high resolution neutron diffraction experiments may be used to answer essential functional questions like the so far unknown mechanism of water splitting and oxygen evolution in Photosystem II.

Introduction

Approximately 30% of all proteins are embedded into biological membranes. Membrane proteins are the major players in important cell processes like cell import and export, recognition, signaling, nerve function, respiration and photosynthesis. Whereas more than 25000 structures of soluble proteins are known, less than 35 different types of membrane proteins structures have been determined so far. The main focus of our research is large membrane protein complexes involved in Photosynthesis. Photosynthesis is the major process on earth that converts solar energy into chemical energy and supplies all higher life on earth with food. Furthermore, the process of Photosynthesis produces all oxygen in the atmosphere. Two membrane protein complexes, Photosystem I and II, catalyze the first and most essential step of Photosynthesis, the light induced charge separation.

Photosystem I

Photosystem I is a large membrane protein complex. It consists of 12 proteins to which 127 cofactors are non-covalently bound. One monomer contains 96 chlorophylls (green pigments), 22 carotenoids (orange pigments), 3 [4Fe4S] clusters, 2 phylloquinones and a Ca atom (Figure 1). In the biological membrane, PS I is a trimer with a molecular weight of 1,000,000 Da. Photosystem I captures the light from the sun by its large antenna system and transfers the energy to the center of the complex, where the transmembrane charge separation takes place. The electron is transferred along a chain of electron carriers to ferredoxin at the stromal side where the electrons are used to reduce $NADP^+$ to NADPH. Re-reduction of PS I at the lumenal side is performed by either plastocyanine or cytochrome c_6.

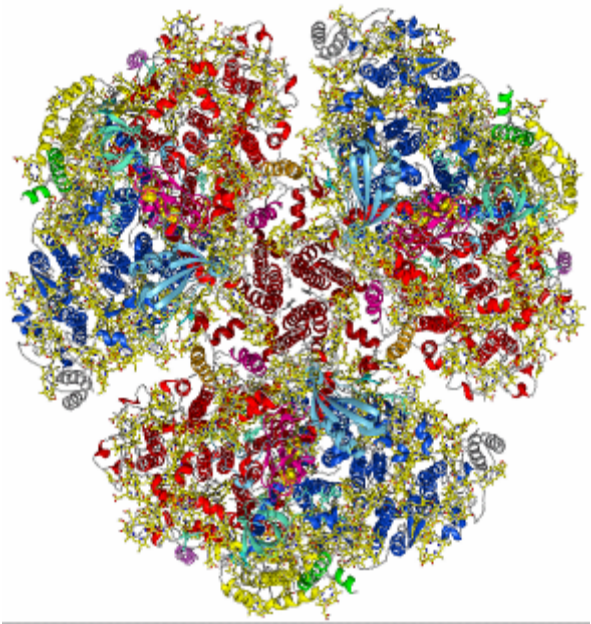

Figure 1. X-ray Structure of PS 1

Photosystem I is embedded into the photosynthetic membrane and has to be solubilized by detergent such as beta-dodecylmaltoside which is used for to form a protein detergent micelle where the detergent surrounds the hydrophobic parts of the protein like a swim-ring. Photosystem I crystallizes by dialysis against low ionic strength. The crystals have the space group $P6_3$ with unit cell constants of a = b = 288 Å, c = 167 Å. The first crystals diffracted to 6 Å resolution and the first structural model at 6 Å resolution was published in 1993 (Krauss et al., 1993). Less than 5% of

the protein surface (as we now know only 4 salt bridges) is involved in crystal contacts. The major problem for the improvement of the crystals was the loose packing of the trimers in the unit cell which contains 78% solvent (water + detergent). We overcame these problems as described below.

Growth of large single crystals suitable for X-ray and Neutron diffraction experiments

Due to the weak crystal contacts and the high solvent content the crystals are very fragile and their growth is influenced strongly by gravity effects like sedimentation of seeds and convection. Therefore experiments to grow larger crystals were performed under microgravity in the space shuttle. The largest crystal ever grown from Photosystem I was grown during the USML-2 mission in the space shuttle Columbia. The crystal had a size of 4 mm in length and 1.5 mm in diameter (volume ≈ 20 mm^3) and diffracted x-rays to 3.4 Å. At that time the best earth-grown crystals diffracted to 5 Å. These crystals would have been optimal for neutron diffraction experiments if a source was readily available and we had this in mind at the time, but they were used instead for x-ray data collection. Room temperature data were collected and an improved structure of PS I based on these data sets was determined (Klukas et al., 1999, 1999).

The experiments under microgravity led to an important increase in our knowledge of the mechanism of nucleation and that the fluid crystalline lamellar phase of the detergent may be involved in nucleation. The next important step was to further improve the crystals on earth. We determined the full phase diagram for the solubility of Photosystem I as a function of the physical-chemical parameters. The determination of the phase diagram was a pre-requisite for the use of seeding techniques that lead to the growth of well ordered single crystals. In the last step (macroseeding) large single crystals are obtained demonstrating that large crystals can now be grown on earth (Figure 2). Their size is mainly limited by the size of the reaction vessel. Recently, we grew crystals of Photosystem I up to 5 mm size in 3 days by macroseeding for ongoing neutron diffraction experiments at ILL in Grenoble. The very large yet very fragile PS I crystals are stable in the neutron beam at room temperature for weeks.

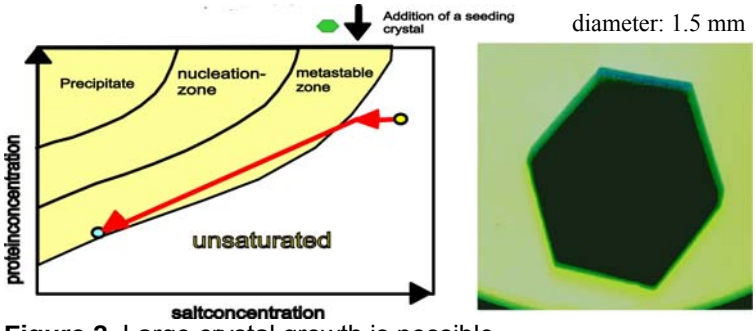

Figure 2. Large crystal growth is possible.

X-ray structure analysis of Photosystem I

The structural model of the PS I trimer at 2.5 Å contains 7098 amino acids (3x12 proteins), 381 cofactors, 620 water molecules. The structure can be described as a cloverleaf with each of the monomers containing 12 proteins and 127 cofactors (Jordan et al., 2001). The electron transport chain is located in the center of each monomer. PS I is very unique in the content of cofactors that contribute 30% to the total mass of the protein. The cofactors not only play an exclusive role in the function of PS I, but also have a very important function in the structure and assembly of the giant membrane protein complex.

Determination of the structure of the detergent in PS I crystals by low resolution Neutron diffraction experiments

Whereas the x-ray structure analysis provided a clear picture of the protein, little to no information about the structure of the detergent can be gained from this method. This is unfortunate because knowledge of the detergent structure is essential for the investigation of the process of nucleation and crystal growth, and this is the limiting factor for structure determination of membrane proteins.

Two models for the arrangement of detergent in membrane protein crystals can be found in text books: Type I crystals where the detergent should form a membrane-like structural arrangement similar to lamellar phases of detergent; and type II crystals where the detergent micelles are building blocks of the unit cell. Low-resolution neutron diffraction experiments provide the best way for determining detergent structures within membrane protein crystals. Recently, the detergent organization in crystals of monomeric outer membrane phospholipase A has been determined (Snijder et al., 2003), and the detergent structure in crystals of the bacterial light harvesting complex has been determined (Prince et al. 2003). These structures show a type II organization of the detergent, as was the case for all other structures of detergent that have been so far determined in membrane protein crystals.

These results raise the question as to whether type I crystals may exist at all. To address this question we initiated neutron diffraction experiments at DB21 at ILL on single crystals of Photosystem I with the aim of determining the detergent structure in PS I crystals. Data collection is in progress and data sets in 100% and 70% D_2O have already been collected in two principle orientations of the crystal. The data sets have been collected from crystals with a length 3 to 5 mm and a diameter of 0.3 to 1 mm (volume 0.5 to 10 mm^3). Data collection was performed at a wavelength of 7.56 Å with rotations of 0.2^o /image, at room temperature. The diffraction patters show a resolution of ≈ 30 Å. Data sets at different contrast (40% and 0% D_2O) have to be collected for phase determination before the structure of the detergent can be calculated. However, even the raw diffraction patterns provide strong indication for the existence of a lamellar phase of the detergent in the crystals. Two symmetric strong reflections of 60,000 counts (compared to ≈ 600 counts for the protein reflections) were detected at the orientation where the neutron beam was exactly perpendicular to the c-axis of the crystals. Such strong reflections at this orientation are what one would expect if an ordered layer of D_2O molecules would be located on top of a lamellar detergent phase. In conclusion, there is evidence from our preliminary neutron diffraction data that the lamellar phase of the detergent may even exist in the single crystals.

Targets for High resolution Neutron diffraction studies on Photosystem I

Will it be possible to perform high-resolution neutron macromolecular crystallography with MaNDi on large membrane protein complexes like photosystem I and II? I believe the answer is yes as our recent test experiments look very promising. We just tested some small PS I crystals (0.5 mm^3, same amount of unit cells like a 0.025 mm crystal of a 100kDa protein) at the LADI beamline in Grenoble and they already diffracted to 8 Å resolution. Taking into account the much larger crystals sizes that we can produce and the higher flux at the planned MaNDi beamline, collection of high-resolution data on Photosystem I crystal could be achieved.

What important questions could be answered with high-resolution neutron experiments on Photosystem I crystals? The structure of PS I has been determined by x-ray structure analysis at 2.5 Å resolution. In addition to the proteins and cofactors, 220 water molecules have been identified per monomeric unit of PS I. Interestingly many of the water molecules are located in the membrane intrinsic part of PS I, raising the important question of the function of these water molecules (Figure 3). Detailed inspection shows that all of these water molecules are located at functional important sites. For example, water molecules coordinate the two chlorophylls that represent the first electron acceptor in the electron transport chain. Another example is water clusters located between the phylloquinone and the first of the FeS clusters, FX. The electron transfer from the phylloquinone to FX is the rate-limiting step of the electron transfer in PS I with a large reorganization energy, i.e. activation energy barrier. The electron chain shows two branches, and one of the most controversy-driven questions is whether only one branch or both branches are active in electron transport. It was observed that the electron transfer along the A-branch might be 20 times slower than the transport along the B-branch. Whereas the cofactor arrangement is identical on both branches, there are large differences in the water clusters located between the phylloquinone and FX. On the slow A-Branch, six water molecules are located between the electron carriers showing no pronounced structural arrangement, whereas the water molecules at the B-branch form a pentamer which is a very stable arrangement that has also been identified in other protein structures. It would be very exciting to locate the hydrogen atoms in the water clusters and unravel the structure of these clusters at atomic detail by high-resolution neutron diffraction studies.

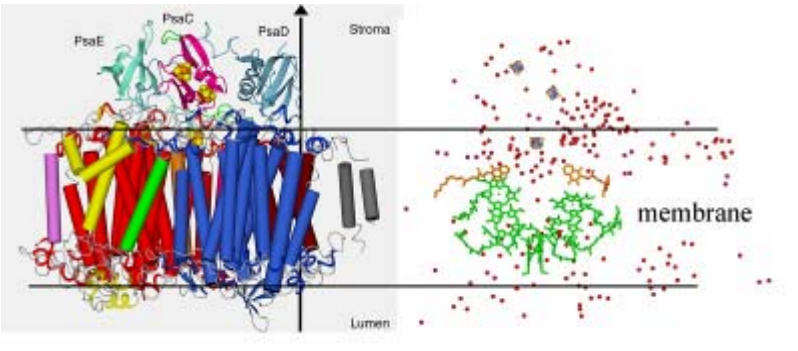

Figure 3. Membrane Bound PS I and the 220 identified waters located in the membrane intrinsic region.

Targets for High resolution Neutron Diffraction Studies on Photosystem II

Photosystem I is one of the most important enzymes on earth and it has changed our entire atmosphere from an anoxygenic atmosphere (~3 billion years ago) to an oxygenic atmosphere. All the molecular oxygen in the atmosphere is produced by Photosystem II, thereby providing the basis for all higher life on earth. Photosystem II drives the light-driven charge separation from water at the lumenal site to plastoquinone at the stromal site of the photosynthetic membrane. The water oxidation is performed in 4 subsequent steps of charge separation, whereby in each step one electron (and one proton?) is extracted from water molecules bound to a tetra-nuclear manganese cluster (Figure 4). Oxygen is thereby evolved following 4 charge separation events.

One of the most exciting questions in science is how water splitting can be achieved. A lot of effort has been put into the synthesis of artificial metallo-organic clusters that mimic the reaction, but so far all of them failed. In the best case, these clusters catalyze an irreversible reaction but none of them can act as a catalyst that performs the same reaction that nature has invented billions of years ago. The first step in unraveling the secrets of water splitting was the successful crystallization of Photosystem II by our group (Zouni et al., 2000; Zouni et al., 2001) in an active oxygen evolving form. PS II crystallizes in the space group $P2_12_12_1$. The most remarkable feature of the crystals is that they are still able to split water. Oxygen bubbles come

out from the crystals when they are excited by strong laser light. The structure of PS II was determined at 3.8 Å resolution showing for the first time the location of the Mn cluster. The electron density of the Mn cluster has the form of a papaya, with three Mn atoms forming a triangle shaped arrangement and the last one building the tip of the structure. This arrangement already excludes the popular "C-model", derived from EXAFS data: an arrangement of dimers of dimers that can already be found in textbooks. New models that are in agreement with the structure may include a funnel or butterfly model.

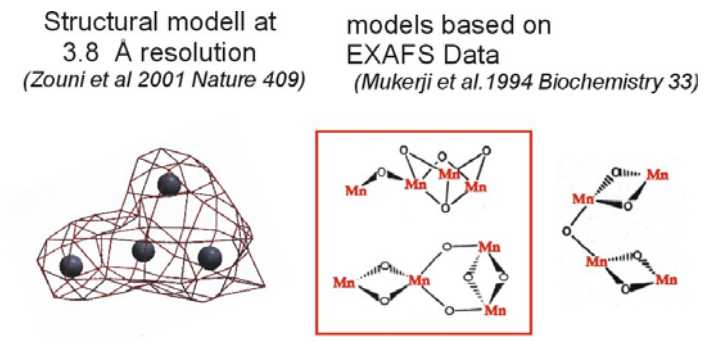

Figure 4. Present knowledge of the manganese cluster.

The 3.8 Å x-ray structure of PS II allows a first glimpse on the structure of the Mn cluster, however it is not sufficient to explain the mechanism of water splitting. It would be of major significance to observe the water molecules at atomic detail bound to the cluster and to unravel the secrets of water splitting. These experiments may best be achieved by utilization of the proposed MaNDi beamline at the SNS.

Neutron diffraction may unravel the mechanism and pathway of the protons that are released during the catalytic cycle. A hypothesis exists that the redox active tyrosine may not only extract electrons but hydrogen atoms from the Mn cluster. The unraveling of the mechanisms of water splitting by Photosystem II would be the ultimate goal for neutron diffraction experiments. The interesting point would be not only to get a static high resolution picture of the complex, but we may also perform the data collection on different oxidation states of the cluster, so that the whole catalytic cycle can be visualized at atomic detail.

Another important question in this respect is the question of water channels in PS II. The Mn cluster is deeply buried into the protein and the question arises as to how water can enter the catalytic site. Recently, we improved the x-ray resolution limit of the crystals to 3.6 Å resolution and saw for the first time details of the extrinsic subunits that stabilize the Mn cluster. The PsbO protein forms a tube like β-barrel structure pointing towards the Mn cluster. *Does this tube contain a water channel that allows the water molecules entering the water oxidation site in a well-defined manner? This important question could also be answered in the near future if MaNDi would become available.*

References

Jordan P, Fromme P, Klukas O, Witt HT, Saenger W, Krauß N (2001) Three-dimensional structure of cyanobacterial photosystem I at 2.5 Å resolution. Nature **411:** 909-917

Klukas O, Schubert WD, Jordan P, Krauss N, Fromme P, Witt HT, Saenger W (1999) Localization of two phylloquinones, Q_K and Q_K', in an improved electron density map of photosystem I at 4 Å resolution. J Biol Chem **274:** 7361-7367

Klukas O, Schubert WD, Jordan P, Krauss N, Fromme P, Witt HT, Saenger W (1999) Photosystem I, an improved model of the stromal subunits PsaC, PsaD, and PsaE. J Biol Chem **274:** 7351-7360

Krauss N, Hinrichs W, Witt I, Fromme P, Pritzkow W, Dauter Z, Betzel C, Wilson KS, Witt HT, Saenger W (1993) Three-dimesional structure of system I of photosynthesis at 6 Å resolution. Nature **361:** 326-361
Prince SM, Howard TD, Myles DA, Wilkinson C, Papiz MZ, Freer AA, Cogdell RJ, Isaacs NW (2003) Detergent structure in crystals of the integral membrane light-harvesting complex LH2 from Rhodopseudomonas acidophila strain 10050. J Mol Biol **326:** 307-315
Snijder HJ, Timmins PA, Kalk KH, Dijkstra BW (2003) Detergent organisation in crystals of monomeric outer membrane phospholipase A. J Struct Biol **141:** 122-131
Zouni A, Jordan R, Schlodder E, Fromme P, Witt HT (2000) First photosystem II crystals capable of water oxidation. Biochim Biophys Acta **1457:** 103-105
Zouni A, Witt HT, Kern J, Fromme P, Krauß N, Saenger W, Orth P (2001) Crystal structure of photosystem II from Synechococcus elongatus at 3.8 Å resolution. Nature **409:** 739-743

Counter-Diffusion Methods in the Growth of Macrocrystals for Neutron Diffraction

Dan Carter
New Century Pharmaceuticals, Inc. Huntsville Alabama

The growth of large protein crystals can be enhanced by the use of the Diffusion Controlled Apparatus for Microgravity (DCAM) and the Counter-Diffusion Cell (CDC; Figure 1: Carter et al., 1999). This crystallization apparatus can also facilitate the exchange of deuterated reagents after crystals have formed. Standard growth of large crystals can take place over a few days to a few weeks depending on how one controls the equilibration rates. Typically in the DCAMs, a 90 day time period is used. If you can grow 0.3 mm crystals by hanging drop methods, you can grow large crystals with the DCAMs.

The DCAMs are commercial systems that were developed by funding from NASA. The normal problem with growing large crystals is that mosaicity increases as the size increases. Therefore, they designed a devise called the counter-diffusion cell which is about the size of a dime. The device controls equilibration between two chambers that is separated by an agarose gel plug. You can change the gel to different diameters and lengths to approach supersaturation differently. If you are interested in working with the DCAMs, you can contact Dan Carter at dcarter@newcenturypharm.com.

Figure 1. DCAM components. See Carter, D. C., Wright, B., Miller, T., Chapman, J., Twigg, P., Keeling, K., Moody, K., White, M., Click, J. Ruble, J., Ho, J. X., Adcock-Downey, L., Bunick, G. J. & Harp, J. M. (1999). J. Cryst. Growth,196, 602-609.

Hydrogen and Hydration in Proteins and DNA Obtained by BIX-3 and BIX-4

Nobuo Niimura
Japan Atomic Energy Research Institute

In this talk hydrogen and hydration in the crystal structures of myoglobin (Mb) [1],wild-type of rubredoxin (Rb-w) [2], mutant of rubredoxin (Rb-m) [3], hen egg-white lysozyme (HEWL) at pH4.9 [4] and Pig Cubic Insulin [5] will be discussed

Hydrogen bond

The hydrogen bond plays an important role in numerous biological phenomena. Hydrogen bonds are directional and form several kinds of networks in many biological macromolecules**.** However, since it is not easy to determine the positions of all the hydrogen atoms in protein molecules using x-rays or NMR alone, any detailed discussion of hydrogen bonds that require the positions of the hydrogen atoms is not possible without more precise information. High resolution neutron protein crystallography enables one to examine H-bonds and identify the weak H-bonds and bifurcated hydrogen bonds in protein structures. Our analysis shows that the bifurcated H-bonds are present at the terminal regions of α-helix and 3_{10} helix in several proteins.

H/D exchange

Studies on the crystals of wild-type rubredoxin [2] in D_2O solution showed that 24 out of 74 hydrogens at potentially exchangeable sites do not have significant positive (deuterium) peaks at the expected positions. Of those, 11 atoms are bonded to nitrogen atoms of the main chain, implying that those positions are not fully accessible to the H/D exchange process. Comparing this result with the distribution of *B*-factors and accessible surface area (ASA) of the main chain atoms, it is seen that the H/D atoms having small H/D exchange ratios also have small B factor values and small ASAs. These results not only show that those atoms are located in the interior of the protein molecule, but also suggest that the regions around those atoms have such a rigid structure that solvent molecules are unable to contact them. H/D exchange studies on rubredoxin (mutant) [3] and myoglobin [1] reveal that results are similar in both cases.

Hydrogens in histidine

The protonation and deprotonation of two nitrogen atoms ($N\pi$, $N\tau$) in imidazole ring of histidine have important implications in the function of insulin and the formation of a metal complex. The cubic insulin is a hetero-dimer with two chains, A-chain and B-chain. Fig. 1 (a) and (b) show neutron diffraction $2|F_o|-|F_c|$ Fourier maps of His5 and His10 in B-chain of cubic insulin at 1.6 Å resolution [5]. In His5 in B-chain, $N\pi$ is protonated and $N\tau$ is deprotonated, while in His10 both $N\pi$ and $N\tau$ are protonated.

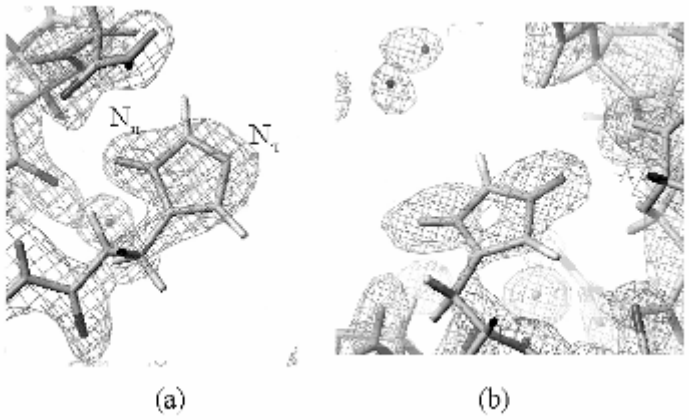

Figure 1. 2|*F*o|-|*F*c| positive nuclear density neutron map of (a) His5 and (b) His10 in the B-chain of cubic insulin.

Acidic hydrogens in histidine residues

Accessible polar hydrogen atoms can be exchanged by deuterium when the protein crystals are grown in D_2O. However, the hydrogen atoms bonded to carbon, in general, are not exchangeable. Interestingly we found that the hydrogen atom bonded to the $C_{\varepsilon 1}$ carbon atom of His97 in metmyoglobin exchanges with deuterium. His97 is located on the proximal side of the heme plane while the ligand binding position is on the distal site. The exchange seems to happen due to the fact that the $C_{\varepsilon 1}$-H imidazole group is the most acidic C-H bond found in amino acids [6]. An occupancy refinement of the deuterium exchange reveals a ratio of 80% D/ 20% H. To our knowledge, this is the first time neutron diffraction has been used to verify the acidic character of the $H_{\varepsilon 1}$ atom of His97 in myoglobin. Similar observation has been made recently in hen egg-white lysozyme [7].

Classification of hydration

We have categorized water molecules in the crystals into the following classes based on their appearance in Fourier maps: triangular, ellipsoidal stick, and spherical shapes. The ellipsoidal stick shapes can be further sub-divided as short and long depending on their appearance in the maps. We found that this classification conveniently reflects the degree of disorder and/or dynamic behavior of a water molecule. Typical examples of different shapes are shown in Figs. 2 (a-d). The green and red contours in ($2|F_o|-|F_c|$) maps correspond to the neutron and x-ray data, respectively. The oxygen positions observed by x-ray and neutron scattering coincide. In the case of the triangular shape (Fig. 2(a)), the 2 D and the O atoms of the water molecule are all H-bonded to (O/N) and deuterium atoms, respectively. Thus, the orientation of this water molecule is well-defined. For short ellipsoidal stick shape (Fig. 2(b)) it is seen that the oxygen position observed by x-rays is located at one end of the neutron Fourier peak, and only one

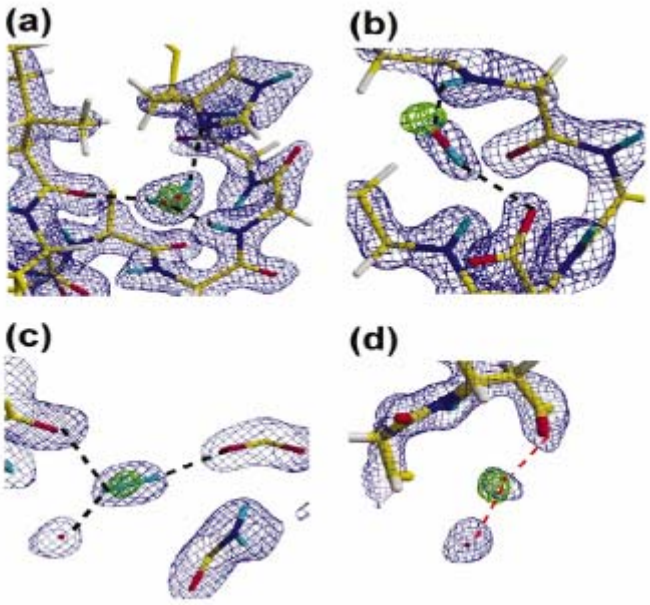

Figure 2. Neutron 2*j*Fo*j*-*j*Fc*j* maps of water molecules in myoglobin and a rubredoxin mutant crystals wherein different shapes of densities are seen for water: (a) triangular shape, (b) short ellipsoidal shape, (c) long ellipsoidal shape and (d) spherical shape. In these maps, the blue contours correspond to neutron peaks, while the green contours correspond to oxygen peaks from x-ray data. Observed atoms from the neutron data are shown as stick diagrams.

deuterium atom is visible. The observed D and O atoms are H-bonded to neighboring O/N and D atoms respectively but the other deuterium atom was not identified because of the molecular rotation (or packing disorder) around the fixed O-D bond. Thus, we interpret short ellipsoidal stick shaped peaks to represent water molecules rotationally disordered around an O-D bond. Fig. 2(c) shows an example of the long ellipsoidal stick-shaped peak. The O position observed by x-rays is located in the middle of the neutron Fourier peak, and the two D atoms are seen in the neutron map. In this case, the two D atoms are H-bonded to neighboring O and/or N atoms, but the O atoms of the D_2O molecule cannot be identified because of the molecular rotation or packing disorder around the D-D axis. Finally, in the case of spherical-shaped peak (Fig. 2(d)) only the center of gravity of this type of water molecule can be defined because its orientation is totally disordered. A spherical peak in a neutron Fourier map implies that the water molecule is freely rotating. Although the above classification has been carried out solely based on the appearance of peaks in Fourier maps, we found a strong correlation between the shapes in the density maps and the number of hydrogen bonds that fixes the positions of atoms of water molecules. The average number of “anchor points” of triangular, ellipsoidal and spherical-shaped density for the water molecules are 2.3, 1.3 and 0.3, respectively. In the three proteins, Mb, Rb-w and Rb-m, the average populations of triangular, ellipsoidal and spherical shapes are 29%, 16% and 55%, respectively [8].

Dynamic behavior of hydration

The dynamic behavior of water molecules can be assessed by plotting the *B*-factors of atoms from neutron and x-ray diffraction [8,9]. The *B*-factors from the neutron analysis are the average values from three atoms (D, O and D), while those from the x-ray analysis correspond to O atoms only. The *B*-factors of oxygen atoms obtained by x-rays are in the range from 13 $Å^2$ to 45 $Å^2$. Interestingly, it turns out that the small, intermediate and large *B*-factors from the x-ray analysis correlate well with the water molecules having the triangular, ellipsoidal and spherical shapes in the neutron maps, respectively.

The role of hydrogen atoms in enzymology of Lysozyme

In the case of lysozyme the enzyme activity is less at pH 7 and maximum at pH 5 at which the carboxylate group of Glu35 is protonated. In the proposed mechanism of reaction of the lysozyme with oligosaccharides this proton gets transferred to the oxygen atom of the substrate (sugar) during its hydrolysis. In order to validate the role of this proton in the enzymology of lysozyme, neutron diffraction experiments were carried out on hen egg-white lysozyme crystals grown at pH 4.9 [4] and 7.0 [10]. Consistent to the above mechanism NMC revealed that the carboxylate oxygen of Glu35 is protonated at pH 4.9, but at pH 7 a water molecule is present at that site. The absence of the proton at the catalytic site residues explains the reduced activity of lysozyme at pH 7.0.

Conclusion and future prospects

1) With the development of the neutron imaging plate (NIP) a breakthrough occurred in the neutron protein crystallography [11] in increasing the data collection efficiency by an order of magnitude and resolution.

2) 1.5 Å resolution neutron protein crystallography provides better information on hydrogen atoms and hydration such as H-bonds, H/D exchanges, solvent dipole moment.

3) Currently neutron protein crystallography requires large protein crystals with a volume ~2 mm^3. Our studies show that a rational way to find the proper condition to grow large single crystals is to first determine the complete crystallization phase diagram including solubility curve. Typically large single crystal are grown under the supersaturated phase close to the solubility curve. Using the phase diagrams of DNA oligomer [12] and insulin [5] we grew large single crystals of insulin, DNA oligomer (Fig. 3) and human lysozyme.

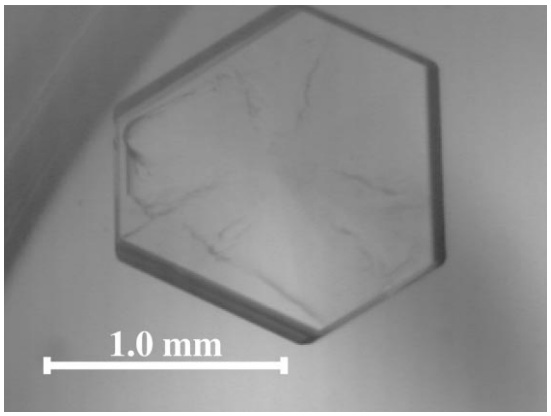

Figure 3. A photograph of a large single crystal (1.7 x 1.3 x 0.6 mm^3) grown under the following conditions: 0.4 ml D_2O solutions of DNA (1.5 mM), $MgCl_2$ (100 mM), MPD [30%(v/v)] at pD 6.6.

References

[1] Ostermann, A., Tanaka, I., Engler, N., Niimura,N. and Parak, F. E. (2002) Hydrogen and deuterium in myoglobin as seen by a neutron structure determination at 1.5 Å resolution. Biohpys. Chem. **95**, 183-193.

[2] Kurihara, K., Tanaka, I., Adams, M. W.W., Jenney.F.E., Jr., Moiseeva, N., Bau, R. and Niimura, N. (2001) Neutron diffraction study on the structure of rubredoxin from *Pyrococcus furiosus*. J. Phys. Soc. Jpn. Suppl., Sect. A, 7**0**, 400-402.

[3] Chatake, T., Kurihara, K., Tanaka, I., Adams, M.W.W., Jenney Jr., F.E., Tsyba, I., Bau, R. and Niimura, N. (2002) Applied Physics A**75**, 1-3
[4] Maeda, M., Fujiwara, S., Yonezawa, Y. and Niimura, N. (2001) Neutron Structure Analysis of Hen Egg-White Lysozyme at pH4.9. J. Phys. Soc. Jpn. **70**, Suppl. A 403-405
[5] Maeda,M., Chatake,T., Ostermann,A., Tanaka,I., Niimura,N. To be submitted.
[6] Matsuo, H., Oe, M., Sakiyama, F. and Narita, K. (1972) A new approach to the determination of pKa's of histidine residues in proteins. J. Biochem. **72**,1057-1060.
[7] Bon, C., Lehmann, M.S. and Wilkinson, C. (1999) Quasi-Laue neutron-diffraction study of the water arrangement in crystals of triclinic hen egg-white lysozyme. Acta Crystallogr. D**55**, 978-987.
[8] Chatake, T.; Ostermann, A.; Kurihara, K.; Parak, F.G.; Niimura, N. Hydration in proteins observed by high-resolution neutron crystallography. Proteins, to be published.
model of a ZnS_4 coordination unit in a protein, Proc. Natl. Acad. Sci U. S. A. **93**, 8836-8840.
[9] Engler, N., Ostermann, A., Niimura, N, and Parak, F.G., (2003) Hydrogen atoms in proteins: Positions and dynamics, PNAS. 100, 10243-10248
[10] Niimura, N., Minezaki, Y., Nonaka, T., Castanga, J-C., Cipriani, F., Hoghoj, P., Lehmann, M. S. and Wilkinson (1997) Neutron Laue diffractometry with an imaging plate provides an effective data collection regime for neutron protein crystallography. Nat Struct Biol. **4** ,909-914.
[11] Niimura, N., Karasawa, Y., Tanaka, I., Miyahara, J., Takahashi, K., Saito, H., Koizumi, S. and Hidaka, M. (1994) An imaging plate neutron detector. Nucl. Instrum. Methods A**349**, 521-525.
[12] Arai, S., Chatake, Y., Minezaki and Niimura, N. (2002) Crystallization of a large single crystal of a B-DNA decamer for a neutron diffraction experiment by the phase-diagram technique, Acta Cryst. D58, 151-153

Protein Crystallography with Spallation Neutrons: Results from the PCS at Los Alamos

Paul Langan
Los Alamos National Laboratory, Life Sciences Division

The protein crystallography station (PCS) is being used by the structural biology community to locate hydrogen (H) atoms and water molecules in proteins, nucleic acids and biological polymers (Figure 1). There are many reasons why it's important to know the location of protons but we've found that the overwhelming reason for most of our users is to determine enzyme mechanisms. In this talk I give a brief overview of the facility and its capabilities.

The Department of Energy Office of Biological and Environmental Research funds the PCS, providing the only resource for neutron protein crystallography in the US. Beam-time is allocated twice a year through a call for proposals and a peer review system and is free and open to everyone. Benno Schoenborn is principle investigator. I was project manager during design and construction and now I act as instrument scientist. The PCS is the first in the world to be built at a spallation source. Spallation neutron sources are a new arena for protein crystallography. Time-of-flight methods are used on the PCS to collect wavelength-resolved Laue protein crystallography data.

Figure 1. Inside the hutch at the PCS

The PCS has come on line at a time when Proteomics is offering the promise of structure-based information in drug design. X-ray diffraction will be the primary tool for establishing proteomics structure libraries. However it is not usually possible to locate H atoms and disordered water molecules using x-ray data, because H atoms are relatively weak x-ray scatterers. Since H atoms or ions are the primary motive force in most enzyme mechanisms, that means it's usually not possible to determine detailed enzymatic mechanism from x-ray data alone. Neutron diffraction can be used locate H atoms. Because of this I think that it can play an important auxiliary role in high throughput proteomics programs by providing information about the detailed mechanism of newly discovered enzymes.

Detailed design and construction of the PCS began in 1998, first beam was obtained in December 2000, the station was fully commissioned in 2001 and since August 2002 we've been running as a user facility. We completed the project ahead of time and within budget ($4.8M). The station was built a Los Alamos Neutron Science Center (LANSCE) as a collaboration between Bioscience Division, LANSCE division and also Brookhaven National Laboratory. At LANSCE neutrons are produced in pulses at a rate of 20Hz, over a wide range of wavelengths. The neutrons travel as a function of their wavelength down the flight path (Figure 2). By recording the time-of-flight information of a detected neutron, its wavelength can be calculated. The data collected in the PCS are resolved in wavelength. The wavelength-resolved Laue method has the advantages of the conventional Laue method, including rapid data collection,

but it does not suffer in the same way from reflection overlap and a build up of background scattering over the wavelength band, because the diffraction spots and the background are resolved in wavelength (Figure 2).

The neutron beam has a divergence of ±0.1^{o} and a size at the sample position of 5 mm or less. Sample sizes are typically ~2 mm^{3} but can be less if the protein is perdeuterated. The wavelength-resolved Laue patterns are collected on a large cylindrical (120^{o} horizontal, 20 cm vertical, radius 70 cm) PSD. The detector sits on the 2θ arm of the goniometer which allows it to swing out for high resolution studies and also to be raised or lowered. The 50^{o} κ goniometer is used to move the crystal through a number of different orientations, recording a wavelength-resolved Laue pattern at each setting. The number of settings required depends on space group symmetry and it can be anything from 6 settings to 24 settings. The collection time at each crystal setting depends on crystal volume and unit cell, and can be anything from 1 hour to more than a day. We've collected data sets in less than 5 days (Li *et al*, 2004, *Acta Cryst. D***60**, 200-202) and as many as 20 days (Hanson *et al*, 2004, *Acta Cryst. D***60**, in press). Data collection is coordinated from a PC that runs a java-based GUI. There are various options for data visualization. Data analysis is carried out used a customized version of d*TREK (Langan *et al*, 2004, *J. Appl. Cryst.* in press, Langan & Greene, 2004, *J. Appl. Cryst.* Submitted, Schoenborn & Langan, 2003, *J. Synchrotron Rad.*, **11**, 80-82).

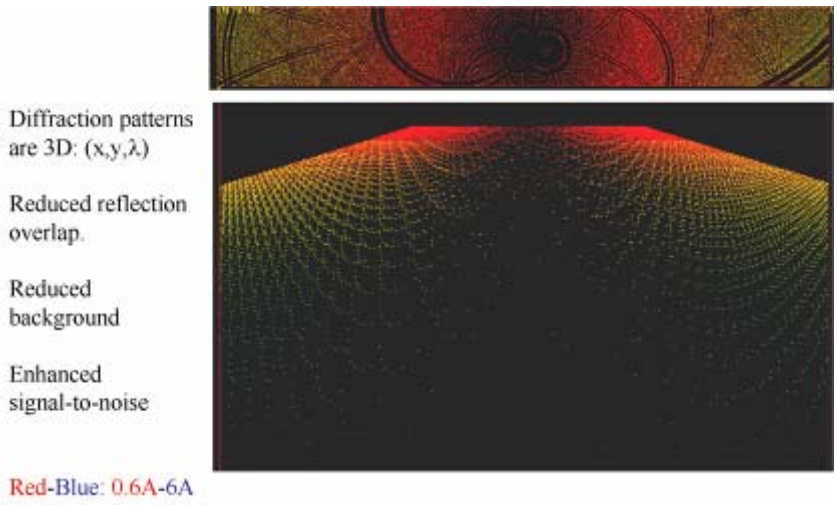

Figure 2. Wavelength resolved Laue in detector space.

Future plans for increasing the capabilities of the PCS include increasing the proton current at LANSCE from 100 μA to 200 μA, a new target moderator, more detector coverage (up to 4X), a perdeuteration laboratory and the development of new computational tools for Neutron Protein Crystallography. We expect that some of these developments will lead to many-fold gains in data collections efficiency.

DISCUSSIONS ON MACROMOLECULAR NEUTRON DIFFRACTION INSTRUMENTATION AT THE SNS

P. Thiyagarajan, Arthur Schultz, Jason Hodges, Christine Rehm, Andrew Mesecar

1. Introduction

By employing well established analytical procedures[1-5] and Monte Carlo simulations[6], the performance of *MaNDi* at both the coupled and decoupled liquid hydrogen moderators at the SNS has been investigated. Although, due to its long pulse widths, a coupled hydrogen moderator can provide higher neutron flux, calculations show that, for the high resolution applications in structural biology, *MaNDi* requires a high resolution moderator such as the decoupled liquid hydrogen moderator at SNS. This moderator can provide a high flux of cold neutrons in the wavelength region 1.5 to 5 Å and narrow pulse widths.

MaNDi has been designed with a 24.5 m flight path wherein a useful wavelength bandwidth of about 2.7 Å (without any frame overlap) will be available, given that the source frequency is 60 Hz at SNS. The instrument will employ a set of 3 choppers at 7.2 m, 8.2 m, and 10.4 m downstream from the moderator, respectively, for the selection of the wavelength band. State-of-the-art high index neutron supermirror guides will be used for the efficient beam transport leading to a flux gain at the sample position in the range of 2 to 10 when compared to that with no guide. A curved guide in the middle section will reduce the overall instrument background and will eliminate any potential radiation damage to the crystals of biological samples by x-rays and high energy neutrons from the target. The combination of a wide wavelength bandwidth and large solid angle detector coverage will provide unprecedented high through-put and resolution for *MaNDi* in comparison to the current facilities for NMC.

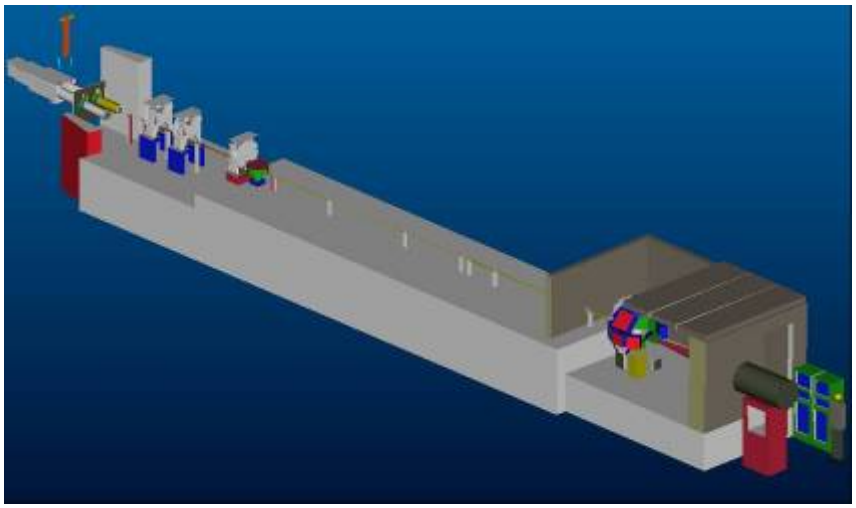

Figure 1. 3D conceptual model of *MaNDi*

2. Layout of *MaNDi*

The layout and the parameters of the *MaNDi* instrument determined from analytical calculations and Monte Carlo simulations are shown in Fig. 1 and Table 1, respectively.

TABLE 1. Instrument parameters of *MaNDi*

Moderator	Moderator type	Top Upstream
	Material	Para-Hydrogen
	Decoupler	Cadmium
	Poison	Gadolinium
	Poison depth	27 mm
	Width	0.10 m
	Height	0.12 m
Curved Guide	Starting point	6 m downstream
	Width	1.5 cm
	Height	1.5 cm
	Length	12 m
	Supermirror coating	$m = 3$
	Total turn angle	0.43°
	Radius of curvature	1599 m
	Line-of-sight lost	≈20 m
Straight Guide	Starting point	18 m downstream
	Width	1.5 cm
	Height	1.5 cm
	Length	Variable: Depends on resolution requirement
	Supermirror coating	m=3
Bandwidth Choppers	Positions	7.2 m, 8.2 m, 10.4 m
Moderator-to-sample distance		24 m
Wavelength range	2.0 Å ≤ λ ≤ 4.69 Å	$\Delta\lambda$ = 2.69 Å
Wavelength resolution		$\Delta\lambda/\lambda \approx 0.15\%$
Sample-to-detector distance		0.5 m
Detectors	Array of 2-D PSDs	1 mm resolution scintillation detectors

3. Moderator Choice

Since high resolution structural biology requires high neutron flux, a coupled hydrogen moderator has been proposed by many for NMC applications. However, when high resolution data for crystals with lattice constants in the range of 150 Å are required, our calculations show that it is important to consider both the flux and the resolution (pulse lengths of the emission time) of the moderator. The increased flux from the coupled moderator (8X that of the decoupled moderator) comes at the cost of a pulse width that is about 8X larger than that of the decoupled moderator[7]. Monte Carlo simulations show that if *MaNDi* views a coupled hydrogen moderator, the long tails in the emission times (pulse width) will be detrimental to the resolution.

3.1 Effective Flux of the Decoupled Hydrogen moderator

In order to make decisions on the optimal wavelength range for the diffraction experiments, an effective flux is calculated by weighting the flux from the moderator for the reflectivity of neutrons.

The integrated intensities I_{hkl} are reduced to structure factor amplitudes $|F_{hkl}|$ based on the Laue formula:

$$I_{hkl} = \phi(\lambda)\frac{V_s}{V_c}\frac{|F_{hkl}|^2}{V_c}\frac{\lambda^4}{2\sin^2\theta} \quad (1)$$

where $\varphi(\lambda)$ is the incident neutron intensity per unit wavelength range at wavelength λ ($n\cdot cm^{-2}\cdot sec^{-1}\cdot Å^{-1}$), V_s is the sample volume, V_c is the crystal unit cell volume, F_{hkl} is the structure factor, and 2θ is the Bragg angle. Terms for the detector efficiency, sample absorption, and extinction have not been included.

Equation (1) can be rewritten as

$$I_{hkl} = \phi(\lambda)\frac{V_s}{V_c^2}|F_{hkl}|^2\lambda^2 d_{hkl}^2 \quad (2)$$

This leads to an effective flux of

$$\phi_{\text{eff}}(\lambda) = \phi(\lambda)\cdot\lambda^2 \quad (3)$$

In this case, one takes into account that for any *hkl*, the *d*-spacing is constant regardless of the angle. Then, the optimal wavelength for measuring all Bragg peaks is the same, but the optimal angle will be different for each *hkl*. Multiplying the flux for the decoupled hydrogen moderator by λ^2 at each wavelength gives the curve shown in Fig. 2. It is clear from Fig. 2 that wavelengths in the range of 1.5 to 5.0 Å provide the highest effective flux.

In Figure 3, the wavelength dependence of the ratios of the total intensity from the coupled and decoupled moderators is plotted. This is the gain in total intensity provided by the coupled moderator. It is seen that for wavelengths of about 2.5 Å or greater a flux gain of 8X can be obtained with the coupled moderator. However, for wavelengths below 2.5 Å the gain decreases dramatically.

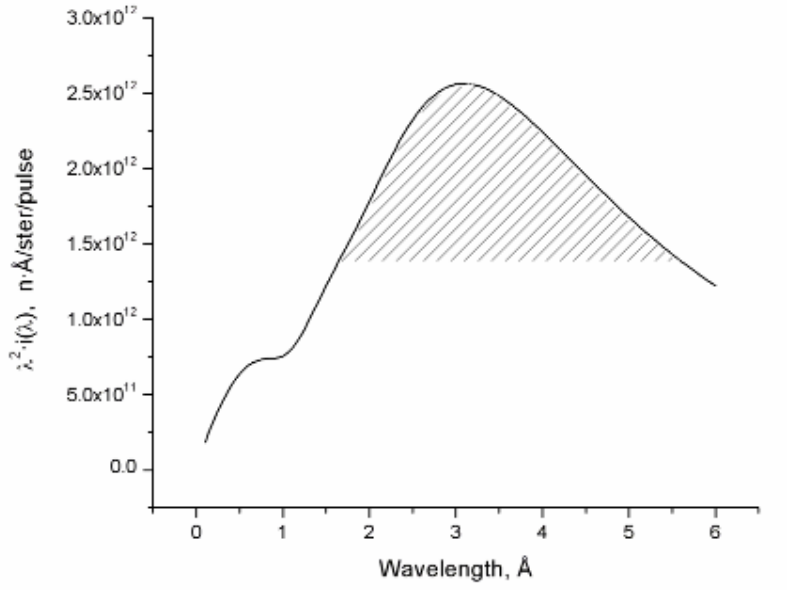

Figure 2. Plot of $\lambda^2\cdot\varphi(\lambda)$, n·Å/ster/pulse, versus wavelength in Å for the decoupled, poisoned hydrogen moderator.

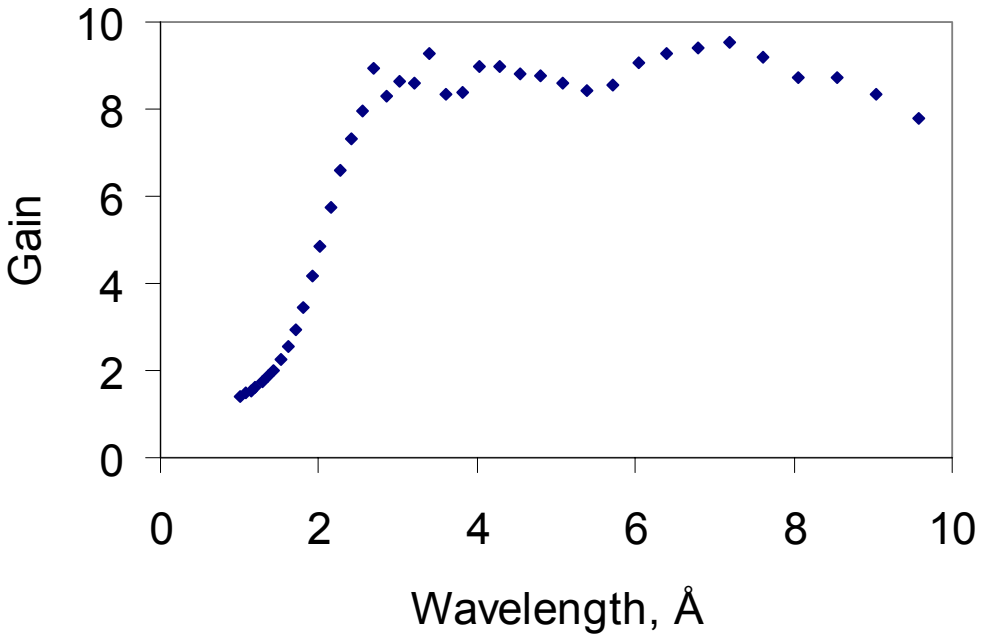

Figure 3. Intensity gain for the coupled hydrogen moderator obtained by calculating the ratio of the total intensities of the pulse at each wavelength of the coupled and decoupled moderators.

3.2 Resolution with Different Moderators

For a cubic unit cell with lattice constant *a*, it can be shown that to resolve two Bragg peaks at d_{min} the condition [3] in Equation (4) has to be fulfilled

$$R_{FW} < \frac{d_{\min}}{a} \tag{4}$$

where R_{FW} is the full width for complete peak separation.. Full width resolution is necessary for single crystal diffraction, since it is not sufficient just to resolve peaks, but rather it must be possible to integrate the intensity under the peak.

The pulse width time resolution contributes primarily to the resolution parallel to the diffraction vector, whereas the angular resolution primarily contributes to that in the perpendicular direction. From Jauch [3], we obtain the maximum allowable pulse length (full width)

$$\Delta t_{pulse}(FW) \leq 504.8L(\frac{d^2_{\min}}{a})\sin\theta \tag{5}$$

which must be met for peaks to be completely separated in the direction of the reciprocal lattice vector at d_{min} for a crystal with lattice constant *a*. In this equation, the units are: *t*, μs; *L*, m; d_{min} and *a*, Å.

Fig. 4 shows the pulse shapes for 2.55 Å neutrons from the coupled and decoupled liquid hydrogen moderators. For the coupled hydrogen moderator, the intensity at the peak region of the pulse is only about 1.5X greater than that from a decoupled hydrogen moderator. However, the pulse width is over 8X larger for the coupled moderator. The values for the

coupled and decoupled moderators are compared in Table 2. Since 99% can be considered as too difficult to achieve, we have adopted a goal of 90% of the total intensity. It is seen from Table 2 that the 8X gain in intensity with the coupled moderator comes at the expense of nearly 10X larger pulse width for the decoupled moderator. The longer pulse widths at the coupled moderator, in addition to affecting the resolution parallel to the q-vector, will increase the background by about 8X, thus affecting the signal to noise ratio of the diffraction peaks.

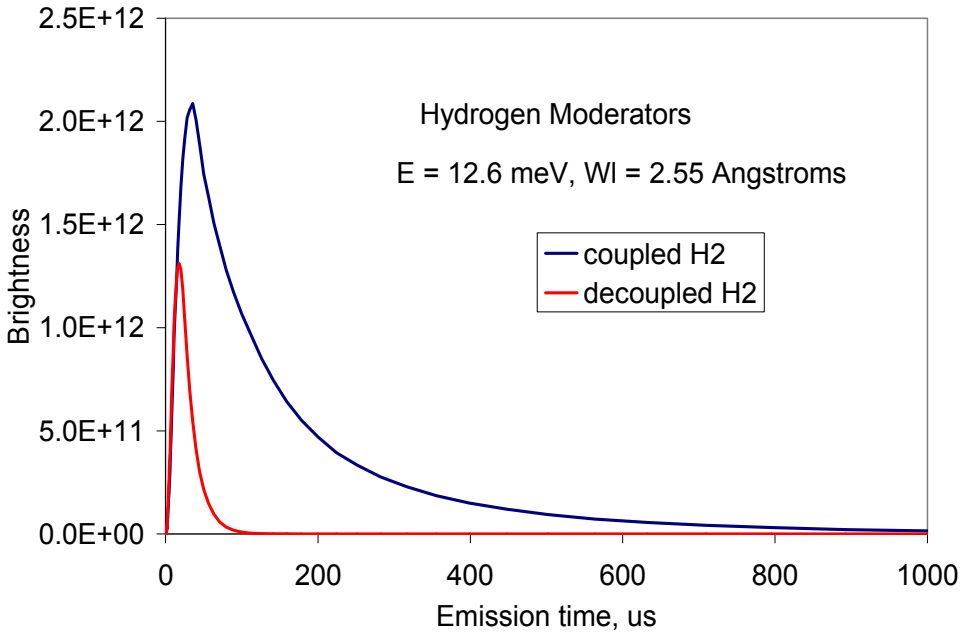

Figure 4. Brightness as a function of emission time in μs for neutrons with λ = 2.55 Å for the coupled and decoupled liquid hydrogen moderator at the HPTS at SNS.

TABLE 2. Comparison of coupled and decoupled H_2 moderators for the pulse corresponding to λ = 2.55 Å

Parameter	Coupled H_2	Decoupled H_2	Ratio
Total intensity (n/ster/pulse/eV)	3.06×10^{14}	3.84×10^{13}	8.0
Gaussian FW = 2.13 FWHM (μsec)	193	52	3.7
Simulated FW at 90% of total intensity (μsec)	430	45	9.6
FW at 10% of max (μsec)	335	58	5.8

TABLE 3. Calculated maximum allowed pulse full widths [Eq. (5)] and the pulse full widths of the moderators for a 24.5 m instrument.

2θ (deg)	λ (Å)	Equation (7) FW (μsec)	Coupled FW (μsec)	Decoupled FW (μsec)	FW Ratio	Intensity Ratio
30	0.776	49	33	17	1.9	1.1
60	1.500	94	300	27	11.1	2.2
90	2.121	132	400	44	9.1	5.8
120	2.598	162	430	58	7.4	8.0
150	2.898	181	445	66	6.7	8.3

Table 3 provides the maximum allowable pulse full widths derived from equation (5) for different wavelengths and corresponding Bragg angles to resolve peaks for a cubic system with a = 150 Å, d_{min} = 1.5 Å, and L = 24.5 m. Also shown are the full widths corresponding to 90% of the total intensity, or 10% of the maximum, whichever is longer, for the pulse from each moderator.

The data in Table 3 lead to the following conclusions:

- The pulse width of the decoupled moderator is more than adequate at all scattering angles and wavelengths. Perhaps a partially coupled moderator or one with a greater poison depth could be useful, but such a moderator is not available at the SNS.
- The FW values for the coupled moderator are higher than the values in Equation (5) and hence a 24.5 m long instrument cannot take advantage of the higher flux with the coupled moderator. One way to use the higher flux from the coupled moderator for NMC is by increasing the length of the flight path to 75 m [see Equation (5)].

Although such a long flight path instrument can be useful for NMC applications, there are several disadvantages.

- Resolution is still borderline as can be seen in Fig. 5, where we have shown the peak shapes for a top hat function corresponding to a d_{min} = 1.5 Å for a cubic unit cell of 150 Å. The peaks are well separated for a 24 m long instrument with a decoupled liquid hydrogen moderator, while there is a large peak overlap for a similar length instrument viewing a coupled moderator. Although the peak overlap has improved for a 75 m long instrument, it is still inferior to the decoupled moderator case.
- The gain factor will be reduced by a factor of 3, as the usable wavelength bandwidth ($\Delta\lambda$) will decrease from 2.67 Å to less than 0.9 Å due to frame-overlap condition.
- Total guide efficiency for longer wavelengths at 75 m will be about 60% (based on MC simulations) and much less for shorter wavelengths. The gain factor will further reduce to 1.6 or less.
- There is a large additional cost associated with the construction of a 75 m long instrument.

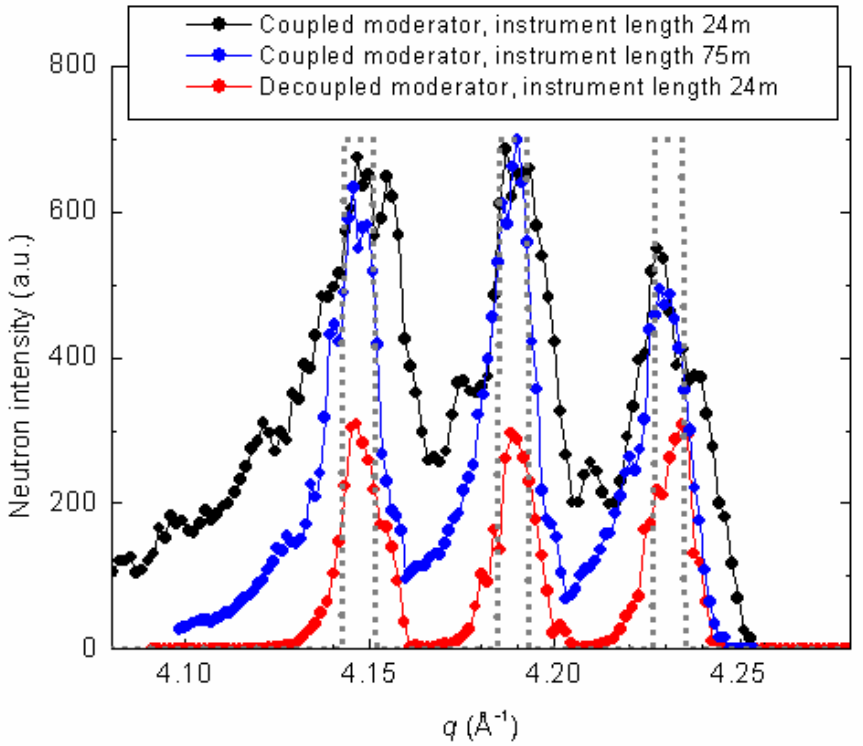

Figure 5. Peak shapes for a top hat function corresponding to a d_{min} = 1.5 Å for a cubic unit cell of 150 Å. MC simulation results for 3 different instrument configurations of *MaNDi*.

4. Neutron Guide System

To efficiently transport cold neutrons from the moderator to the sample position, *MaNDi* will use high index curved and straight guides because of their following advantages:

- Neutron guides offer significant gain in flux when compared to natural collimation viewing the whole moderator.
- Curved guides in the middle section of the beam line make it possible to gently steer the neutron beam such that the sample is completely out of line-of-sight of the source.
- Small widths of the beam allow for the more efficient operation of bandwidth choppers for wavelength selection.

A curved guide provides two advantages: (1) It has a clear cut-off wavelength, i.e., it prevents leakage of high-energy neutrons through absorbing beam conditioning devices (chopper blades, slits etc.), and (2) It will make the operation of *MaNDi* easier from the safety and sample stability points of view because it will allow only cold neutrons in the beam at the sample position.

Monte Carlo (MC) simulations using the *IDEAS* package [6] were used to optimize the length, location, curvature, and type of supermirror coating of the neutron guide system, and the distance from the guide exit to the sample. The *MaNDi* guide system starts at a distance of 6 m

from the moderator, and consists of a 12-m-long curved guide followed by a straight guide (Fig. 6) whose length can be selected based on the resolution requirement. The sample position is at

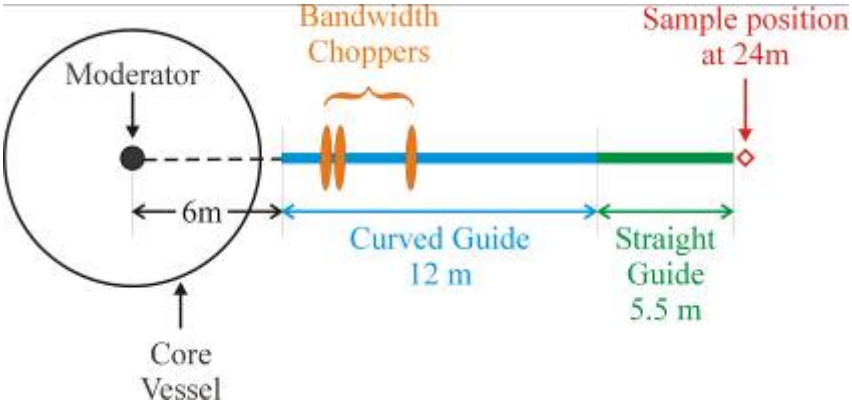

Figure 6. Schematic layout of the neutron guide system and choppers

24 m and the distance between sample and detector will be on the order of 0.5 m. However, the sample-to-detector distance will be defined at a later stage giving due consideration to the spatial resolution of the detector, cost, Δq resolution, etc. Fig. 7 shows the ratio of the intensity values at the sample position with and without guides as a function of wavelength. It follows that substantial gain in flux can be achieved by using a guide system (supermirror coating m = 3) when compared to the natural collimation. The gain in intensity is related to the increase in the angular divergence of the beam (e.g. for neutrons with λ = 2 Å the FWHM beam divergence is ≈ 0.3°). However, the increase in divergence can be exploited to match the resolution requirements of a given experiment by using a variety of collimators at the sample position.

5. Beam Defining Optics

A variety of beam defining optics such as Soller collimators, polycapillary focusing optics[8], tapered guides, and pinhole collimators will be inserted between the guide exit and the sample to optimize the beam divergence to experimental requirements. Such flexibility will not be possible without the use of neutron guides.

6. Detectors

An array of state-of-the-art high efficiency position sensitive area detectors with a spatial resolution of 1 mm will be used to cover a wide solid angle around the sample. Recently developed scintillation detectors for the time-of-flight single crystal neutron diffractometer SCD at IPNS can potentially be used. One detector will be used to measure the low angle reflections.

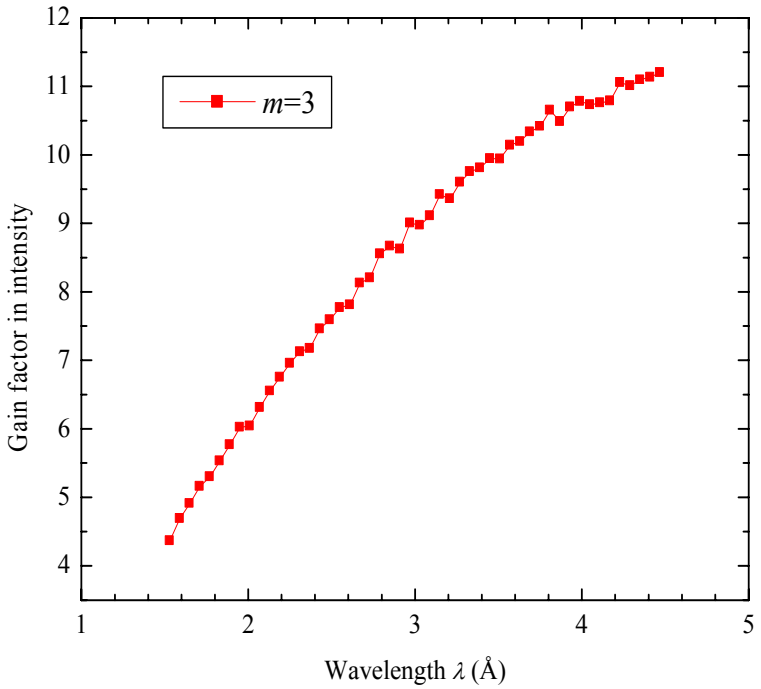

Figure 7. Gain in intensity versus wavelength in Å when using an *m=3* neutron guide relative to no guide

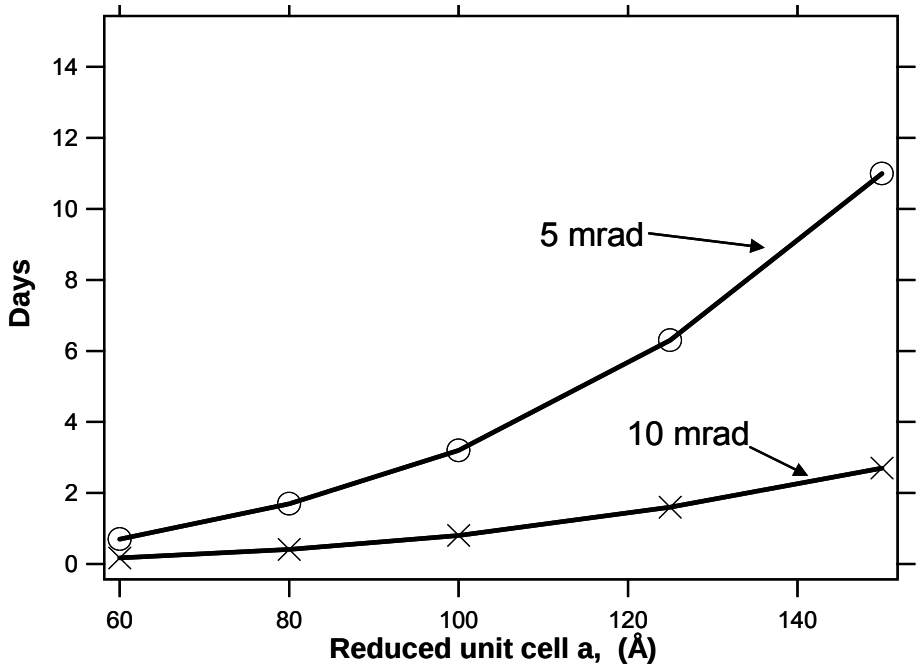

Figure 8. Data collection times for *MaNDi* for 0.125 mm^3 95% deuterated protein crystals with different unit cell dimensions. The flux on the sample can be increased at the expense of higher beam divergence (10 mrad vs. 5 mrad). However, for crystals that can tolerated the higher divergence, the data collection time is significantly reduced.

7. Instrument Performance

The performance of *MaNDi* has been calculated based on counting times necessary to obtain a complete data set for protein crystals with different unit cell sizes, by taking into consideration of the data precision, Debye-Waller factor, flux, and incoherent background.

We calculated counting times based on an equation proposed by Jauch [3]. Fig. 8 shows the data collection times for MaNDi. Validation of this approach was achieved by using the published beam time data used for a few protein crystals of known volume from PCS, BIX3, and LADI.

For crystals of deuterated proteins with a volume of 0.125 mm^3 a complete data set for d_{min} = 2 Å can be obtained from *MaNDi* in a few days (Fig. 8). Our calculations indicate that a similar amount of beam time will be required to obtain data of similar precision for 1 mm^3 normal protein crystals.

The counting times for d_{min} = 1.5 Å for the above systems will be an order of magnitude higher than those for d_{min} = 2.0 Å. For instance, crystals with a 60 Å unit cell will require about 7 days, while those with a 100 Å unit cell will require about 30 days to obtain data of similar precision. Current instruments for NMC will require 10 to 50 times longer than the above times. Thus the performance of *MaNDi* promises to open up new avenues thus far not available for NMC.

8. References

1. Jauch, W. *Prospects of ISIS in single-crystal diffractometry*. In *ISIS Workshop*. 1986. Rapallo, Italy.
2. Jauch, W., *Transactions ACA*, 1993. **29**: p. 55-61.
3. Jauch, W., *J. Neutron Research*, 1997. **6**: p. 161-171.
4. Jauch, W. and H. Dachs, *SNQ Information*, 1984 (Issue No. 5): p. 12-18.
5. Jauch, W. and H. Dachs, in *Neutron Scattering Instrumentation for SNQ*. 1984, KFA-Jülich: Jülich. p. 31.
6. Lee, W.-T. and X.-L. Wang, *Neutron News*, 2002. **13**: p. 30-34.
7. Iverson, E.B., *SNS Moderators*. 2002: http://www.sns.anl.gov/components/moderator/HPTS-sct.shtml.
8. Gibson, W.M., et al., *J. Appl. Cryst.*, 2002. **35**: p. 677-683.

INSTRUMENT DEVELOPMENT TEAM

Bau	Robert	University of Southern California	bau@usc.edu
Beamer	Lesa	University of Missouri-Columbia	beamerl@missouri.edu
Blessing	Robert H.	State University of New York, Buffalo	blessing@hwi.buffalo.edu
Bunick	Gerard J.	Oak Ridge National Laboratory	bunickgj@ornl.gov
Carter	Dan	New Century Pharmaceuticals, Inc.	dcarter@newcenturypharm.com
Cowan	John	Argonne National Laboratory	jacowan@anl.gov
Davidson	Victor	University of Mississippi Medical Center	vdavidson@biochem.umsmed.edu
Dealwis	Chris	University of Tennessee	cdealwis@utk.edu
Egli	Martin	Vanderbilt University	martin.egli@vanderbilt.edu
Fromme	Petra	Arizona State University	pfromme@asu.edu
Gardberg	Anna	University of Illinois at Chicago	gardberg@uic.edu
Ginell	Stephan	Argonne National Laboratory	ginell@anl.gov
Glusker	Jenny	Fox Chase Cancer Center	JP_Glusker@fccc.edu
Guo	Hong	University of Tennessee	hguo1@utk.edu
Harrison	David H.	The Chicago Medical School	David.Harrison@finchcms.edu
Hanson	Debra	Argonne National Laboratory	dkhanson@anl.gov
Hanson	B. Lief	University of Toledo	bryant.hanson@utoledo.edu
Hasson	Miriam S.	Purdue University	mhasson@purdue.edu
He	Chuan	The University of Chicago	chuanhe@midway.uchicago.edu
Helliwell	John	University of Manchester	john.helliwell@man.ac.uk
Hodges	Jason	Oak Ridge National Laboratory	hodges@anl.gov
Huq	Ashfia	Argonne National Laboratory	ahuq@anl.gov
Joachimiak	Andrzej	Argonne National Laboratory	andrzejj@anl.gov
Johnson	Michael E.	University of Illinois at Chicago	mjohnson@uic.edu
Koetzle	Thomas	Argonne National Laboratory	tkoetzle@anl.gov
Kolesnikov	Alexander	Argonne National Laboratory	akolesnikov@anl.gov
Kossiakoff	Anthony	University of Chicago	koss@cummings.uchicago.edu
Kundrot	Craig	NASA/Marshall Space Flight Center	craig.e.kundrot@nasa.gov
Laible	Phillip	Argonne National Laboratory	laible@anl.gov
Lal	Jyotsana	Argonne National Laboratory	jlal@anl.gov
Langan	Paul	Los Alamos National Laboratory	langan_paul@lanl.gov
Littrell	Kenneth	Argonne National Laboratory	klittrell@anl.gov
Loong	Chun	Argonne National Laboratory	ckloong@anl.gov
Loria	J. Patrick	Yale University	j.patrick.loria@yale.edu
Mathews	F. Scott	Washington University	mathews@biochem.wustl.edu
Mesecar	Andrew	University of Illinois-Chicago	mesecar@uic.edu
Myles	Dean	Oak Ridge National Laboratory	mylesda@ornl.gov
Niimura	Nobuo	JAERI	niimura@mx.ibaraki.ac.jp
Pahl	Reinhard	University of Chicago	pahl@cars.uchicago.edu
Petsko	Gregory A.	Brandeis University	petsko@brandeis.edu
Plapp	Bryce V.	University of Iowa	bv-plapp@uiowa.edu
Podjarny	Alberto	IGBMC	podjarny@igbmc.u-strasbg.fr
Pokkuluri	Raj	Argonne National Laboratory	rajp@anl.gov
Ramaswamy	S	University of Iowa	s-ramaswamy@uiowa.edu
Rehm	Christine	Oak Ridge National Laboratory	rehmc@ornl.gov
Ringe	Dagmar	Brandeis University	ringe@brandeis.edu

INSTRUMENT DEVELOPMENT TEAM - cont'd

Rosenbaum	Gerold	Argonne National Laboratory	rosenbaum@anl.gov
Rosenberg	John M.	University of Pittsburgh	rosenbrg@pitt.edu
Sanishvili	Ruslan	Argonne National Laboratory	rsanishvili@anl.gov
Santarsiero	Bernard	University of Illinois at Chicago	bds@uic.edu
Savage	David	University of California	savage@msg.ucsf.edu
Schiffer	Marianne	Argonne National Laboratory	mschiffer@anl.gov
Schoenborn	Benno	Los Alamos National Laboratory	schoenborn@lanl.gov
Schultz	Arthur	Argonne National Laboratory	ajschultz@anl.gov
Snell	Edward	NASA Laboratory for Structural Biology	eddie.snell@msfc.nasa.gov.
Stamper	Geoffrey	Abbott Laboratory	geoffrey.stamper@abbott.com
Sukumar	Narayanasami	Cornell University	sukumar@aps.anl.gov
Tanaka	Ichiro	JAERI	tanaka@neutrons.tokai.jaeri.go.jp
Teeter	Martha	University of California/Boston College	mmteeter@ucdavis.edu
Thiyagarajan	P. (Thiyaga)	Argonne National Laboratory	thiyaga@anl.gov
Timmins	Peter	Institut Laue Langevin	timmins@ill.fr
Wlodawer	Alexander	National Cancer Institute	wlodawer@ncifcrf.gov
Worcester	David	University of Missouri	worcesterd@missouri.edu

IDT EXECUTIVE COMMITTEE

Andrew Mesecar (Chair)

Gerard J. Bunick
Jenny Glusker
Chris Dealwis
Martin Egli
John Helliwell
Anthony Kossiakoff
Paul Langan
Dean Myles
Alberto Podjarny
Benno Schoenborn
Arthur Schultz
P. Thiyagarajan

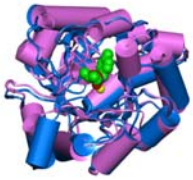

Workshop on
NEUTRON MACROMOLECULAR CRYSTALLOGRAPHY AT THE SPALLATION NEUTRON SOURCE

Argonne National Laboratory - Intense Pulsed Neutron Source

October 2-3, 2003

LIST OF ATTENDEES

Ian Anderson
Oak Ridge National Laboratory
Spallation Neutron Source
701 Scarboro Rd.
Oak Ridge, TN 37831-6477
Phone: 865-574-0548
FAX: 865-241-5177
andersonian@ornl.gov

R. Kent Crawford
Oak Ridge National Laboratory
Spallation Neutron Source
701 Scarboro Rd.
Oak Ridge, TN 37831
Phone: 865-241-6481
FAX: 865-241-5177
crawfordrk@ornl.gov

Stephan Ginell
Argonne National Laboratory
Biology CAT
9700 S. Cass Ave., Bldg. 202
Argonne, IL 60439
Phone: 630-252-3972
FAX: 630-252-6126
ginell@anl.gov

Robert Bau
University of Southern California
Chemistry Dept.
Building: ACB 101, Mail Code: 0744
Los Angeles, CA 90089
Phone: 213-740-2692
FAX: 213-740-0930
bau@usc.edu

Victor Davidson
University of Mississippi Medical Center
Dept. of Biochemistry
2500 N. State St.
Jackson, MS 39216-4505
Phone:
FAX:
vdavidson@biochem.umsmed.edu

Hong Guo
University of Tennessee
Biochemistry & Cellular & Molecular Biology
1414 W. Cumberland Ave.
Knoxville, TN 37996
Phone: 865-974-3610
FAX:
hguo1@utk.edu

Gerry Bunick
Oak Ridge National Laboratory
Life Sciences Division
PO Box 2009 MS8080
Oak Ridge, TN 37831-8080
Phone: 865-576-2685
FAX: 865-574-1274
bunickgj@ornl.gov

Chris Dealwis
University of Tennessee
Biochemistry & Cellular & Molecular Biology
M407 Walters Life Science Bldg.
Knoxville, TN 37996
Phone: 865-974-4088
FAX:
cdealwis@utk.edu

Deborah Hanson
Argonne National Laboratory
Biology CAT
9700 S. Cass Ave., Bldg. 202
Argonne, IL 60439
Phone: 630-252-4189
FAX: 630-252-5517
dkhanson@anl.gov

Jack Carpenter
Argonne National Laboratory
Intense Pulsed Neutron Source
9700 S. Cass Ave., Bldg. 360
Argonne, IL 60439
Phone: 630-252-5519
FAX: 630-252-4163
jmcarpenter@anl.gov

Martin Egli
Vanderbilt University
Dept. of Biological Sciences
Medical Research Building III, Room 5270 B
Nashville, TN 37235
Phone: 615-343-8070
FAX: 615-322-7122
martin.egli@vanderbilt.edu

L. Bryant Hanson
University of Tennessee
Genome Science & Technology
PO Box 2009
Oak Ridge, TN 37831-8080
Phone: 865-574-1210
FAX: 865-574-1274
blm@ornl.gov

Dan Carter
New Century Pharmaceuticals, Inc.
895 Martin Road
Huntsville, AL 35824
Phone:
FAX:
dcarter@newcenturypharm.com

Petra Fromme
Arizona State University
Dept. of Chemistry & Biochemistry
Physical Science Building PS-C155
Tempe, AZ 85287-1604
Phone: 480-965-9028
FAX: 480-965-2747
pfromme@asu.edu

David H. Harrison
Finch University/The Chicago Medical School
Biochemistry Dept.
3333 Green Bay Road
North Chicago, IL 60004
Phone: 847-578-8609
FAX:
David.Harrison@finchcms.edu

John Cowan
Argonne National Laboratory
Intense Pulsed Neutron Source
9700 S. Cass Ave., Bldg. 360
Argonne, IL 60439
Phone: 630-252-3593
FAX: 630-252-4163
thiyaga@anl.gov

Anna Gardberg
University of Illinois at Chicago
Biochemistry Department
900 S. Ashland Ave.
Chicago, IL 60607-7173
Phone: 312-996-6299
FAX:
gardberg@uic.edu

Chuan He
The University of Chicago
Dept. of Chemistry
5735 S. Ellis Avenue
Chicago, IL 60637
Phone: 773-702-5061
FAX: 773-702-0805
chuanhe@midway.uchicago.edu

John Helliwell
University of Manchester
Department of Chemistry
Oxford Road
Manchester, M13 9PL United Kingdom
Phone: 44 (0)161 275 4970
FAX: 44 (0)161 275 4734
john.helliwell@man.ac.uk

Jason Hodges
Oak Ridge National Laboratory
Spallation Neutron Source
IPNS Room-A137
Argonne, IL 60439
Phone: 630-252-9761
FAX: 630-252-4163
hodges@anl.gov

Ashfia Huq
Argonne National Laboratory
Intense Pulsed Neutron Source
9700 S. Cass Ave., Bldg. 360
Argonne, IL 60439
Phone: 630-252-8135
FAX: 630-252-7722
ahuq@anl.gov

Andrzej Joachimiak
Argonne National Laboratory
Structural Biology Center
9700 S. Cass Ave.
Argonne, IL 60439
Phone: 630-252-3926
FAX:
andrzejj@anl.gov

Michael E. Johnson
University of Illinois at Chicago
Center for Pharmaceutical Biotechnology

900 S. Ashland Ave., M/C 870
Chicago, IL 60607-7173
Phone: 312-996-9114
FAX: 312-413-9303
mjohnson@uic.edu

Tom Koetzle
Argonne National Laboratory
Intense Pulsed Neutron Source
9700 S. Cass Ave.
Argonne, IL 60439
Phone: 630-252-6485
FAX: 630-252-4163
tkoetzle@anl.gov

Alexander Kolesnikov
Argonne National Laboratory
Intense Pulsed Neutron Source
9700 S. Cass Ave., Bldg. 360
Argonne, IL 60439
Phone: 630-252-3555
FAX: 630-252-4163
akolesnikov@anl.gov

Anthony Kossiakoff
University of Chicago
Dept. Biochemistry & Molecular Biology
920 East 58th Street
Chicago, IL 60637
Phone: 773-834-2776
FAX: 773-834-2777
koss@cummings.uchicago.edu

Craig Kundrot
NASA/Marshall Space Flight Center
Microgravity Sciences and Applications Department
NASA Mail Code SD41
Marshall, AL 35812
Phone: 256-544-2533
FAX: 256-544-9305
craig.e.kundrot@nasa.gov

Philip Laible
Argonne National Laboratory
Biology CAT
9700 S. Cass Ave., Bldg. 202
Argonne, IL 60439
Phone: 630-252-4875
FAX: 630-252-5517
laible@anl.gov

Jyotsana Lal
Argonne National Laboratory
Intense Pulsed Neutron Source
9700 S. Cass Ave., Bldg. 360
Argonne, IL 60439
Phone: 630-252-6042
FAX: 630-252-7722
jlal@anl.gov

Paul Langan
Los Alamos National Laboratory
Life Sciences Division
Los Alamos, NM 87545
Phone: 505-665-8125
FAX: 505-665-3024
langan_paul@lanl.gov

Kenneth Littrell
Argonne National Laboratory
Intense Pulsed Neutron Source
9700 S. Cass Ave., Bldg. 360
Argonne, IL 60439
Phone: 630-252-3423
FAX: 630-252-4163
klittrell@anl.gov

Chun Loong
Argonne National Laboratory
Intense Pulsed Neutron Source
9700 S. Cass Ave., Bldg. 360
Argonne, IL 60439
Phone: 630-252-5596
FAX: 630-252-4163
ckloong@anl.gov

J. Patrick Loria
Yale University
Dept. of Chemistry
New Haven, CT 06520
Phone: 203-436-4847
FAX:
j.patrick.loria@yale.edu

Lee Magid
University of Tennessee
Joint Institute for Neutron Scattering
425 Andy Holt Tower
Knoxville, TN 37996-0140
Phone: 865-974-1407
FAX: 865-974-2805
lmagid@utk.edu

Andrew Mesecar
University of Illinois-Chicago
Center for Pharmaceutical Biotechnology
Room: 3070 MBRB, Mail Code: 870
Chicago, IL 60612
Phone: 312-996-1877
FAX:
mesecar@uic.edu

Dean Myles
Oak Ridge National Laboratory
PO Box 2008 MS6100
Oak Ridge, TN 37831-6100
Phone: 865-576-5230
FAX: 865-576-7956
mylesda@ornl.gov

Nobuo Niimura
JAERI
2-4 Shirane, Tokai-mura
Naka-gun, Ibaraki-ken, 319-1195
Phone: 81-294-38-5254
FAX: 81-294-38-5272
niimura@mx.ibaraki.ac.jp

Reinhard Pahl
University of Chicago
CARS CAT
9700 S. Cass Ave., Bldg. 434
Argonne, IL 60439
Phone: 630-252-0467
FAX: 630-252-0443
pahl@cars.uchicago.edu

Alberto Podjarny
IGBMC
Dept. of Structural Biology
Strasbourg, France
Phone: 33-3886-53311
FAX:
podjarny@igbmc.u-strasbg.fr

Raj Pokkuluri
Argonne National Laboratory
Biosciences Division
9700 S. Cass Ave., Bldg. 203
Argonne, IL 60439
Phone: 630-252-4197
FAX: 630-252-3387
rajp@anl.gov

Christine Rehm
Oak Ridge National Laboratory
Spallation Neutron Source
701 Scarboro Rd.
Oak Ridge, TN 37830
Phone: 865-576-5375
FAX: 865-241-5177
rehmc@ornl.gov

Jim Richardson
Argonne National Laboratory
Intense Pulsed Neutron Source
9700 S. Cass Ave., Bldg. 360
Argonne, IL 60439
Phone: 630-252-3554
FAX: 630-252-7722
jwrichardson@anl.gov

Gerold Rosenbaum
Argonne National Laboratory
APS-CAT
9700 S. Cass Ave., Bldg. 436
Argonne, IL 60439
Phone: 630-252-0643
FAX: 630-252-0652
rosenbaum@anl.gov

Ruslan Sanishvili
Argonne National Laboratory
Biology CAT

9700 S. Cass Ave., Bldg. 436
Argonne, IL 60439
Phone: 630-252-0665
FAX: 630-252-0667
rsanishvili@anl.gov

Bernard Santarsiero
University of Illinois at Chicago
Center for Pharmaceutical Biotechnology
900 S. Ashland Ave., M/C 870, 3100MBRB
Chicago, IL 60607
Phone: 312-413-0339
FAX: 312-413-9303
bds@uic.edu

David Savage
University of California
Biophysics Dept.
600 16th St.
San Francisco, CA 94107
Phone: 415-637-4450
FAX:
savage@msg.ucsf.edu

Marianne Schiffer
Argonne National Laboratory
Biosciences Division
9700 S. Cass Ave., Bldg. 202
Argonne, IL 60439
Phone: 630-252-3883
FAX: 630-252-3387
mschiffer@anl.gov

Benno Schoenborn
Los Alamos National Laboratory
Bioscience Division
Mail Stop M880
Los Alamos, NM 87544
Phone:
FAX:
schoenborn@lanl.gov

Arthur Schultz
Argonne National Laboratory
Intense Pulsed Neutron Source
9700 S. Cass Ave., Bldg. 360
Argonne, IL 60439
Phone: 630-252-3465
FAX: 630-252-4163
ajschultz@anl.gov

Geoffrey Stamper
Abbott Laboratory
Dept. of Structural Biology
100 Abbott Park Road
Abbott Park, IL 60064
Phone: 847-935-5930
FAX:
geoffrey.stamper@abbott.com

Narayanasami Sukumar
Cornell University
ANL-APS, NE-CAT
9700 S.Cass Ave., Bldg. 436E, Sector 24
Argonne, IL 60439
Phone: 630-252-0681
FAX: 630-252-0687
sukumar@aps.anl.gov

Ichiro Tanaka
JAERI
2-4 Shirakata-shirane
Tokai, Ibaraki 319-1195 Japan
Phone: 81-29-284-6736
FAX: 81-29-284-3822
tanaka@neutrons.tokai.jaeri.go.jp

Martha Teeter
University of California/Boston College
Chemistry Dept.
One Shields Avenue
Davis, CA 95616
Phone:
FAX:
mmteeter@ucdavis.edu

Ray Teller
Argonne National Laboratory
Intense Pulsed Neutron Source
9700 S. Cass Ave., Bldg. 360
Argonne, IL 60439
Phone: 630-252-4999
FAX: 630-252-4163
rteller@anl.gov

P. (Thiyaga) Thiyagarajan
Argonne National Laboratory
Intense Pulsed Neutron Source
9700 S. Cass Ave., Bldg. 360
Argonne, IL 60439
Phone: 630-252-3593
FAX: 630-252-4163
thiyaga@anl.gov

Peters Timmins
Institut Laue Langevin
DS Division
6, rue Jules Horowitz
Grenoble Cedex 9, BP 156-38042 France
Phone: 33 476 207 263
FAX: 33 476 207 120
timmins@ill.fr

Vijaya Tirumala
Argonne National Laboratory
APS-XFD
9700 S. Cass Ave.

Argonne, IL 60439
Phone: 630-252-1797
FAX:
vijay@aps.anl.gov

Alexander Wlodawer
National Cancer Institute
NCI at Frederick
P.O. Box B, Building 536, Room 5
Frederick, MD 21702-1201
Phone: 301-846-5036
FAX: 301-846-6128
wlodawer@ncifcrf.gov

David Worcester
University of Missouri
Biology Division
Columbia, MO 65211
Phone: 573-882-6864
FAX: 573-882-0123
worcesterd@missouri.edu

Workshop on
Neutron Macromolecular Crystallography At The Spallation Neutron Source
October 2-3, 2003
Argonne National Laboratory, Argonne, IL, USA

Background

Neutron macromolecular crystallography (NMC) can play a critical role in structural biology and functional genomics by providing accurate information on the positions of the protons and water molecules at active sites of enzymes that will enable the elucidation of the mechanistic details involved in their function. In order to exploit the high neutron flux that will become available by 2006 at the Spallation Neutron Source (SNS), and to leverage the enormous interest shown by the macromolecular crystallography community, it is proposed to develop a dedicated best-in-class high throughput and high resolution time-of-flight single crystal macromolecular neutron diffractometer (MaNDi) at the SNS high power target station (HPTS). Design calculations show that the data rates at the MaNDi instrument will be over 50 times greater than that for the best existing facilities. Furthermore, it will enable studies of crystals with larger lattice constants than is possible at the current facilities for NMC. It is expected that the unprecedented high data rates and resolution with MaNDi for the high resolution neutron macromolecular crystallography (NMC) will greatly advance the fields of structural biology and enzymology.

Objective

- To discuss the exciting opportunity that exists at the SNS for the development of a powerful facility for high resolution neutron macromolecular crystallography (NMC). NMC has been proven to provide accurate positions of hydrogens, protonation states of the atoms and the hydration in biological macromolecular crystals which is of interest to the scientific community in the fields of structural biology, enzymology, biochemistry, and macromolecular crystallography.
- To obtain input from the scientific community on the exciting scientific challenges that can be addressed by neutron macromolecular crystallography. Also, to obtain input on the design aspects of MaNDi with regard to the size of the unit cell, resolution, detectors, sample environment, and deuteration facilities, as well as any other requirements at the Spallation Neutron Source.
- To officially form an instrument development team (IDT) and to document a strong scientific case in order to obtain funding for the design and construction of the MaNDi instrument.

Confirmed Speakers

Ian Anderson (SNS)
Robert Bau (USC)
Gerry Bunick (ORNL)
Dan Carter (New Century Pharmaceuticals, Inc.)
Victor Davidson (U Of MS)
Chris Dealwis (UTK)
Martin Egli (Vanderbilt U)
Petra Fromme (Arizona State U)
Hong Guo (UTK)
Leif Hanson (ORNL)
John Helliwell (U of Manchester, UK)
Andrzej Joachimiak (ANL-SBC)
Michael E. Johnson (UIC)
Anthony Kossiakoff (U of C)
Paul Langan (LANL)
J. Patrick Loria (Yale)
Lee Makowski (ANL-BIO)
Dean Myles (ORNL)
Nobuo Niimura (JAERI, Japan)
Alberto Podjarny (IGBMC-Strosborg, France)
Benno Schoenborn (LANL)
Geoffrey F. Stamper (Abbott Labs)
Ichiro Tanaka (JAERI, Japan)
Martha Teeter (Boston College)
Peter Timmins (ILL, France)
Alexander Wlodawer (NCI)

Workshop Website: www.pns.anl.gov/events/conferences/mandi/flyer.pdf
Conference Site: Bldg. 360, Intense Pulsed Neutron Source (IPNS), Argonne National Laboratory
Accommodation: Argonne Guest House
Organizing Committee: Andrew Mesecar (UIC), Arthur Schultz (ANL) and P. Thiyagarajan (ANL)
Conference Secretary: Carolyn Peters, IPNS, ANL (cpeters@anl.gov)
Registration Fee: $100.00 US cash or check only payable to Carolyn Peters-Workshop Account 467290.

ORAU OAK RIDGE ASSOCIATED UNIVERSITIES
SNS SPALLATION NEUTRON SOURCE

SPONSORS

Joint Institute for Neutron Sciences (JINS)

UIC University of Illinois at Chicago

IPNS